5-7-2016

Interrogating Raf-1 Kinase Inhibitor Protein (RKIP) as a Novel Therapeutic Target for Modulating Inflammatory Responses

Kyle T. Wright
kwright@uchc.edu

Interrogating Raf-1 Kinase Inhibitor Protein (RKIP) as a Novel Therapeutic Target for Modulating Inflammatory Responses

Kyle T. Wright, M.D., Ph.D.

University of Connecticut, 2016

The studies presented here were designed to test if Raf-1 kinase inhibitor protein (RKIP) plays a functionally significant role in immunity, and to interrogate its possibility of providing a novel therapeutic target for modulating inflammatory responses. Based on previous studies from other laboratories that attributed negative regulatory functions to RKIP in the context of MAPK and NF-κB signaling in cell lines, we tested the hypothesis that its function was to suppress the production of pro-inflammatory cytokines, proliferation, and cell survival. However, after extensive investigation, our data clearly demonstrate that RKIP is actually necessary for the production of certain cytokines, namely Type-I and Type-II interferons, but had less robust effects on cell survivability and proliferation. Specifically, this work shows that RKIP is integrated in the signaling pathway downstream of TCR triggering in $CD8^+$ T cells and TLR ligation in APCs. Finally, these studies highlight RKIP as a druggable protein, and through its targeted inhibition, cytokine responses can be significantly diminished. Thus, this provides elementary rationale for its potential clinical applicability in therapeutic interventions for inflammatory diseases, especially those associated with dysregulated IFN responses. Through this current work, we have provided a solid foundation for future studies that seek to investigate further the molecular mechanisms of RKIP function within the immune system, as well as its advancement into clinically relevant inflammatory disease models.

Interrogating Raf-1 Kinase Inhibitor Protein (RKIP) as a Novel Therapeutic Target for Modulating Inflammatory Responses

Kyle T. Wright

B.S., University of Illinois Urbana-Champaign, 2008

A Dissertation

Submitted in Partial Fulfillment of the

Doctor of Philosophy

at the

University of Connecticut

2016

APPROVAL PAGE

Doctor of Philosophy Dissertation

Interrogating Raf-1 Kinase Inhibitor Protein (RKIP) as a Novel Therapeutic Target for Modulating Inflammatory Responses

Presented by:

Kyle T. Wright

Major Advisor 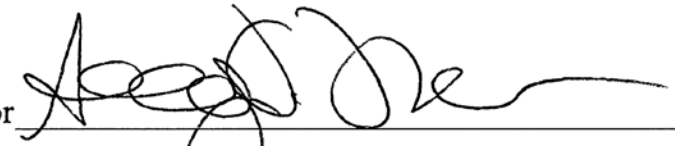

Anthony T. Vella, Ph.D.

Associate Advisor 

Robert B. Clark, M.D.

Associate Advisor 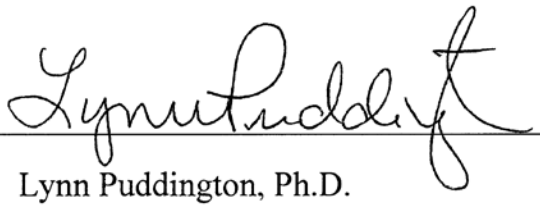

Lynn Puddington, Ph.D.

Associate Advisor 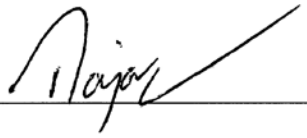

Thiruchandurai V. Rajan, M.D., Ph.D.

University of Connecticut- 2016

ACKNOWLEDGEMENTS

First and foremost, I would like to thank Tony for his invaluable guidance and support throughout the development of this thesis project, as well as challenging me both intellectually and personally during my time in his laboratory. Not only did he bolster my training of how to think about and conduct scientific research, but he also taught me how to be a scientist. This is perhaps his greatest gift to me, and for this I will always be grateful. I would also like to thank my thesis committee members Drs. Robert Clark, Lynn Puddington, and T.V. Rajan for their support and ever poignant feedback during the course of our scientific discussions.

I am also grateful to the members of the Vella Lab group which have helped guide and strengthen not only my project through intelligent discussions and (occasionally pointed) feedback, but also my desire to learn, teach, and advocate science for the long-term. I've learned so much from them: Drs. Adam Adler, Francisco Sylvester, Antoine Ménoret, Soo-Mun Ngoi, Sanjeev Kumar, Andrew Draghi, Raghunath Ramanarasimhaiah, Naomi Tsurutani, Wenhai Liu, and all other past and present lab members.

Most importantly, I would like to thank my mom for instilling in me at an early age a desire to always strive for greatness in everything I do, but never at the cost of doing it the right way; and also to my wife, Bo, for providing unwavering emotional and intellectual support throughout this process. I can only ever hope to be half as good at what I do, as what she does. Finally, I want to acknowledge all of my family and friends that are constant reminders of the fact that although having a strong devotion to your craft is important, it's equally as important to, every once in a while, sit on the couch with a bottle of wine and watch a good movie.

TABLE OF CONTENTS

LIST OF TABLES

LIST OF FIGURES

CHAPTER 1

INFLAMMATION IN HEALTH AND DISEASE:

HOW UNDERSTANDING DIFFERENT INFLAMMOMES MAY LEAD TO ENHANCED THERAPUETIC INNOVATION AND CLINICAL IMPLEMENTATION

I. INTRODUCTION

Inflammation, to use a timeworn axiom, is a double-edged sword. Under normal physiological circumstances, it operates as the most significant defense system that the human body has developed to ward off incursion of foreign pathogens (1); however, if inappropriately directed or poorly regulated, it can lead to significant morbidity and mortality (2). It is truly a unique circumstance within physiology that one of the greatest assets for developing Darwinian fitness (3), and certainly important for survival and propagation of many species, can abruptly become one of the most substantial agents for tissue dysfunction and disease development.

Although the mechanisms by which inflammation develops have gained significant complexity and efficiency over evolutionary time, there are still only but a handful of molecular signaling pathways and professional immune cell types that drive the entire effective output of inflammatory processes (4). Nevertheless, inflammation as a term in its clinical sense, and certainly as it is portrayed to the general public, has been, until recently, used too broadly. This is most likely responsible for the stagnation in therapeutic options for patients suffering from "inflammatory" diseases until the advent of cytokine-specific biologicals in the 1990 (5, 6). In reality, inflammation can vary depending on a myriad of factors including the following: 1) the initiating stimulus or trigger (e.g. pathogenic infection, cell injury, molecular mimicry, or inappropriate responses to a self and innocuous antigens), 2) the cell types, receptors, and signaling pathways involved, 3) the generation of specific effector cytokine-chemokine milieus, 4) temporality (e.g. acute vs. chronic or early vs. late phase dynamics), and 5) the type of pathology that results (e.g. systemic vs. local, tissue destruction vs. repair, etc.). The compilation of these factors in a given mechanistic context is the inflammome (7). Humans and other higher order mammals have, over evolutionary time, developed several discrete inflammomes in order

to antagonize the effects of certain pathogens (Figure 1-1). However, when these inflammomes are induced inappropriately, they drive the development of distinctive disease causing effector molecules that have become the basis of new interventional therapies (8). The vast majority of biological anti-inflammatory treatments currently being researched and developed are focused on the *post hoc*, direct inhibition of these downstream effectors by anti-cytokine monoclonal antibodies or through receptor antagonists. This prevailing thought process of "end-point treatment" has even directed a new approach to disease classification, namely a cytokine-based disease taxonomy (9), as opposed to a traditional diagnosis based on particular tissue or organ system dysfunction. Although this approach is a much improved way of organizing groups of distinct diseases, it omits the processes that led to the generation of these effectors in the first place. In this review, we will focus on delineating not only the pathogenic sequelae of these inflammation-driving effector cytokines, but also the distinct inflammomes that lead to their synthesis. Through this, we hope to expand the idea of a cytokine-based disease taxonomy into an inflammome-based disease taxonomy, while directing the focus of future therapeutic development toward those interventions that subvert *a priori* cytokine development, rather than *post hoc* inhibition.

II. THE MAJOR INFLAMMOMES

A. INNATE (TNF DOMINANT)

The innate immune response is composed of different cell types that respond to diverse endogenous or exogenous signals and mediate distinct downstream effects within minutes to hours of activation. However, there are at least three major cytokine milieus that can be generated based on all of these factors: tumor necrosis factor (TNF) dominant, interferon (IFN) dominant, and inflammasome dominant. The word “dominant” is used because, in reality, all of these responses are generated to varying degrees with any given inflammogen. For clinical purposes, thinking about the innate response in the context of these three major divisions allows one to clearly see that these milieus are generated by separate signaling cascades that provide opportunity for specific therapeutic interventions.

A TNF dominant response can be generated by either pathogenic infection or trauma that results in cell injury (10). These initiating triggers are recognized by the innate immune system through the production of pathogen associated molecular patterns (PAMPs), or in the case of cell injury, damage-associated molecular patterns (DAMPs) ((1, 11, 12). PAMPs, as the name implies, are usually structural components of bacteria, viruses, or fungi that are recognized through pattern recognition receptors (PRRs) on immune cells such as macrophages, dendritic cells, B cells, and others (13, 14). On the other hand, DAMPs are factors found in host cells that are normally sequestered away from immune recognition; however, in the face of cell injury or death, these DAMPs, such as the nucleosome associated protein HMGB1, are released from cells and are recognized by the same PRRs as PAMPs (15, 16).

PRRs, such as the toll-like receptors (TLRs) will activate two distinct signaling pathways after ligation, depending on which PAMP is recognized by its corresponding TLR. In the case of TNF dominated responses, the major contributing pathway involves activation of the MyD88 adaptor protein which is activated most strongly in the context of lipopeptides (TLR1/2 or 2/6), LPS (TLR4), flagellin (TLR5), profilin (TLR11, 12), ribosomal RNA (TLR13), or CpG oligodinucleotide sensing (TLR9) (14). MyD88 is responsible for coupling TLR ligation to the activation of the pro-inflammatory transcription factor NF-κB through a complex signaling pathway involving interleukin-1 receptor-associated kinase (IRAK) 1 and 4, TNF receptor associated factor 6 (TRAF6), TAK1, IκB kinase (IKKα/β/γ), and finally poly-ubiquitinylation and degradation of the inhibitor of NF-κB (IκBα) (17, 18). NF-κB function results in the transcription of factors important for cell survival, as well as initiating a pro-inflammatory program. Specifically, in conjunction with MAPK signaling, this leads to synthesis of the transcription factor activator protein 1 (AP-1), which induces transcription of *Tnf* (19). After TNF protein is produced, it exerts pleiotropic effects on the body including: activation of the underlying tissue endothelium which directs other immune cells to sites of inflammation, activation of the pro-inflammatory acute phase response from the liver (interleukin-6, C-reactive protein, serum amyloid A, etc.), enhancement of phagocytosis and oxidative burst from phagocytic cells, and during prolonged or systemic exposure, insulin resistance, muscle wasting, and substantial vasodilation (10, 20, 21). Additionally, TNF signaling through its receptors can lead to further activation of NF-κB, and subsequently more TNF production, creating a very potent and potentially dangerous cycle of activation (22, 23).

TNF is produced in nearly every inflammatory disease; however, there are several where the TNF predominates the response, so much so that interventional anti-TNF interventions have

been introduced as therapies. These include inflammatory bowel diseases (Chron's disease and ulcerative colitis), rheumatoid arthritis, ankylosing spondylitis, psoriasis, several vasculitides including giant cell arteritis, and asthma that is refractory to other therapies ((6, 24, 25)). Systemic TNF, via activation of the acute phase response, can also result in a "cytokine storm" which leads to the initiation of systemic inflammatory response syndrome (SIRS) or sepsis for triggers involving bacteremia, viremia, or mass tissue damage (e.g. electrocution, severe burns, etc.) (26-28). Current anti-TNF therapies being used in the clinical setting include: anti-TNF monoclonal antibodies (Infliximab, Adalimumab) and soluble TNF decoy receptors (29, 30). However, many disease processes do not respond to anti-TNF therapy. In fact some, as in the case of multiple sclerosis (31), are exacerbated with anti-TNF therapy; clearly demarcating the importance of understanding specific inflammomes before institution of a given therapy. As anti-TNF treatment was the first biologic anti-cytokine therapy to be FDA approved (in 1998)(32), it is not surprising that this field is also the first to realize the need for *a priori* therapeutics, exemplified by the recent wave of NF-κB inhibitors currently in clinical trials (33-35), as well as TLR antagonists to prevent sepsis (36, 37).

B. INNATE (IFN DOMINANT)

The innate IFN dominant inflammome is initiated in an analogous way as to the TNF dominant inflammome (i.e. PAMP-TLR interaction); however, the ligands recognized in these responses are generally nucleic acids from viruses, and to a lesser extent bacteria, or even endogenous DNA and RNA in the context of autoimmune diseases like systemic lupus erythematosus. The signaling mechanisms of type-I IFN generation are complex but are becoming well described. Briefly, these nucleic acid PAMPs are recognized by endosomal (TLR3, TLR7, TLR8) or cytoplasmic (RIG-I, MDA-5, STING) sensors, and converge downstream at the level of

interferon regulatory factor 3 (IRF3) and IRF7 phosphorylation (38, 39). IRF3 and IRF7 act to initiate the transcription of type-I IFNs (IFNα/β/δ/ε/ω) which, like TNF, can also enhance their own production via a positive feed-forward loop (40). Type-I IFNs can be made by most cell types, but plasmacytoid dendritic cells (pDCs) have been identified as professional IFNα producing cells in response to nucleic acid PAMPs (41). The importance of pDCs in type-I IFN production is exemplified by the fact that they have a cell-type specific alteration in their signaling machinery that permits IFNα production directly after stimulation with TLR7 and TLR9 ligands through a TRAF3-independent mechanism involving IKKα and IRF7 (42). Type-I IFNs, like TNF, also have pleiotropic effects at different levels of the immune system including activation of anti-viral response genes, the establishment of CXCR3-mediated chemokine gradients via CXCL9 and CXCL10, and the enhancement of IFNγ from Th1 and Tc1 T cells and NK cells (43, 44). They can also lead to STAT3 phosphorylation in macrophages and Tregs which can induce an anti-inflammatory response via up-regulation of IL-10 and PD-L1 (45, 46). Some diseases associated with altered type-I IFN production include SLE (47), psoriasis (48), multiple sclerosis (therapeutic) (49), insulin-dependent diabetes mellitus (50, 51), rheumatoid arthritis (52, 53), myasthenia gravis (54), and some hematologic malignancies (55). Therapeutically, anti-IFN treatments for diseases like SLE and polymyositis have shown promise is reducing symptom severity (56, 57), whereas recombinant IFNβ has been established as a treatment for relapsing-remitting multiple sclerosis (58).

C. INNATE (INFLAMMASOME DOMINANT)

The third major inflammome driven by innate immune cells centers on activation of inflammasomes, which are pentameric or heptameric protein complexes that serve to couple PAMP and DAMP sensing with the proteolytic cleavage of pro-IL-1β and pro-IL-18 via caspase

1 (59). Several different inflammasomes exist and differ somewhat by structure, but each contains a PRR-like protein (i.e. NOD-like receptor (NLRs) or the interferon-inducible AIM2) which is connected to pro-caspase 1 by the adaptor protein ASC (60). These inflammasomes also have been reported to confer resistance to different kinds of pathogens based on the PRR that is affiliated with them. For example, the NLRP3 inflammasome responds to *Staphylococcus spp.*, *Listeria spp.*, and influenza viruses (61), the NLRC4 inflammasome is activated by intracellular pathogens bearing flagella (62), and the AIM2 inflammasome responds to dsDNA from *Francisella tularensis*, and herpes viruses (63). The exact nature of inflammasome activation and regulation are still active areas of investigation; however, several consensuses have been reached. First, inflammasomes usually require two signals in order to become fully responsive: 1) substrates for the inflammasome (i.e. pro-IL-1β and pro-IL-18) are generated in response to signaling cascades downstream of other PRRs including NF-κB and Type-I IFN signaling, and 2) the inflammasome must have a second signal that allows for the activation of pro-caspase 1 into bioactive caspase 1, and subsequently the production of mature IL-1β and IL-18 (64). There are many theories as to what can supply signal 2 and those include: intracellular potassium efflux (65), extracellular ATP sensing (66), exposure to lysosomal enzymes like cathepsin B (67, 68), and reactive oxygen species (69). Inflammasome regulation is less well understood, but factors involved in chronic infections like prolonged IFNγ exposure can lead to inflammasome destabilization through nitric oxidize-mediated nitrosylation (70).

The inflammasome dominant inflammome becomes medically relevant not only in response to bacterial and viral pathogens, but also in the context of situations involving “frustrated phagocytosis” which can result from chronic infections of *Mycobacteria spp.* or incidents of sterile inflammation such as exposure to particulate antigens (71). Diseases associated with the

inflammasome dominant inflammome include gout (uric acid crystals), asbestosis (asbestos fibrils), berylliosis (beryllium), silicosis (silica), sarcoidosis, and amyloidosis (proteins) (72). Each of these disease result lead to localized inflammation of the area where these particulates are deposited which is usually the lung (beryllium, silica, asbestos), joints (uric acid), or small blood vessels and soft tissue (amyloid). Inflammasomes are also implicated in both metabolic disease and atherosclerosis, and may be main player in the development of insulin resistance in type-2 diabetes mellitus (73-75). Antagonistic IL-1 therapies such as anakinra (receptor antagonist (76)), canakinumab (anti-IL-1 mAb (77)), and rilonacept (soluble decoy receptor (78)) have proved efficacious in these types of diseases, including gout (79, 80). Many of these therapies were initially developed for the treatment of rheumatoid arthritis; however, they have shown limited long-term efficacy in humans (81). This illustrates that the presence of a particular cytokine within the inflammatory milieu in a given disease, and thus an attempt to block it therapeutically, is not sufficient in most cases to effectively decrease symptom severity. However, a full understanding of the inflammome of a given disease can better guide clinicians to more rational interventions.

D. ADAPTIVE (T CELL CENTRIC)

T cells are perhaps the best studied of all immune cells, namely due to their importance of facilitating nearly every immune response in some way (82). T cells are activated after their T cell receptor (TCR) encounters peptide antigens in the context of the major histocompatibility complex (MHC) that have been processed and presented by APCs (83). Naïve T cells also require a second signal in the form of co-stimulatory molecules that drive their proliferation (clonal expansion) via the production of IL-2 (84). These are usually in the form of CD28 on the T cell and CD80/CD86 on the APC; however, ligation of other co-stimulatory molecules such as

ICOS, OX40, and 4-1BB can also provide this necessary signal (20). Finally, a third signal in the form of cytokines results in the differentiation of the activated T cell towards a specific effector subtype which has a specific cytokine potential. Thus, the T cell centric inflammome can take on different characteristics depending on the context in which it was induced (85). The major T cell subsets include Th1 (driven by IL-12, IL-18, IFNα/β), Th2 (IL-4, IL-33), Th17 (TGFβ & IL-1, IL-6, IL-21, IL-23), and T regulatory cells (TGFβ), but other, less well defined subsets also exist including cytotoxic T helper cells, Th9, Th22, Tfh, and Tr1 (86, 87). For the purpose of this review, we will focus on Th1, Th2, and Th17 subtypes as they have been the best studied in the context of mediating human disease.

Th1 T cells are produced when activated in the context of IL-12, IL-18, and Type-I IFNs and inhibited in the presence of IL-4 (88). They are defined by the major transcription factor T-bet which is necessary for their ability to produce the effector cytokine IFNγ. Th1 T cells also provide help to $CD8^+$ cytotoxic T lymphocytes (CTLs) that respond to cells infected with intracellular pathogens or altered self (cancerous cells), and kill them by production of several soluble effector molecules including IFNγ, granzymes, granulysin, and perforin (89). CTLs can also induce death through contact-mediated, caspase 8 dependent apoptosis by Fas-FasL (CD95-CD95L) and TNF-related apoptosis-inducing ligand (TRAIL)-DR5 (90). Th1 cells have been implicated in the pathogenesis of numerous autoimmune diseases through inappropriate activation by self-antigens, and also the potentiation of innate immune responses through the positive feedback effects of IFNγ (91).

Th17 T cells are produced in the context of TGFβ and other pro-inflammatory cytokines such as IL-6, IL-1β, IL-21, IL-23, and others (92). Their differentiation to Th17 can be enhanced through autocrine production of IL-21 (93), and also stabilized by subsequent IL-23 after the up-

regulation of IL-23R after TCR activation (94). Th17 polarization is controlled by the master transcription factor RORγT, RORC2 in humans (95), which facilitates the production of IL-17A, IL-17F, IL-21, and IL-23 production from Th17 T cells (96). A major known function of IL-17 is to recruit neutrophils to the sites of infection by stimulating the production of IL-8, CCL2, CCL7, CXCL1, and CXCL5 (97). IL-17 can also promote synthesis of TNF, IL-6, and IL-1β from epithelial cells and macrophages. Th17 cells have been implicated as pathogenic in several mouse models of RA, IBD, psoriasis, and type-1 diabetes mellitus (98), as well as several diseases in humans: multiple sclerosis, RA (99), SLE (100), psoriasis (101), and IBD (102). These associations have been largely based on finding elevated IL-17 levels in either sera or tissue biopsies from afflicted patients or direct visualization of Th17 cells within diseased tissue biopsies (103). Several therapies exist to target the Th17 pathway including (104) (monoclonal antibody that targets the IL-12p40 subunit shared by IL-12 and IL-23) and several anti-IL17 antibodies that are not yet FDA approved (brodalumab, ixekizumab, and secucinumab). Ustekinumab treatment has seen some success in treating patients with psoriasis, but that success has not translated to other Th17 implicated diseases to date (105, 106).

The final T cell subset that can define the T cell centric inflammome are Th2 T cell which differentiate in the presence of IL-4 or IL-33 and the absence of IFNγ (107, 108). Th2 cells are potent promoters of IL-4, IL-5, and IL-13 production and are defined by their master transcription factor GATA3 (109). Th2 cells can also efficiently provide help to B cells through CD40-CD40L interactions. In the presence of IL-4, B cells secrete antibodies of the IgE isotype which are critical for protection against helminthic infection (110), but are also the main driving force of allergic responses in humans (111). The concomitant actions of IgE, by binding its receptor FcεRI, and Th2 cytokines potently induce granulocyte chemotaxis and degranulation of

mast cells, eosinophil, and basophils. This degranulation releases vasoactive amines (like histamine), serine proteases, and eicosanoids (such as prostaglandins and leukotrienes), all of which facilitate symptoms of allergy (erythema, pruritus, bronchoconstriction) (112). Once again, most therapies currently approved for treatment of allergic reactions are typically based on *post hoc* approaches. These interventions involve blockade of histamines and leukotrienes, or management of symptoms (e.g. bronchodilators) (113). Investigation into blocking these responses at the level of T cell (or B cell) initiation is an area that requires attention, as too few studies have been conducted to answer these questions.

The T cell centric inflammome can assume very diverse outcomes, and be the driving force behind many different types of inflammatory diseases. However, because T cells undergo clonal expansion in response to activation, they are susceptible to many of the broadly immunosuppressive agents that aim to kill dividing cells (114, 115) . For example, corticosteroids block the production of IL-2, and immunophilins (such as tacrolimus, and cyclosporine) prevent calcineurin-mediated activation of NFAT, a transcription factor critical for T cell responses (116). Also, cyclostatic drugs (e.g. methotrexate, azathioprine, mercaptopurine) that block all cell proliferation, and are typically used in cancer therapy, are sometimes used to prevent T cell expansion in inflammatory diseases (117). All of these therapeutic options prevent pro-inflammatory cytokine production; however, they also suffer from lack of specificity. Future studies aimed at improving T cell based therapeutic interventions should seek to combine the *a priori* blockade of cytokine synthesis with the specificity of a biologic treatment in order to prevent such broad immunosuppression.

E. ADAPTIVE (B CELL CENTRIC)

The main effectors of the B cell centric inflammome are antibodies, which are generated after the integration signals from PRR triggering, B cell receptor ligation, T cell help, and sensing of the cytokine milieu (118). The effector functions of antibodies are well defined and include opsonization and neutralization of pathogens, initiation of the complement cascade, and activation of other effector cells as described above. Different antibody isotypes are generated by activation-induced cytodine deaminase (AICD) in response to sensing the cytokine milieu by B cells. For example, in humans the presence of IFNγ will trigger production of IgG1, IL-4 will give IgE, while TGFβ will yield IgA (119, 120).

However, B cells can also be significant contributors to cytokine synthesis in their own right. B cells that are primed by Th1 cells and BCR ligation will begin to produce a "Th1-like" cytokine profile including synthesis of IFNγ and even IL-12, a cytokine not made explicitly by Th1 cells but key for Th1 differentiation (B effector type 1 or Be-1 cells). By analogy, those primed with Th2 cells will produce IL-2, IL-4, and IL-13 (Be-2) (121). Additionally, B cells can also produce regulatory cytokines, such as TGFβ and IL-10, in some circumstances (Bregs). Each of the B cell cytokine-producing subtypes have been identified *in vivo* (122, 123), and have documented functional significance, especially in the context of pathogen clearance and autoimmune diseases that result from the inappropriate production of autoantibodies like SLE (124). Nevertheless, much remains to be studied regarding their role in cytokine-based inflammation.

F. REVERSE-PHASE IMMUNITY

Recently, more evidence is coming to light that exemplifies the bi-directionality of the immune response, in that exposure to molecules that directly activate T cells, such as superantigens, can

lead to T-cell mediated activation of the innate immune system (125, 126). This concept outlines an emerging reverse-phase inflammome that relies on bystander activation of the innate immune response through cytokines produced by the adaptive arm of the immune system, rather than PAMP or DAMP exposure. The exact mechanism(s) by which this activation occurs is still an area of active investigation; however, production of IL-17 by TCR γδ T cells after cooperative activation by TCRαβ T cells has been implicated (127, 128). This novel route of innate immune system activation will generate an inflammatory-milieu that is largely similar to those generated by the innate inflammomes discussed previously. In cases such as *Staphyloccal* enterotoxin A (SEA) mediated acute lung injury or SIRS, a physician may see a clinical picture, based on cytokines, that heavily implicates the innate immune system as the main driving force in disease pathogenesis; however, when trying to treat such a disease process with therapeutics such as anti-TNF, they may encounter much difficulty because the actual pathogenic mechanism is directed by T cells and may be better treated by agents that affect IL-17 or IL-2 production. This illustrates that although a cytokine-based disease taxonomy allows for a better understanding of how to treat diseases that share related milieus, it may in some cases lead clinicians to incorrect assumptions that could be insignificant, or even deleterious to the patient.

III. RKIP: A NEW THERAPUETIC TARGET?

Raf-1 kinase inhibitor protein (RKIP) is part of the highly evolutionarily conserved phosphatidylethanolamine-binding protein (PEBP) superfamily. This family of proteins has been found in species from bacteria to plants to humans (129, 130), and is ubiquitously expressed, to different degrees, in all tissues (131). RKIP (PEBP-1) was originally shown to interact with Raf-1 by yeast-two hybrid screening in 1999 (132), which prevented the downstream phosphorylation of MEK and ERK (Figure 1-2). Since this time, RKIP has been implicated as a

regulator (both positive and negative) of important signaling pathways within cells. The functional significance of these interactions is poorly understood, and most likely varies between cell types. It has been shown to interact with upstream proteins involved in the NF-κB cascade, and may facilitate the assembly or stabilization of these complexes (133). The affinity for RKIP and its ligands can be altered based on post-translational modification events, the best example of which is its transition from Raf-1 inhibition to GRK-2 inhibition after phosphorylation of Ser $(Thr)_{153}$. RKIP is also a positive regulator exemplified by its ability to enhance GSK-3β (134) through the prevention of an inhibitory (Thr_{390}) phosphorylation and by enhancing production of the microRNA let-7 (135). RKIP has also been described as a suppressor of epithelial to mesenchymal transition, and subsequently, invasion and metastasis of cancerous cells (136) through a mechanism involving GSK-3β and its downstream target cyclin D1 (137).

Despite these well-defined roles for RKIP in cancer cells, its function within primary cells and within the immune system is unknown. However, recent studies have suggested that RKIP may be linked to immune function and potentially cytokine production. First in 2006, studies implicated RKIP induction in successful macrophage and dendritic cell maturation in cell lines that included the up-regulation of the scavenger receptor CD36 and decreased nuclear localization of NF-κB (138). In 2009, Reumer and colleagues found that RKIP overexpression in *Drosophila melongaster* (PEBP1 or CG18594) protected them from infection by pathogenic bacteria through the enhanced production and secretion of immunity-related proteins (139). Also in 2009, Ménoret et. al. demonstrated that RKIP was altered (either at the level of expression or post-translational modification) between primed OT-I T cells that were either resting or recalled with the cognate peptide SIINFEKL from ovalbumin (140). By blocking RKIP using the small molecule inhibitor locostatin, the production of IFNγ and TNF was attenuated through an

unknown mechanism. Taken together, these studies suggest that RKIP may have an immunological function that may result in altered cytokine responses. Also, the fact that RKIP can be inhibited exogenously allows for the possibility that it may provide a therapeutic target for modulating *a priori* cytokine production.

IV. CONCLUSIONS

Inflammation is one of our body's greatest assets as it is responsible for the defense against harmful pathogens and facilitates removal and repair of dead or dying cells. However, inflammation is also the pathogenic mechanism by which many diseases are manifest, leading to significant medical and financial burdens for patients. Our ability to therapeutically intervene in these pathophysiological processes is key to preventing undue morbidity and mortality in these patients. Before the 1990s, the standard of care for many auto-inflammatory diseases involved broad immunosuppression using corticosteroids or direct killing of proliferating cells, both of which lead to significant immunosuppression and the inability to ward off potential infections. With the advent of cytokine-specific biologics, clinicians and scientific investigators became much more interested in specific, targeted therapies that attenuated disease, while allowing for most of the immune response to continue unabated. This led many to consider a disease diagnostic schema that centered on a particular cytokine milieu. This has resulted in the development of successful therapeutic endeavors for some diseases (IBD, RA), but also to significant failures (anti-TNF in MS, anti-IL-1 in sepsis, and anti-IL-17 in Chron's disease) (141-143). These errors were due largely in part to the analysis of *post* hoc cytokine production rather than examination of the underlying inflammome that led to the generation of these cytokines in the first place. By understanding the inner workings of the body's different inflammomes (Figure

1-1), even better therapies can be developed that stop altered cytokine production at the source, rather than after the fact.

Figure 1-1: An Inflammome-based Disease Taxonomy

A schematic representation of the cytokine networks established by the host's major inflammomes; the size of each circle pictorially represents the relative abundance of a given cytokine within its respective inflammome. Human diseases associated with each inflammome are listed in non-bold script.

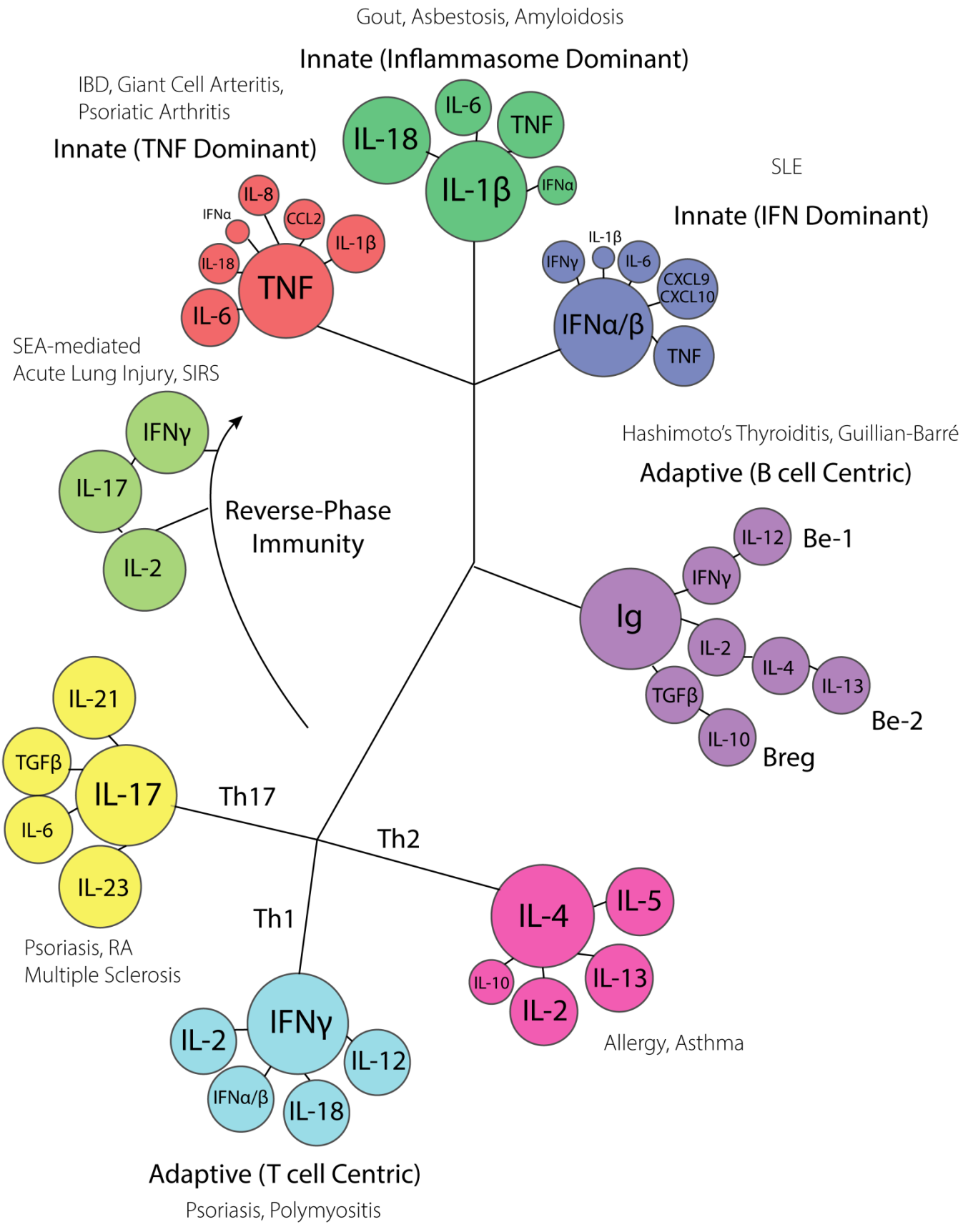
Gout, Asbestosis, Amyloidosis
Innate (Inflammasome Dominant)
IL-18
IL-6
TNF
IL-1β
IFNα
IBD, Giant Cell Arteritis,
Psoriatic Arthritis
Innate (TNF Dominant)
IL-8
IFNα
CCL2
IL-1β
IL-18
TNF
IL-6
SLE
Innate (IFN Dominant)
IL-1β
IFNγ
IL-6
CXCL9
CXCL10
IFNα/β
TNF
SEA-mediated
Acute Lung Injury, SIRS
IFNγ
IL-17
IL-2
Reverse-Phase
Immunity
Hashimoto's Thyroiditis, Guillian-Barré
Adaptive (B cell Centric)
IL-12
Be-1
IFNγ
Ig
IL-2
IL-4
IL-13
TGFβ
Be-2
IL-10
Breg
IL-21
TGFβ
IL-17
Th17
IL-6
IL-23
Th2
Th1
IL-4
IL-5
IL-10
IL-13
IL-2
Psoriasis, RA
Multiple Sclerosis
Allergy, Asthma
IFNγ
IL-2
IL-12
IFNα/β
IL-18
Adaptive (T cell Centric)
Psoriasis, Polymyositis

Figure 1-2: RKIP: A regulator of kinase-mediated signaling cascades (A) Schematic diagram outlining previously described RKIP function. RKIP suppresses both the Raf-MEK-ERK and canonical NF-κB signaling cascades in the resting state; however, after stimulation RKIP is phosphorylated at $Ser(Thr)_{153}$ by protein kinase C which allows is to dimerize and lose affinity for Raf-1 and IKK complex members while gaining affinity for GRK-2. This system allows for the coordinated activation of multiple pathways within the cell, theoretically leading to enhanced cytokine production, cell survival, proliferation, and locomotion. (B) A list of known RKIP binding partners and their functions;

A

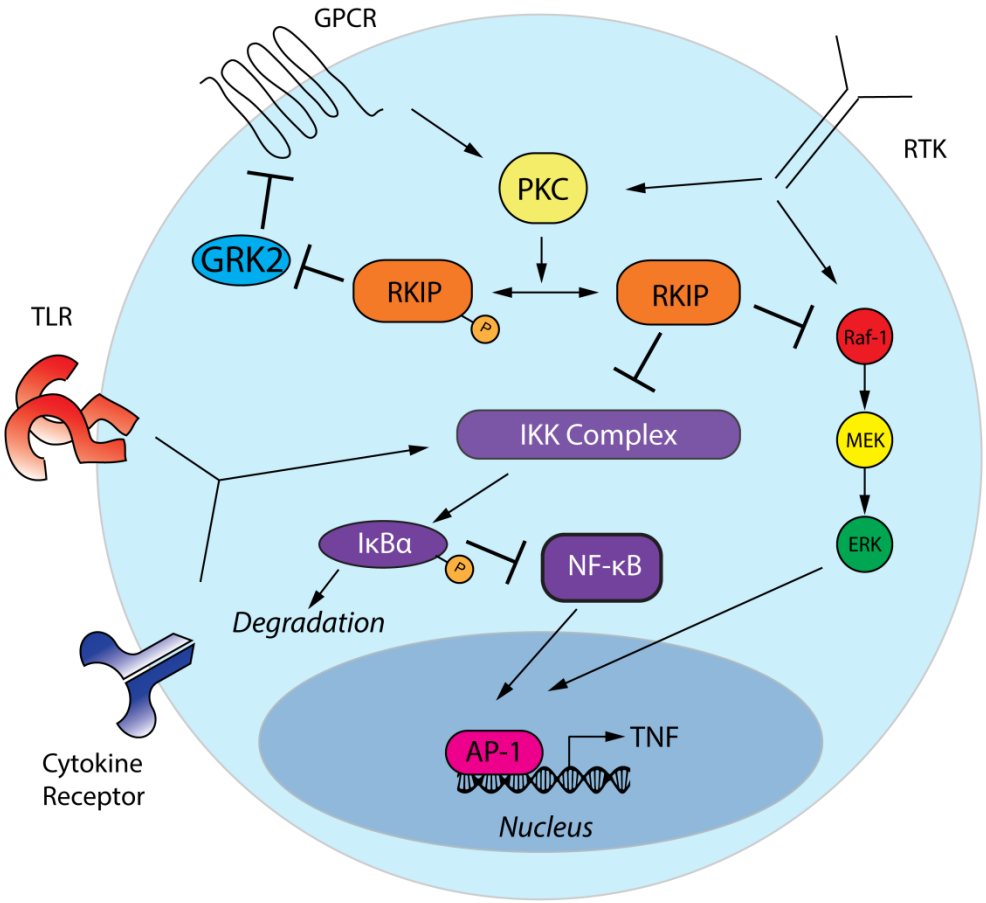

B

RKIP – A List of Known Binding Partners

Molecule	Function	Reference
Raf-1	MAPKKK for the Raf-MEK-ERK cascade; bound by and inhibited by non-phosphorylated RKIP	Yeung K. et. al. *Nature* (1999).
Lipids	Phosphotidalethanolamine>>Phosphotidalinositol = Phosphotidalcholine; binds to polar head groups	Bernier et. al. *Biochem Biophys Acta* (1986).
Opioids	Shown to bind morphine in rat brains and may be associated with opioid receptors, but does not bind them directly;	Grandy et. al. *Mol. Endocrine. (1990).*
ATP/ADP	Found to contain ATP binding site;	Banfield et. al. *Structure* (1998).
Aurora B Kinase	Evidence of RKIP regulation; indirect evidence of binding; also binds centrosome proteins & kinetichore regions	Eves et. al. *Mol. Cell.* 2006
GRK2	Phosphorylates GPCRs and causes their uncoupling; inhibits NF-κB activity; activity is inhibited by p-RKIP	Lorenz et. al. *Nature.* (2003).
NIK	Non-canonical activator of NF-κB; induced by LT-β	Yeung K. et. al. *Mol. Cell. Biol.* (2001).
IKKα/β	Components of the complex responsible for the phosphorylation and degradation of IκB; RKIP acts as scaffold	Yeung K. et. al. *Mol. Cell. Biol.* (2001).
TAK1	Activating kinase directly upstream of IKK; RKIP acts as a scaffold and helps to facilitate its ubiquitination and subsequent phosphorylation	Yeung K. et. al. *Mol. Cell. Biol.* (2001).
TRAF6	E3 ubiquitin ligase upstream of IKK and downstream of TLR signaling; responsible for ubiquitination of TAK1; RKIP acts as scaffold	Tang et. al. *FEBS Letters* (2010).
GSK3β	GSK family members are involved in the inhibition of oncogenes that stabilize cyclins (specifically cyclin D); RKIP stabilizes GSK3β via its binding	Al-Mulla F. et. al. *Cancer Research* (2011).

CHAPTER 2

MATERIALS AND METHODS

Mice

C57BL/6 mice were purchased from Jackson Laboratory (Bar Harbor, ME, USA). $RKIP^{-/-}$ mice were engineered by the Dr. Jan Kylsik Laboratory (Department of Neuroscience, Brown University, Providence, RI, USA) (144) and received from the laboratory of Dr. Kam Yeung (Department of Biochemistry and Cancer Biology, University of Toledo, Toledo, OH, USA). Once in-house, $RKIP^{-/-}$ mice were rederived by the Gene Targeting and Transgenic Facility (GTTF) at the University of Connecticut Health Center (UCHC) following a standard protocol (145). After successful rederivation, $RKIP^{-/-}$ were bred to C57BL/6J mice to obtain wild type littermate controls. All mice at UCHC were housed in specific pathogen-free conditions and handled in accordance with institutional and federal guidelines outlined by the National Institutes of Health.

Immunizations and *in vitro* Stimulations

For SIRS induction, staphylococcal enterotoxin A (SEA; Toxin Tech; Sarasota, FL, USA) was injected at 1μg per mouse diluted in 0.2ml of BSS intraperitoneally (i.p.). 48 h later a second i.p. injection of SEA was administered and tissues harvested at 48 or 72 h after the second injection (2°). For PAMP-TLR studies, 1μg SEA was i.p. injected followed by an i.p. injection of 10μg lipopolysaccharide (LPS) derived from *Salmonella typhimurium* (Sigma-Aldrich; St. Louis, MO, USA) 18 h after SEA and tissues were harvested 12 d after SEA administration. Doses for *in vitro* stimulations with TLR ligands are as follows unless otherwise indicated: LPS 50μg/ml, CpG-A 9μg/ml, CpG-B 9μg/ml, Poly I:C 50μg/ml, Pam_3CSK_4 50μg/ml (Invivogen; San Diego, CA, USA).

Tissue Processing

Spleens were crushed through 100 μm nylon mesh strainers (Flacon/BD Biosciences; San Jose, CA, USA) and treated with ammonium chloride for 5 min at room temperature to lyse red blood cells (RBCs). Pooled peripheral lymph nodes (inguinal, axillary, and brachial) were crushed through nylon mesh strainers. Liver leukocytes were obtained as previously described (146). Briefly, livers were perfused using a solution of PBS and sodium heparin (Sigma-Aldrich) crushed through nylon mesh strainers, and separated by a 35% percoll gradient (Sigma-Aldrich). Blood was obtained from the tail veins of mice before and 1.5 h after 2° SEA administration. Blood was kept at room temperature for 30 min to allow for coagulation and then stored for 1 h at 4°C to shrink the absolute size of the clot. Samples subsequently underwent centrifugation at 13,000 rpm at 4°C for 10 min, and the upper aqueous fraction (serum) was collected and stored at -80°C until analysis.

Cell Purification and Sorting

For studies involving purified cell populations, splenocytes were isolated from tissue as described above and were subjected to depletion using MicroBeads specific for CD8, CD4, and DX5 (Miltenyi Biotec; Gladbach, Germany) and MACS LD purification columns (Miltenyi Biotec) following the manufacturer's protocol to obtain purified splenic APCs or subjected to positive selection using CD8 or CD4 MicoBeads and MACS LS purification columns (Miltenyi Biotec) to obtain purified CD8 and CD4 T cell populations. B cells were isolated using negative selection with the B cell isolation kit (Miltenyi Biotec). Purities for bead-isolated cell populations are routinely greater than 93% as assessed by flow cytometry.

Cell Culturing and Flow Cytometry

For *in vitro* restimulations, 5 x 10^5 cells were cultured at 37°C and 5% CO_2 in 0.2ml of complete tumor medium (CTM) which consists of minimal essential medium (MEM) supplemented with 10% fetal bovine serum, dextrose, salts, amino acids, and antibiotics. As indicated, cells were restimulated with 0.1μg/well SEA, 50ng/ml phorbol 12-myristate 13-acetate (PMA) (Calbiochem; Gibbstown, NJ, USA) plus ionomycin (1μg/ml) (Invitrogen; Carlsbad, CA, USA). For studies involving locostatin (Calbiochem), 5μM solutions diluted in CTM were used as the effective dose with an equal volume by percent DMSO in CTM acting as the vehicle control. These reagents were used as indicated within the corresponding figure legends. Cultures analyzed for intracellular cytokine production by flow cytometry were stimulated in culture for 4-5 h, while cultures being utilized to assess cytokine production by ELISA were stimulated overnight. The following mAbs were purchased from BD Biosciences: Phycoerythrin-conjugated TNFα, IL-10, Vβ3; Biotin-conjugated CD86; Allophycocyanin-conjugated CD44, Rat IgG2a, Rat IgG2b; FITC-conjugated Rat IgG2a, Hamster IgG; Alexa Fluor-700-conjugated CD3; PerCP-conjugated CD4, B220, Rat IgG2a; and Pacific Blue-conjugated CD8. The following mABs were purchased from eBioscience (Sand Diego, CA, USA): PE-conjugated CD11b, CD25, CD80, Rat IgG1, Rat IgG2b, Hamster IgG; Biotin-conjugated Rat IgG2a; Alexa Fluor 700-conjugated MHC-II, Rat IgG2b; APC-conjugated IFNγ, B220, Rat IgG1, Rat IgG2b; FITC-conjugated Foxp3, CD11c; PE-Cy7-conjugated Streptavidin; and PerCP-conjugated Rat IgG2a. FITC-conjugated Annexin V was purchased from BD Biosciences.

Surface and intracellular staining was performed as previously outlined (147). Briefly, cells were suspended in a wash buffer containing BSS, 3% FBS, and 0.1% sodium azide. Blockade of nonspecific binding (Fc Block) was performed by treating cells for 10 min prior to initial

extracellular antibody staining with a solution containing mouse serum, human IgG, and anti-Fc mAb 2.4G2 (148). Surface staining of approximately 1 x 10^6 cells/well was performed with the aforementioned antibodies at concentrations determined by individual titration studies, ranging from 1:50 to 1:200, for 30 min at 4°C in the dark. After incubation, cells were washed twice with wash buffer to remove any non-bound antibody and were subsequently fixed with 2% paraformaldehyde. For intracellular staining, the cells were additionally permeabilized with wash buffer containing 0.25% saponin (Sigma-Aldrich) and stained with antibodies against intracellular antigens overnight at 4°C in the dark. The following day cells were washed twice to remove any non-bound antibody. For analysis of Foxp3 containing cells, a commercially available staining buffer set from eBioscience was used. Flow cytometric analysis was conducted in the UCHC flow cytometry core on a Becton Dickinson (Franklin Lakes, NJ, USA) LSR II flow cytometer and data was analyzed using FlowJo 9.5.2 software (Tree Star; Ashland, OR, USA).

Enzyme-linked Immunosorbent Assay (ELISA)

IFNγ, IL-10, CCL2, IL-1β, and IL-2 OptEIA ELISA kits were purchased from BD Biosciences. ELISA kits for CCL3, CXCL10, and CCL5 were purchased from R&D Systems (Minneapolis, MN, USA), and IFNα and IFNβ ELISA kits were purchased from PBL Interferon Source (Piscataway, NJ, USA). All ELISAs were performed according to the manufacturer's instructions. Briefly, capture antibody (1:250 dilution) was coated overnight on MaxiSorp 96-well plates (Thermo Scientific; Rochester, NY, USA) in coating buffer (0.1 M sodium carbonate or 0.1M sodium phosphate). The following day, the plates were washed with PBS+0.05% Tween-20 and blocked with PBS+10% FBS for 1 h at room temperature. Next, the plates were washed again and incubated with supernatants from overnight cultures or from mouse sera for 2

h at room temperature. Following, the plates were washed again and incubated with a 1:250 dilution of capture antibody plus streptavidin-HRP conjugate solution for 1 h at room temperature. Finally, the plates were washed and incubated with substrate solution (tetramethylbenzidine-TMB; BD Biosciences) for 30 min in the dark and stopped with 1M phosphoric acid. Absorbance was read on a Bio-Rad iMark microplate reader (Bio-Rad; Hercules, CA, USA) and concentrations were calculated using a standard curve line of best fit on Microplate Manager Software (Bio-Rad). Mouse SAA ELISA kit was purchased from Immunology Consultants Laboratory Inc. (Portland, OR, USA) and used according to the manufacturer's protocol. All reagents, including an antibody pre-coated plate were contained within the kit. For assessment of serum LDH activity, sera were diluted 1:10 in a 96-well microtiter plate (100 µl) in tandem with a 1:2 serial dilution (11600-1.33 U/ml) of native bovine LDH standard (Cell Sciences, Canton, MA, USA). Next, 100 µl of a 1:50 mix of two colorimetric reagents from a commercially available LDH assay kit (Clontech, Mountain View, CA, USA) was added to the sera samples. Absorbance was measured every 10 min for 30 min at 490 nm (600 nm reference) and converted into activity units (U/ml) based on the prepared standard curve. Because LDH can be released from disrupted RBCs, any serum samples that showed visible signs of hemolysis were excluded from the study.

Multiplex Cytokine Analysis

Sera samples and culture supernatants were subjected to multiplex cytokine analysis using the 32-analyte Miliplex MAP kit (Millipore; Billerica, MA, USA) according to the manufacturer's instructions. This kit measures the following cytokines between 3.2 and 10,000 pg/ml and is standardized by internal quality controls: G-CSF, GM-CSF, IFNγ, IL-1α, IL-1β, IL-2, IL-3, IL-4, IL-5, IL-6, IL-7, IL-9, IL-10, IL-12 (p40), IL-12 (p70), IL-13, IL-15, IL-17, CXCL10, CXCL1,

LIF, LIX, CCL2, M-CSF, CXCL9, CCL3, CCL4, CXCL2, CCL5, TNFα, and VEGF. The Miliplex MAP kits were run using the Bio-Plex reader and software package (Bio-Rad).

Immunofluorescence Microscopy

Cells were isolated (~2 x 10^5) in PBS and affixed to 1" x 3" frosted poly-lysine coated slides (BD Falcon) using the Cytospin 4 (Thermo Shandon; Pittsburgh, PA, USA). Cells were fixed using 4% PFA in PBS at 4°C for 30 min. After fixation, the cells were washed three times in PBS and then permeabilized with 0.3% Triton X-100 in PBS for 20 min at room temperature. Next, the cells were washed again as before and then blocked using 10% naïve goat serum and 0.2% BSA in PBS for 10 min at room temperature. After blocking, the cells were incubated in the dark overnight at 4°C in a humidified chamber using a FITC-conjugated anti-RKIP antibody (Biorbyt; Cambridge, UK) or FITC-conjugated rabbit-anti mouse isotype control at several concentrations. The next day, the cells were washed again as before and then mounted using Vectasheild mounting medium (Vector Labs; Burlingame, CA, USA) containing DAPI. Slides were visualized using the Axioplan 2 inverted fluorescence microscope (Carl Zeiss; Thornwood, NY, USA).

Quantitative Real-Time Polymerase Chain Reaction

Total RNA was isolated from cells (~3 x 10^6) using the Qiagen RNeasy Mini kit (Qiagen Inc: Valencia, CA, USA) according to the manufacturer's instructions. Total RNA was quantified using the NanoDrop 2000 (Thermo Scientific) spectrophotometer and then 250ng-1μg RNA was reverse transcribed using the iScript cDNA synthesis kit (Bio-Rad). Next, transcript levels for IRF3 (fwd. GAGAGCCGAACGAGGTTCAG, rev. CTTCCAGGTTGACACGTCCG), IRF5 (fwd. GGTCAACGGGGAAAAGAAACT, rev. CATCCACCCCTTCAGTGTACT), IRF7 (fwd.

GAGACTGGCTATTGGGGGAG, rev. GACCGAAATGCTTCCAGGG), TRAF3 (fwd. CAGCCTAACCCACCCCTAAAG, rev. TCTTCCACCGTCTTCACAAAC), MDA-5 (fwd. AGATCAACACCTGTGGTAACACC, rev. CTCTAGGGCCTCCACGAACA), TBK1 (fwd. ACTGGTGATCTCTATGCTGTCA, rev. TTCTGGAAGTCCATACGCATTG), IKKε (fwd. ACCACTAACTACCTGTGGCAT, rev. CCTCCCCGGATTTCTTGTTTC), IFNAR1 (fwd. AGCCACGGAGAGTCAATGG, rev. GCTCTGACACGAAACTGTGTTTT), IFNα (fwd. CCTGATGGTCTTGGTGGTGAT, rev. CAGTTCCTTCATCCCGACCAG), IFNβ (fwd. AGCTCCAGCTCCAAGAAAGGACGAACAT, rev. GCCCTGTAGGTGAGGTTGATCT), and actin (fwd. GTGGGCCGCTCTAGGCACCA, rev. CTCTTTGATGTCACGCACGA) were determined from cDNA using the SYBR Green PCR Master Mix kit (Life Technologies; Grand Island, NY, USA) on an ABI 7300 Real-Time PCR system (Applied Biosystems by Life Technologies). The primer sequences were chosen from those previously validated in PrimerBank (149) (Center for Computational and Integrative Biology, Harvard Medical School, Cambridge, MA, USA) and were purchased from Integrated DNA Technologies (Coralville, IA, USA). Relative fold changes between experimental and control groups were determined using the $\Delta\Delta C_T$ method.

RNA Sequencing and Pathway Analyses

Total RNA was isolated as before and sent to Otogenetics Crp. (Atlanta, GA, USA) for next generation RNA-sequencing. RNA was sequenced using the HiSeq 2000 platform (Illumina inc., San Diego, CA, USA) at a depth of 20 million reads and analyzed using both proprietary software capable of handling Illumina based scripts, and differential expression of FPKM (fragments per kilobase mapped) normalized data was determined using the public domain software: Cufflinks (UC Berkeley, Johns Hopkins University, Cal Tech). Genes of interest were

identified by taking all genes that were found to be statistically significantly different between experimental groups and had a relative fold change of $> \pm 1.2$. These genes of interest were next subjected to functional pathway analysis using the IPA knowledge database (Ingenuity Systems; Redwood City, CA, USA). IPA cross-references a user's list of genes of interest to known canonical signaling pathways and determines the level of enrichment of a given pathway using the user's gene list and fold changes. IPA then calculates a *P* value based on this enrichment using Fisher's exact test. Functional pathway analysis by IPA was also confirmed using the Database for Annotation, Visualization and Integrated Discovery (DAVID) (Laboratory of Immunopathogenesis and Bioinformatics, Frederick, MD, USA) (150).

Oxygen Consumption Rate (OCR) Measurements

Cells were seeded at a concentration $3x10^5$/well in an XF96 tissue culture plate (Seahorse Bioscience; North Billerica, MA) that had been coated with BD Cell-TAK (BD Biosciences) overnight to improve adherence of non-adherent cells. Cells were cultured in DMEM supplemented with 25mM glucose, 2 mM glutamine, and 1mM pyruvate. Basal, maximum and reserve OCR was measured using the Seahorse XF 96 extracellular flux analyzed (Seahorse Biosciences), and mitochondrial function was tested using the following reagents: oligomycin (1μM), FCCP (2μM), rotenone (1μM) and antimycin (1μM).

Immunoblot

Whole cell lysates were generated using a solution consisting of 50mM Tris-HCl, 150mM NaCl, 5mM EDTA, 5mM EGTA, 10mM NaF, 0.5% Triton X-100, and 0.5% n-ocytl-β-D-glucopyranoside. To prevent nucleic acid contamination, the whole cell lysis buffer was supplemented with DNAse (0.67μg/μl) and RNAse (0.33μg/μl). Additionally the phosphatase

inhibitor sodium orthovanadate (1mM) was added to prevent loss of phosphorylated proteins. Cell lysates were centrifuged at 25,000 x g for 10 min at 4°C. Subsequently, lysates were resolved on 4-15% SDS-PAGE (Bio-Rad) at 100V for 60 min and the transferred to 0.2μm nitrocellulose membranes (Bio-Rad) by semi-dry transfer at 25 V for 60 min at 4°C. Membranes were blotted with antibodies for the following antigens: RKIP, p44/p42 ERK, ERK-1 (Cell Signaling Technologies, Danvers, MA, USA), and Actin (Sigma-Aldrich) at 1:1000 in blocking grade milk solution overnight at 4°C. Next, membranes were washed thrice with PBS + 0.1% Tween-20 and blotted with goat anti-rabbit conjugated to horseradish peroxidase (Santa Cruz Biotechnologies, Santa Cruz, CA, USA) at 1:1000 in blocking grade milk solution at room temperature for 2-4 h. Finally, membranes were washed again as before and visualized using ECL chemiluminescence (GE Healthcare Biosciences; Piscataway, NJ, USA). For subcellular fractionation studies, nuclear and cytoplasmic lysates were generated using the NE-PER reagent kit (Thermo Scientific, Waltham, MA, USA) following the manufacturer's instructions. Densitometric quantification of immunoblots was conducted using GeneTools software (Syngene; Federick, MD, USA).

PF 2D Proteomics

PF 2D lystaes were generated by lysing ~ 50 x 10^6 purified splenic B cells using a lysis buffer consisting of: 7.5 M urea, 2.5 M thiourea, 12.5% glycerol, 62.5 mM Tris-HCl, 2.5% n-octyl β-D-glucopyranoside, 6.25 mM TCEP, 1.25 mM protease inhibitor mixture (Sigma-Aldrich) and centrifuged at 25,000 × g for 1 h at 18°C. Subsequently, the buffer used for cell lysis was exchanged using PD-10 columns (GE Healthcare Biosciences) equilibrated with PF 2D start buffer (6M Urea, 25 mM Bis-Tris, 0.2% n-ocytl- β-D-glucopyranoside). Next, the complex protein sample was quantified by bicinchoninic acid (BCA) Protein Assay Kit (Thermo

Scientific; Rockford, IL, USA). Proteomic samples (2 mg) were injected into the Beckman Coulter ProteomeLab PF 2D platform (Beckman Coulter; Brea, CA, USA) and subjected to two-dimensional protein fractionation. First, the complex protein mixture was fractionated over a ProteoSep HPCF column (Eprogen; Downers Grove, IL, USA) by isoelectric focusing with a linear gradient between pH 8.0 and 4.0. Before first dimension fractions were purified further, the fraction collector/injector (FC/I) apparatus was cleaned with a series of washes: 1) 100% H_2O, 2) 50% NH_4OH, 3) 100% H_2O, 4) 50% methanol, 5) 100% H_2O, and 6) 100% start buffer. This allows for an increased level of quality control prior to second dimension fractionation. Next, each of these corresponding fractions was further purified over a ProteoSep HPRP column (Eprogen) with a 0-100% acetonitrile + 0.8% trifluoroacetic acid gradient at 50°C that separates proteins based on their hydrophobicity. Protein spectra were generated with UV light measured at 214 nm and fractions were collected in 0.5 min intervals into 96-deep well plates and stored at −80°C. Proteomic maps for each sample were created using ProteoView software (Beckman Coulter) and maps between groups were analyzed for regions of similarity (signatures) and dissimilarity (fingerprints) using the DeltaView/MultiView software package (Beckman Coulter). It is projected that fractions of interest will be boiled at 100°C for 10 min and further resolved by 4-15% SDS-PAGE and stained using Oriole fluorescent protein stain (Bio-Rad). Any bands correlating to proteomic differences between groups will be excised from the gel and sent for subsequent analysis and identification by matrix-assisted laser desorption/ionization time of flight (MALDI-TOF) and liquid chromatography-tandem mass spectrometry (LC/MS/MS).

Statistical Analysis

Unpaired, two-tailed Student's *t* tests were performed with $P < 0.05$ representing statistical significance in all figures except Figure 3-1B (paired, two-tailed Student's *t* test). For tests

involving unequal standard deviations between groups, Welch's correction was used. Homogeneity of variance was determined by *F* test, with $F > 0.05$ as a threshold for equal variance. *F*-tests were performed using Microsoft Excel 2010 software (Microsoft; Redmond, WA, USA) and *P* values were determined using GraphPad Prism 6.01 (GraphPad Software; LaJolla, CA, USA).

CHAPTER 3

RKIP CONTRIBUTES TO IFNγ SYNTHESIS BY $CD8^+$ T CELLS AFTER SERIAL TCR TRIGGERING IN SYSTEMIC INFLAMMATORY RESPONSE SYNDROME

Kyle T. Wright and Anthony T. Vella. *The Journal of Immunology*. July 15th, 2013, 191: 708-716.

ABSTRACT

Systemic inflammatory response syndrome (SIRS) is associated with the development of severe medical complications including progression to multiple organ dysfunction syndrome and even death. To date, only marginal improvements in terms of therapeutic options have been established for patients affected by SIRS. Raf kinase inhibitor protein (RKIP) is a regulator of MAPK and NF-κB signaling cascades which are both critical for production of the proinflammatory cytokines responsible for SIRS initiation. By testing a T cell dependent mouse model of SIRS which utilizes staphylococcal enterotoxin A (SEA) specific for $V\beta3^+$ T cells, we show that RKIP is necessary for the exaggerated production of IFNγ from SIRS splenocytes. This effect was not due to differences in T cell expansion, IL-10 production, or APC priming, but rather a cell intrinsic defect lying downstream of the T cell receptor in SEA-specific $CD8^+$ T cells. Importantly, mice lacking RKIP were still able to proliferate, survive, and contribute to cytokine production in response to PAMP-TLR mediated stimuli, despite the TCR-dependent defects seen in our SIRS model. Finally, by blocking RKIP in wild type SIRS splenocytes, the IFNγ response by $CD8^+$ $V\beta3^+$ T cells was significantly diminished. These data suggest that RKIP may be a potential therapeutic target in SIRS by curbing effector cytokine production from $CD8^+$ T cells during serial TCR triggering.

INTRODUCTION

Systemic inflammatory response syndrome (SIRS) results from the general release of large quantities of proinflammatory cytokines into circulation. This cytokine storm has the potential to lead to many clinical complications for patients including respiratory failure from acute respiratory distress syndrome, gastrointestinal bleeding, anemia, deep vein thrombosis, metabolic abnormalities, hypotension, disseminated intravascular coagulopathy, multiple organ dysfunction syndrome, and many times death (26, 151, 152). SIRS can be prompted from many initiators including infectious and non-infectious etiologies. These triggers range from uncontrolled bacterial, viral, and fungal infections to pathogenic toxin exposure, organ ischemia, trauma, autoimmune disorders, pancreatitis, hemorrhage, and substance abuse. Several studies have shown that between 30-60% of all hospital admissions meet the clinical diagnostic criteria for SIRS (27, 153). Even though not all patients that meet these criteria progress to severe sequelae, SIRS remarkably carries a baseline mortality rate of ~7%, which climbs to >40% if the patient develops symptoms of shock (27). Taken together, it is no surprise that SIRS is a both a widespread and costly problem for health care systems nationally and globally (154).

Despite affecting a large number of patients, few therapeutics exist for SIRS. Clinical trials attempting to inhibit inflammatory factors such as TNFα and IL-1β failed to show significant efficacy (155, 156). A current therapeutic regimen typically involves an antimicrobial agent, if an infection is present, medications to restore cardiac and respiratory abnormalities if needed, and a broadly immunosuppressive corticosteroid (157, 158). Using drugs that inhibit beneficial inflammatory responses in patients that have either concomitant infections or increased susceptibility due to hospitalization is likely to be counterproductive.

SIRS is very difficult to study in humans because the onset and progression is rapid, and it is likely challenging to enroll patients that are acutely ill into clinical studies. Also, because of its heterogeneity of origins, no unified mouse model of SIRS exists. We sought to utilize a model system that was clinically relevant to human disease, which contained a known trigger of human SIRS that followed the natural history of the disease in terms of its acute onset and patterns of systemic cytokine release. One model incorporating these important facets of human SIRS is exposure to staphylococcal enterotoxin A (SEA). SEA is produced by the human pathogen *Staphylococcus aureus,* and other *S. aureus* enterotoxins, like toxic shock syndrome toxin-1 (TSST-1), induce rapid release of proinflammatory cytokines into the systemic circulation in significant quantities and importantly, can cause SIRS in humans (159, 160). This robust cytokine storm is mediated by the rapid expansion and activation of T cells that specifically bear the Vβ3 chain of the T cell receptor (161). In addition, exposure to these superantigens has explicitly illustrated many other aspects of SIRS pathology including the induction of acute lung injury after vascular damage (140, 162, 163) as well as transient immunosuppression similar to the compensatory anti-inflammatory response syndrome (CARS) seen in a number of SIRS patients (152, 164, 165).

The major cytokine network in SIRS involves production of proinflammatory factors, such as IL-6, IFNγ, and TNFα, which are dependent on the NF-κB and the MAPK signaling pathways (166, 167). It is critical to discover ways to modulate these cascades in order to control SIRS without affecting immunocompentence. Raf kinase inhibitor protein (RKIP) negatively regulates these pathways by binding and inhibiting the kinase activities of several important signaling factors including Raf, MEK, ERK, TRAF6, TAK1, NIK, and IKKα/β (132, 133, 168, 169). RKIP has

also been associated with metastatic disease in many human cancers including prostate (170) and breast (171), but its role in the immune system is undefined.

Here we report that serial triggering of the T cell receptor with SEA models many aspects of human SIRS and identifies IFNγ as a potential intersection between the damage associated with SIRS and the diminished inflammation seen in CARS. This is illustrated by the fact that wild type T cells continue to make IFNγ in SIRS even if they fail to make IL-2, and thus retain the capability to potentiate disease. Importantly, RKIP is shown to be a critical player in these processes because genetic loss of this protein prevents the ability of specific T cells to make exorbitant amounts of IFNγ while only moderately affecting the anti-inflammatory cytokine, Interleukin-10. In addition, by inhibiting RKIP using the small molecule inhibitor locostatin (172), IFNγ production was blocked in wild type SIRS T cells. The data herein suggest that RKIP may be a key therapeutic target for dampening the robust inflammation seen in SIRS while preserving the CARS response.

RESULTS

RKIP drives IFNγ production in mice undergoing SIRS

Systemic Inflammatory Response Syndrome is associated with significant morbidity and mortality in patients, and results from the exorbitant release of inflammatory factors from immune cells (152). To study and model human SIRS in mice, we used a regimen involving multiple administrations of Staphylococcal enterotoxin A (SEA) that induces potent T cell expansion by 48 h (173) and systemic proinflammatory cytokine production (Fig. 3-1A). To verify that we had indeed prompted systemic inflammation, serum from mice 90 min after the secondary administration of SEA was used to measure IFNγ, IL-6, SAA, and LDH. These cytokines were chosen since they are considered prognostic markers for SIRS in human patients (174-177). As expected, significantly increased levels of IFNγ, IL-6, SAA, and LDH were detected in sera after SEA (Fig. 3-1B).

To determine if RKIP played a role in a SIRS response, we compared the cytokine output of SIRS and naïve splenocytes restimulated *in vitro* with SEA from RKIP$^{-/-}$, wild type littermates, and C57BL/6J mice at the height of the SIRS response. Splenocytes from all mice stimulated with SEA *in vivo* produced decreased levels of IL-2 when compared to naïve controls, signifying that the T cells in these cultures were anergic or immunosuppressed similar to CARS T cells. However, the production of the effector cytokine IFNγ was increased dramatically in wild type mice relative to naïve, but maintained or reduced in mice lacking RKIP, suggesting that RKIP may play a role in the optimal production of IFNγ during a SIRS response (Fig. 3-1C). Figure 3-1D shows that in each individual experiment the C57BL/6 splenocytes, from now on referred to as wild type unless otherwise specified, produced substantially more IFNγ in SIRS mice versus

naïve. The RKIP$^{-/-}$ SIRS splenocytes did not make increased IFNγ levels over their naïve counterparts in this overnight culture.

To investigate the reason for reduced IFNγ production seen in Figure 3-1C/D, we phenotyped primary and secondary lymphoid organs from naïve RKIP$^{-/-}$ mice and determined that there were no underlying deficits in T cell, B cell, NK cell, or CD11b^{+} antigen presenting cell (APC) populations (Fig. 3-2A), as well as important thymic subsets (Fig. 3-3A). Also, we found that there were no deficiencies in baseline cytokine production potential of IFNγ in a multitude of lymphoid organs (Fig. 3-2B). Next, we hypothesized that the reduced IFNγ production could be due to a reduction in the expansion of SEA-specific (Vβ3^{+}) T cells. No difference in either SEA-specific CD8^{+} or CD4^{+} splenic T cells by percentage or total number after SIRS induction was detected (Fig. 3-4A/B). Based on these results we hypothesized that reduction in IFNγ production might be T cell intrinsic.

SEA-specific CD8^{+} T cells are responsible for suboptimal IFNγ production in RKIP$^{-/-}$ mice

To test our hypothesis suggesting that if the lower levels of IFNγ were due to a defect in a specific cell type or if it was generalized amongst all splenocytes, we harvested splenocytes from naïve and SIRS induced RKIP$^{-/-}$ and wild type mice and examined IFNγ production in specific cell populations by flow cytometry after a short-term (4 h) *in vitro* restimulation with SEA (Fig. 3-5A). After SIRS induction there was a marked decrease in the percentage of IFNγ producing CD8^{+} Vβ3^{+} T cells from RKIP$^{-/-}$ mice compared to wild type (Fig. 3-5B). Furthermore, of the CD8^{+} Vβ3^{+} T cells producing IFNγ, RKIP$^{-/-}$ cells produced lower amounts compared to wild type cells when using mean fluorescence intensity as a measurement (Fig. 3-5C). This defect in IFNγ production was not observed in SEA-specific CD4^{+} T cells (Fig. 3-5B/C), bystander T

cells, or in splenic non-T cell populations (data not shown). Importantly, naïve T cells did not produce IFNγ in these short-term cultures, as opposed to the overnight stimulation in Figure 1. Perhaps this is due to the IFNγ gene locus not having sufficient time to open and translate IFNγ mRNA into protein in 4 h. These data suggest that the suboptimal IFNγ production seen in RKIP$^{-/-}$ SIRS splenocytes is due to a cell intrinsic defect specifically in CD8^{+} Vβ3^{+} T cells.

Because of the reduced IFNγ production by CD8^{+} Vβ3^{+} T cells, we tested if higher levels of the anti-inflammatory cytokine Interleukin-10 (IL-10) could explain this result, since there is a known reciprocity between these cytokines (178). IL-10 can be induced by *S. aureus* enterotoxins (179) and T regulatory cells (Tregs) proficiently synthesize this suppressive cytokine (180), thus they were examined during SIRS in our model. Tregs from SIRS-induced RKIP$^{-/-}$ mice had a decreased propensity to synthesize IL-10 during stimulation with PMA + ionomycin when compared to wild type controls (Fig. 3-6A, left panel). This was not due to a difference in the percentage of Tregs between groups (Fig. 3-6A, right panel) or a baseline alteration in IL-10 production potential from naïve Tregs (Fig. 3-6B). Interestingly, when whole splenocytes from RKIP$^{-/-}$ and wild type mice were restimulated with SEA and compared for IL-10 induction, a slight, but not statistically significant, reduction was seen in the RKIP$^{-/-}$ group (Fig. 3-6C). This implies that other cell types within the spleen have the ability to compensate, to a degree, for the loss of IL-10 production in Tregs during SIRS associated inflammation.

SIRS CD8^{+} RKIP$^{-/-}$ T cells have an intrinsic signaling defect that lies downstream of the T cell receptor

In order to better localize the lesion that was responsible for suboptimal IFNγ production from RKIP$^{-/-}$ CD8^{+} Vβ3^{+} T cells after TCR-triggering, we wanted to determine if these cells ever had

the potential to make IFNγ or not. Therefore, we tested RKIP$^{-/-}$ and wild type splenocytes after initiation of SIRS with PMA + ionomycin restimulation as opposed to SEA. The defect in IFNγ production by RKIP$^{-/-}$ SIRS CD8^{+} Vβ3^{+} T cells was no longer apparent (Fig. 3-7A, upper panel). Furthermore, there was also no longer a difference in the release or secretion of IFNγ between RKIP$^{-/-}$ and wild type splenocytes after PMA + ionomycin stimulation (Fig. 3-7B). Hence, the signaling defect seen in RKIP$^{-/-}$ SIRS CD8^{+}, but not SIRS CD4^{+}, T cells most likely lies downstream of TCR engagement, but upstream of the factors induced by Ca^{2+} influx and phorbol esters.

Blockade of RKIP using the small molecule inhibitor locostatin greatly diminishes IFNγ production from wild type CD8^{+} T cells in SIRS

In order to test the therapeutic potential of RKIP blockade in SIRS, we restimulated 48 h post-SIRS induction splenocytes from wild type mice overnight with SEA or PMA + ionomycin in the presence of locostatin or vehicle control. The optimal effective dose of locostatin was chosen based on titration studies which elicited a dose that showed both a biological effect while leaving the vast majority of T cells viable, even after overnight stimulation (Fig. 3-8A/B). As in RKIP$^{-/-}$ SIRS splenocytes, inhibition of RKIP function with locostatin significantly decreased IFNγ production after TCR re-triggering with SEA, but not after PMA + ionomycin restimulation, suggesting once again that RKIP is playing a role downstream of the TCR (Fig. 3-7C).

Because SEA crosslinks T cells with APCs, we investigated whether the loss of IFNγ production was due to poor APC presentation. First, we assessed expression of MHC II and the costimulatory molecules CD80/CD86 on splenic APC populations and found no difference between RKIP$^{-/-}$ and wild type littermate controls (Fig. 3-9A/B). Additionally, we isolated APCs

and $CD8^+$ T cells from the spleens of $RKIP^{-/-}$ and wild type littermate mice 48 h after SIRS induction. We then restimulated cultures of $RKIP^{-/-}$ APCs and wild type (or $RKIP^{-/-}$) $CD8^+$ T cells overnight with SEA and unlike stimulation of the intact splenocyte population (Fig. 3-1) we observed no difference in IFNγ production (data not shown). Thus, in order to rule out any unappreciated developmental defect that may have confounded these results, we isolated APCs and $CD8^+$ T cells from spleens of C57BL/6 mice 48 h after SIRS induction and treated them separately with either locostatin or vehicle *in vitro* for 1 h. Cells were washed twice to remove residual locostatin or vehicle, untreated APCs or $CD8^+$ T cells were added, and restimulated overnight with SEA. We observed that by pre-treating wild type $CD8^+$ SIRS T cells with locostatin, IFNγ production was diminished to 30% of untreated or vehicle treated controls (Fig. 3-7D). However, blocking RKIP in APCs before restimulation had little effect of IFNγ output, once again suggesting that RKIP is playing a role at the level of the T cell and can be therapeutically targeted to diminish IFNγ responses from $CD8^+$ T cells during SIRS.

$RKIP^{-/-}$ T cells retain the ability to mount an effective response to PAMP-TLR mediated stimuli

Because $RKIP^{-/-}$ SIRS $CD8^+$ T cells have an intrinsic defect downstream of TCR triggering, we hypothesized that $RKIP^{-/-}$ cells may also have difficulty with proliferation, survival, and cytokine production during a vaccination response. In order to address this question, we replaced the second *in vivo* administration of SEA in our SIRS induction model with the vaccine adjuvant lipopolysaccharide (LPS) (Fig. 3-10A). This model mimics a standard vaccination protocol which results in the expansion and survival of SEA-specific T cells, which become Th1-like cells (147). We found no difference in the survival of $CD4^+$ $V\beta3^+$ or $CD8^+$ $V\beta3^+$ T cells between $RKIP^{-/-}$ and wild type in terms of percentage or total number at day 12 after SEA-LPS

immunization. This was seen in both spleen (Fig. 3-10B, Table 3-1) and liver (Fig. 3-10D, Table 3-1), as well as in pooled peripheral lymph nodes (Table 3-1). Also, there were no observable differences in contraction of SEA-specific cells after SEA immunization alone (Table 3-1). These data are consistent with the lack of changes in clonal expansion during the SIRS model seen in Figure 3-4. Unexpectedly, when cells were harvested from the spleen and liver at day 12 post immunization and restimulated *in vitro* with SEA overnight, $RKIP^{-/-}$ cells now made equal or greater amounts of IFNγ (Fig. 3-10C/E). These results were also recapitulated when cells were restimulated with plate-bound anti-CD3 acting as the TCR-trigger instead of SEA, although a slight reduction in IL-2 production was seen in this instance (Fig. 3-3B). Importantly these data suggest that, although $RKIP^{-/-}$ $CD8^{+}$ T cells have a defect in effector cytokine production during SIRS mediated inflammation, they can still expand, survive, and contribute to effector cytokine production in response to PAMP-TLR mediated reactions.

DISCUSSION

SIRS is an extensive and profound burden on the U.S. healthcare system (153). One well known cause of SIRS induction is exposure to superantigens, most famously TSST-1 enterotoxin from *Staphylococcus aureus* which was directly responsible for many cases of toxic shock syndrome in the 1980s. TSST-1 and SEA bypass canonical antigen processing and activate a large percentage of the T cell repertoire by cross-linking β-chain variable regions, specifically Vβ3, of the T cell receptor (TCR) to constant domains of the major histocompatibility complex on APCs (126). T cells are critically important for mediating SIRS because they can directly release proinflammatory factors themselves and potentiate the inflammatory and destructive effects of innate immune cells (160). In fact IFNγ, an important T cell effector cytokine, has been shown to be necessary for certain clinical sequelae of SIRS including acute lung injury (ALI) (163). By utilizing a T cell-dependent model of SIRS we sought to identify proteins that could alter cytokine production in T cells, thus lessening the inflammatory response at several different levels. We show that RKIP represents a new, and potentially valuable, therapeutic target since its inhibition curbs IFNγ synthesis without shutting down responses to PAMPs. From a mechanistic perspective, we demonstrate that $CD8^+$ T cells may be a spring for cytokine production during a SIRS response, and have demonstrated that RKIP is coupled to continued IFNγ potential in anergic or immunosuppressed $CD8^+$ T cells.

However, like all animal models, SEA exposure does not recapitulate all aspects of human SIRS perfectly. As with many inflammatory mouse models, especially ones on the C57BL/6 genetic background, most are resistant to the typical symptomology seen in human SIRS patients (i.e. fever, lethargy, malaise, hypovolemia, organ dysfunction, death). This may be due to inflammatory reactions in humans and mice eliciting different genetic responses to burns,

trauma, or endotoxemia, all of which trigger SIRS (181). Nevertheless, we feel that this model provides at least a reasonable starting point to analyze potential molecular targets that can modify systemic inflammatory responses.

The NF-κB and MAPK pathways are both critical for the production of proinflammatory cytokines (166, 167) and RKIP has been previously shown to be a negative regulator of these pathways. RKIP imparts control by interfering with the kinase activities of several signaling factors in these cascades. Little is known regarding the *in vivo* effects of RKIP, especially within the immune system. Based on the findings of these previous studies, we anticipated that mice lacking RKIP would be more prone to exaggerated cytokine production during T cell activation, but contrary to our hypothesis we found that RKIP was actually important for enhancing IFNγ production in $CD8^+$ SIRS T cells after serial triggering of the TCR with SEA (Figs. 3-1,3-5). This is critical because SEA induces a SIRS response in mice that results in T cells that are anergic (characterized by their failure to produce IL-2 (182), but can continue to perpetuate inflammation due to their ability to make IFNγ in large quantities. On a molecular level we showed that RKIP is playing a role in the signaling machinery downstream of the TCR, as evidenced by the fact that the diminished IFNγ production from $CD8^+$ T cells lacking RKIP was rescued if the TCR is bypassed using PMA and ionomycin (Fig. 3-7). Interestingly, expansion of these T cells, which is another critical process mediated by MAPK signaling, was unaltered in our model of SIRS (Fig. 3-4). This implies that RKIP's role within effector T cells may be more critical for cytokine output rather than proliferation.

Currently, no choice drug exists for the treatment of SIRS. Therapy focuses on treating specific infections, if one is present, in combination with therapies that stabilize the respiratory and cardiovascular systems if a patient has signs of shock (157). Clinical trials centered on

antagonizing the function of TNFα and IL-1β failed to show efficacy (28); however, our data suggests that perhaps inhibiting the effects of IFNγ may be a better therapeutic strategy. The only treatment to target the robust inflammation of SIRS that has shown marginally better outcomes is the usage of low-dose steroids like hydrocortisone (183). This therapeutic approach is broadly immunosuppressive, thereby minimizing inflammatory reactions that are advantageous to the host, such as productive responses to vaccines or pathogens. This is critical for a patient pool that might be afflicted with established bacterial, viral, or fungal infections. Nevertheless, this is in contrast to patients suffering from autoimmunity where steroid-mediated suppression of the immune system would provide beneficial effects with a diminished risk of infection compared to SIRS. However, an ideal therapeutic for either scenario would be one which dampens the inflammatory effects of T cells that are being chronically stimulated through the TCR (e.g. enterotoxins in SIRS or self-antigen in autoimmunity) while leaving advantageous immune responses, such as to a vaccine or new infection, largely intact.

RKIP may be one potential molecule that, if targeted, could possibly achieve these optimal therapeutic goals. For example, when RKIP is absent from the immune system, or when therapeutically targeted, effector T cells, serially triggered through their TCR, produce significantly less IFNγ than wild type while impinging only marginally on overall IL-10 production (Fig. 3-6). In addition, when the TCR is engaged only once *in vivo* and adjuvanted with TLR stimulation from LPS, splenocytes synthesize normal levels of IFNγ (Fig. 3-10). Thus, it is possible that blockade of RKIP could diminish IFNγ production from effector T cells during SIRS while permitting a relatively unabated response to PAMPs. Although, it remains to be determined what would occur in a complex response where both serial TCR triggering and PAMP-TLR mediated stimuli both exist simultaneously or what the exact role, if any, that RKIP

plays in these responses. Finally, therapeutically targeting RKIP may provide a substantial benefit over direct inhibition of IFNγ because it allows for the alleviation of IFNγ effects at the level of synthesis rather than receptor binding. This may be especially important in acute SIRS where it could be too late to impact disease outcomes once IFNγ has been produced.

Although our data suggests that a loss of RKIP leads to a T cell intrinsic defect in optimal IFNγ production, it still does not exclude the possibility of potential T cell extrinsic effects as well. In fact in 2006, Schuierer and colleagues showed that RKIP expression may play a role in appropriate macrophage and dendritic cell differentiation (138). Since APCs are critical for the activation of T cells in response to classically presented antigens, as well as superantigens, any deficit in APC function could also impart effects onto cytokine production from T cells. We show that RKIP is playing a role at the level of the $CD8^+$ T cell in responses to superantigens because inhibition of RKIP in APCs specifically had no effect on IFNγ production, but inhibition in $CD8^+$ T cells did (Fig. 3-7D). Also, if T cell extrinsic effects such as this were playing a large role in our model systems, we would have expected to see little or no response in our SEA-LPS studies, which was not the case. However, this does not explicitly rule out a potential extrinsic defect in response to MHC-restricted peptide antigens that must undergo canonical processing and presentation within APCs.

Another facet that makes RKIP a unique therapeutic target is that it is a druggable protein. A small molecule inhibitor of RKIP, locostatin, is available (184). Locostatin exerts its inhibitory effects on RKIP by alkylating a conserved histidine residue (His86) within its ligand-binding pocket (172). Modification of this residue prevents RKIP from binding to its aforementioned ligands, thus preventing their inhibition. In addition to abating IFNγ production from wild type cells during SIRS (Fig. 3-7C), locostatin also potently blocks IFNγ and TNFα production upon

triggering mouse OT-I or human antigen-specific T cells against influenza with cognate peptide and human PBMCs treated with LPS (140). However, the specificity of this inhibitor is still being investigated as it has several potential off target effects (184). Furthermore, the target analyses for locostatin have largely been conducted in immortalized cell lines (185), and thus, the exact mechanism of how it mediates its inhibitory effects within an *in vivo* immunological system remains unclear. This allows significant room for improvement in developing better target-specific inhibitors of RKIP before use in a clinical setting. Nevertheless, our new data pin points a locostatin effect on $CD8^+$ T cells, but not APCs, in response to the pathogenic enterotoxin SEA (Fig. 3-7D). In sum, our data suggests that RKIP represents a potentially new therapeutic target for reducing the effects of IFNγ from $CD8^+$ effector T cells during the serial TCR triggering events in SIRS.

ACKNOWLEDGEMENTS

We would like to thank Drs. Antoine Ménoret and Sanjeev Kumar for their intellectual contributions and help conducting several experiments. We are also grateful to Drs. Adam Adler, Robert Clark, and Francisco Sylvester for their helpful discussions and feedback.

Footnotes

1 This work was supported by National Institute of Health grants R01-AI042858 and Project 3 PO1-AI05172 to A.T.V and K.T.W. was supported by T32-AI007080.

[2] Nonstandard abbreviations used in this article: ALI, Acute Lung Injury; CARS, Compensatory Anti-inflammatory Response Syndrome; CTM, Complete Tumor Medium; RKIP, Raf Kinase Inhibitor Protein; SEA, Staphylococcal Enterotoxin A; SIRS, Systemic Inflammatory Response Syndrome; TSST-1, Toxic Shock Syndrome Toxin-1.

Figure 3-1: RKIP is necessary for optimal production of IFNγ by splenocytes during SIRS. (A) Schematic of SIRS induction protocol. (B) Serum was isolated from C57BL/6 mice before 1° SEA and 90 min post 2° SEA treatment, and then quantified for IL-6, IFNγ, SAA, and LDH by ELISA. Data are from 3 independent experiments, N=5-8/group. (C) Splenocytes from C57BL/6J, WT littermate, and $RKIP^{-/-}$ mice were harvested 72 h after 2° SEA as depicted in Figure 1A. 5 x 10^5 cells/well were stimulated overnight with 0.1μg SEA, supernatants were collected and analyzed for IFNγ and IL-2 by ELISA. Data are from 5 independent experiments, N=10-13/group, are expressed as a percent change from naïve splenocytes cultured and stimulated similarly. (D) Absolute values of IFNγ for C57BL/6J and $RKIP^{-/-}$ from each independent experiment in Figure 1C with Standard Error of the Mean (SEM). *P* values were determined by unpaired *t* test between groups in Figure 3-1C/D and by paired *t* test in Figure 3-1B **P*<0.05, ***P*<0.01, ****P*<0.001, *****P*<0.0001.

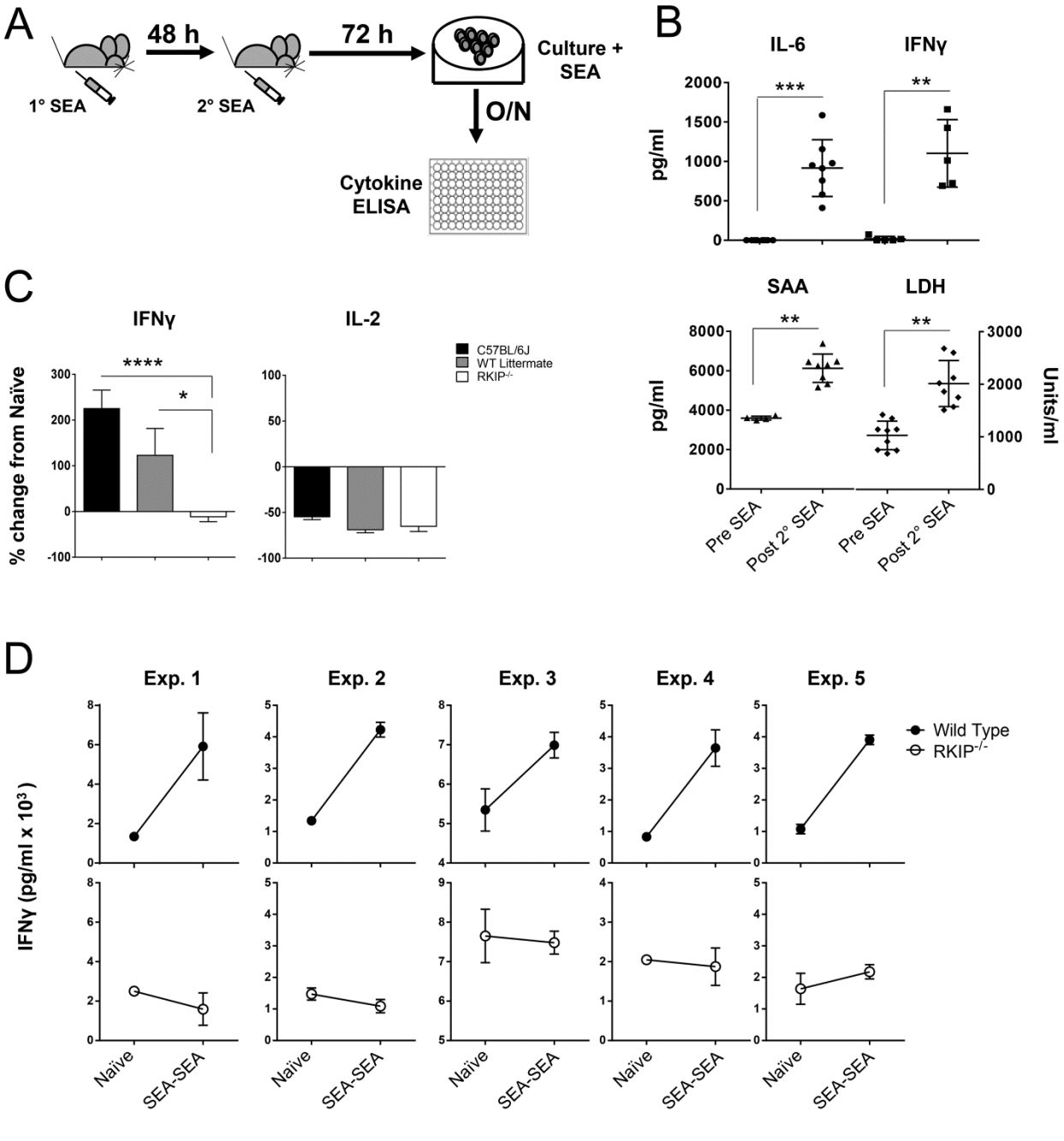
A
48 h
72 h
1° SEA
2° SEA
Culture + SEA
O/N
Cytokine ELISA
B
IL-6
IFNγ
pg/ml
***
**
C
IFNγ
IL-2
% change from Naïve
****
*
C57BL/6J
WT Littermate
RKIP-/-
SAA
LDH
pg/ml
Units/ml
Pre SEA
Post 2° SEA
D
Exp. 1
Exp. 2
Exp. 3
Exp. 4
Exp. 5
IFNγ (pg/ml x 10³)
Wild Type
RKIP-/-
Naïve
SEA-SEA

Figure 3-2: RKIP-/- mice show no overt developmental deficits in important immunological cell populations. (A) Cells from spleen, inguinal lymph node (ILN), axillary lymph node (ALN),and mesenteric lymph node (MLN) were isolated from 4 week and 11 week old RKIP-/- and wild type littermate mice. Cells populations were phenotyped by flow cytometric analysis. Data are from 3 independent experiments, N=8 mice/group. Error bars represent SEM. *P<0.05. **RKIP-/- mice show no overt defects in baseline cytokine production potential**. (B) Cells from in Figure 3-2A were stimulated in vitro with PMA + Ionomycin including Brefeldin A for 4 h. After stimulation, cells were analyzed by intracellular cytokine staining. Data are from 3 independent experiments, N=8 mice/group. Error bars represent SEM. *P<0.05, **P<0.01.

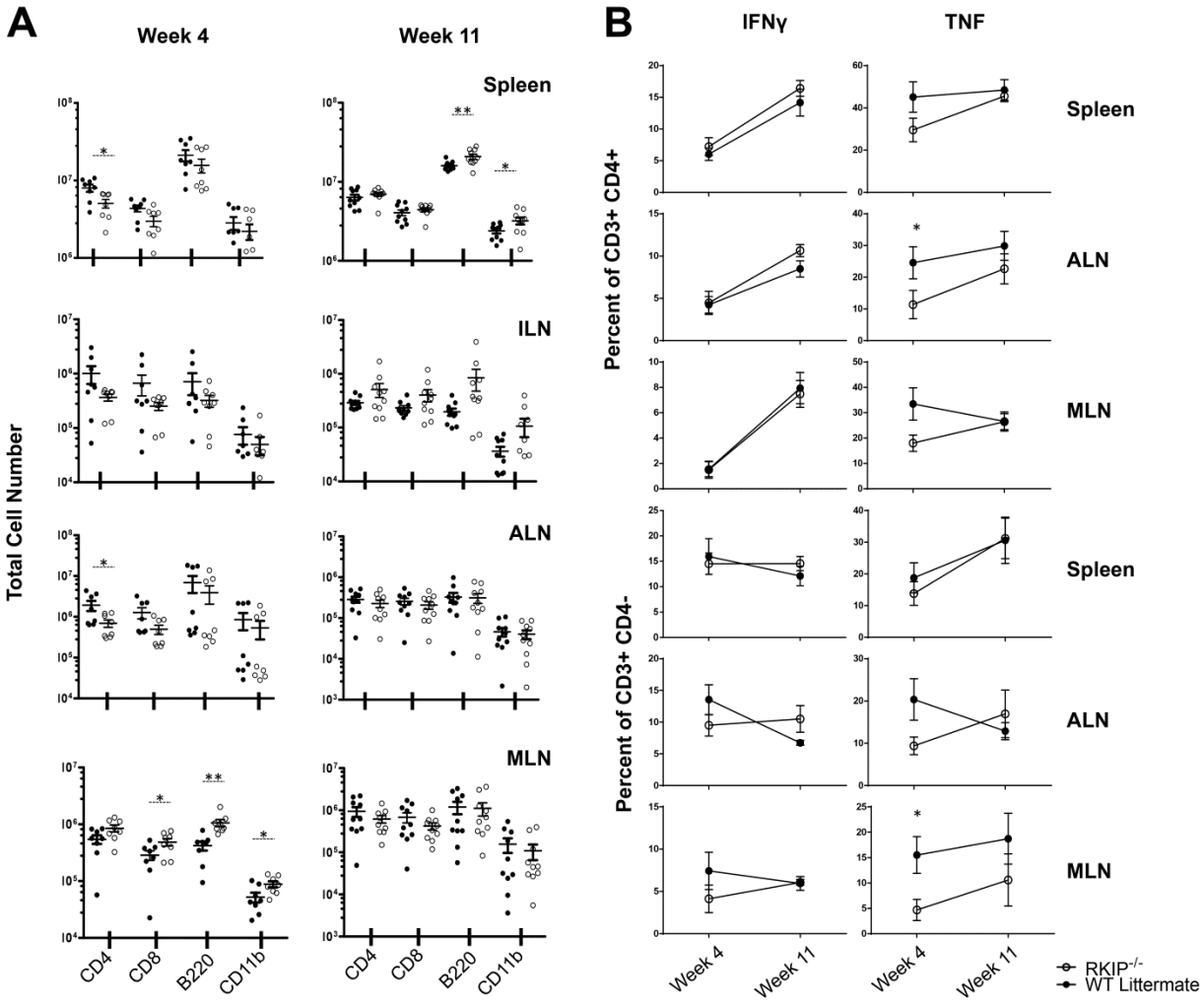
A
Week 4
Week 11
Spleen
ILN
ALN
MLN
Total Cell Number
CD4
CD8
B220
CD11b
B
IFNγ
TNF
Percent of CD3+ CD4+
Percent of CD3+ CD4-
Spleen
ALN
MLN
Week 4
Week 11
RKIP-/-
WT Littermate

Figure 3-3: RKIP-/- mice show no loss of Thymic T cell populations. (A) Thymocytes from Figure 3-2 mice were isolated and stained directly ex vivo for CD3, CD4, CD8, CD25, and CD44 to determine important thymocyte populations by flow cytometric analysis. Error bars represent SEM. *P* values determined by unpaired t test between groups. **Plate bound anti-CD3 restimulation as a substitute TCR-trigger during SEA-LPS vaccination shows IFNγ production is unaltered in RKIP-/- splenocytes**. (B) Cells from spleen and liver in Figure 3-10 were harvested, treated, and analyzed as in Figure 3-10C and Figure 3-10E respectively. Error bars represent SEM. *P* values determined by unpaired t test between groups $*P<0.05$.

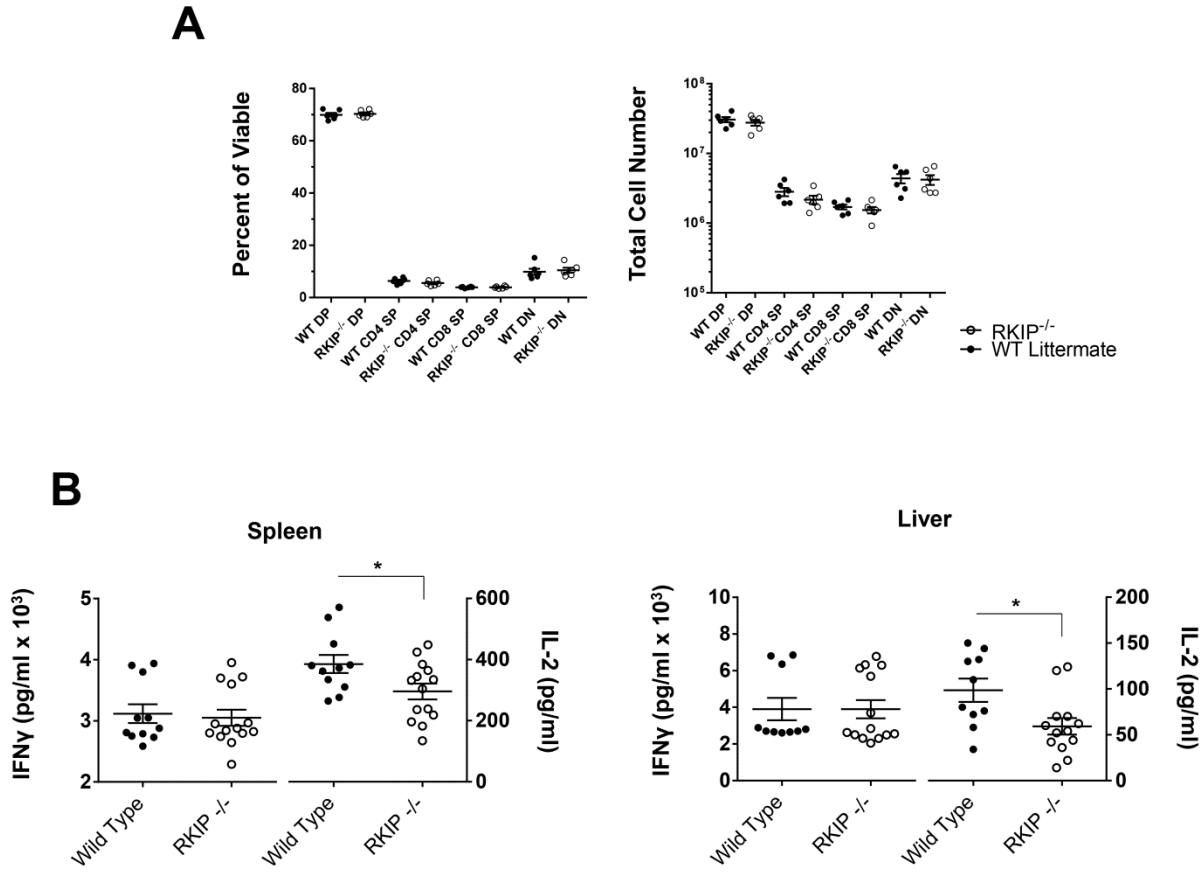
A
Percent of Viable
Total Cell Number
WT DP
RKIP-/- DP
WT CD4 SP
RKIP-/- CD4 SP
WT CD8 SP
RKIP-/- CD8 SP
WT DN
RKIP-/- DN
RKIP-/-
WT Littermate
B
Spleen
Liver
IFNγ (pg/ml x 10^3)
IL-2 (pg/ml)
Wild Type
RKIP -/-
*

Figure 3-4: Reduced IFNγ production in RKIP$^{-/-}$ mice during SIRS is not due to reduced expansion of SEA-specific Vβ3^{+} T cells. (A) Splenocytes from C57BL/6J and RKIP$^{-/-}$ mice were harvested 72 h after 2° SEA as depicted in Figure 3-1A, stained directly *ex vivo* with antibodies against CD3, CD4, CD8, and Vβ3, and CD3^{+} CD8^{+} or CD3^{+} CD4^{+} T cells were gated to determine the percent Vβ3^{+} T cells in spleen. (B) Total cell numbers of Vβ3^{+} T cells from spleen. Data in Figure 3-4A-B are from 5 independent experiments, N=15-16/group. Error bars represent SEM and *P* values were determined by unpaired *t* test between groups.

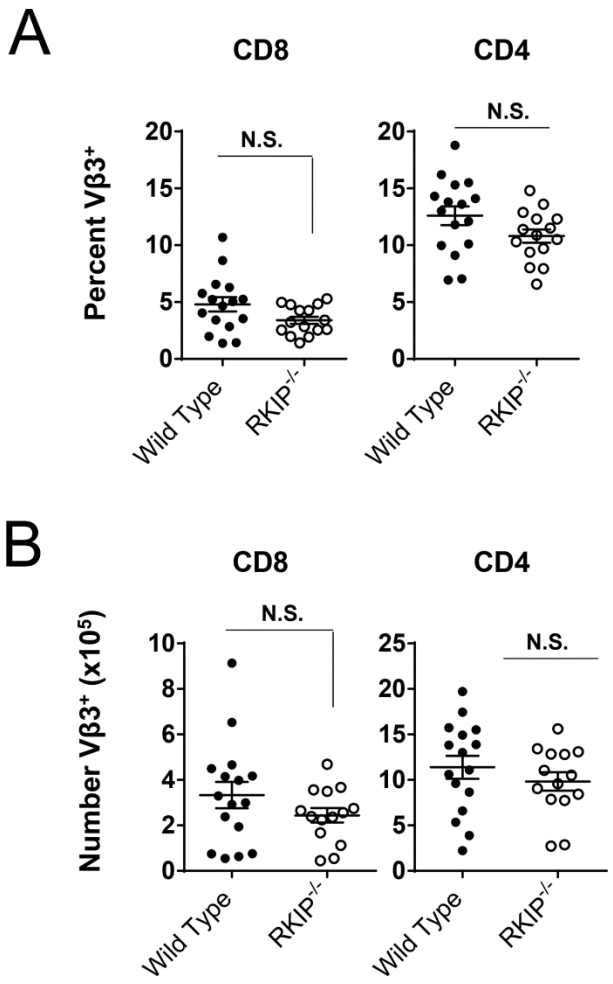
A
CD8
CD4
N.S.
N.S.
Percent Vβ3+
20
15
10
5
0
Wild Type
RKIP-/-
B
CD8
CD4
N.S.
N.S.
Number Vβ3+ (x10^5)
10
8
6
4
2
0
25
20
15
10
5
0
Wild Type
RKIP-/-

Figure 3-5: SEA-specific $CD8^+$ effector T cells are responsible for suboptimal IFNγ production in $RKIP^{-/-}$ mice. (A) Gating strategy for flow cytometric analysis utilized in Figure 3B-C. (B) Splenocytes were harvested as described in Figure 3-1A and restimulated *in vitro* with 0.1μg of SEA/well + Brefeldin A for 4 h. After restimulation, cells were analyzed by intracellular cytokine staining for IFNγ production. Data are plots from a representative experiment displaying median values. (C) The left panels show the mean +/- SEM of IFNγ-producing T cells and (right panels) display Mean Fluorescence Intensity (MFI) of $IFN\gamma^+$ T cells. Data are from 3 independent experiments, N=8 mice/group. Error bars represent SEM and *P* values were determined by unpaired *t* test between groups $*P<0.05$.

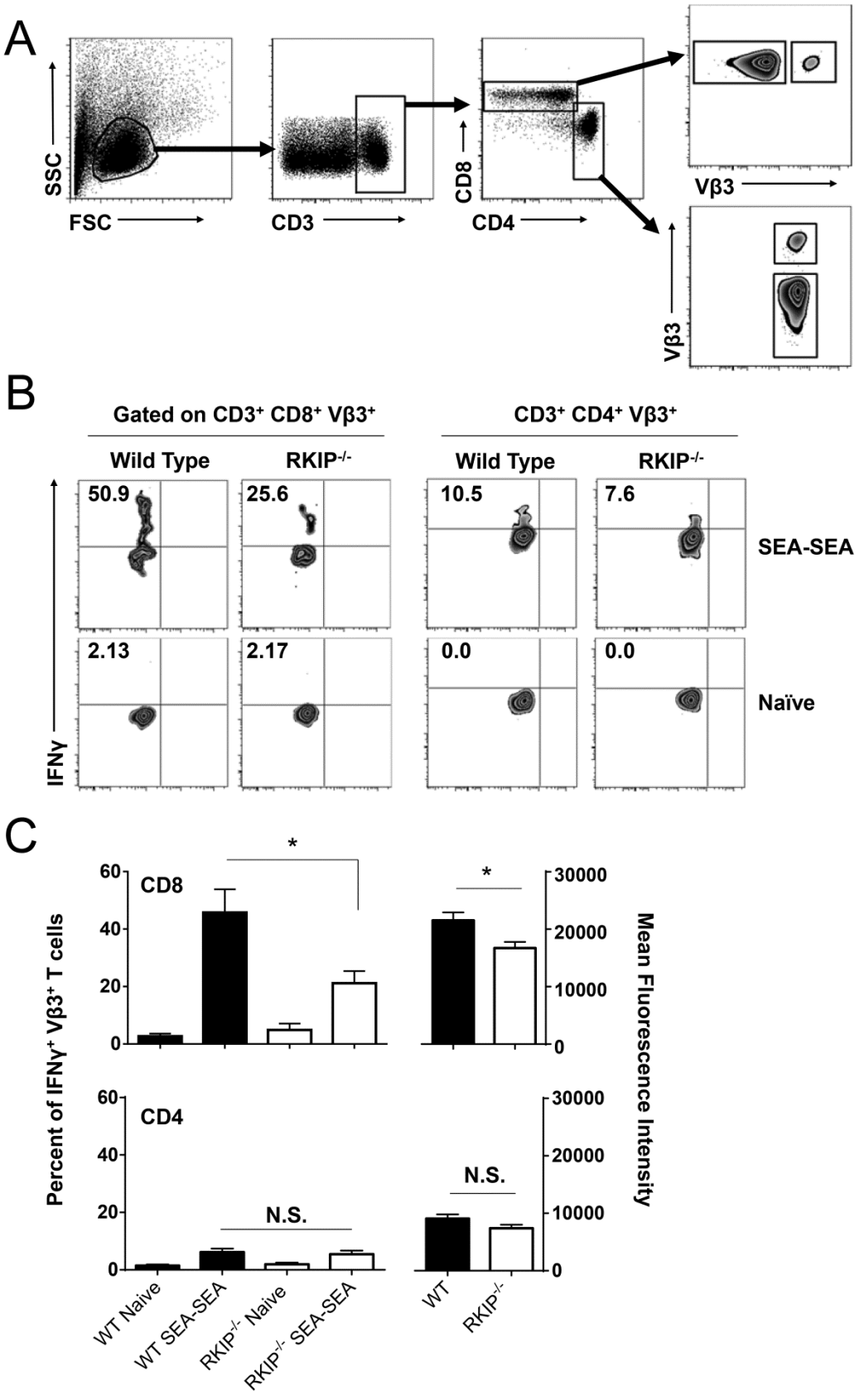
A
SSC
FSC
CD3
CD8
CD4
Vβ3
Vβ3
B
Gated on CD3+ CD8+ Vβ3+
CD3+ CD4+ Vβ3+
Wild Type
RKIP-/-
Wild Type
RKIP-/-
50.9
25.6
10.5
7.6
SEA-SEA
2.13
2.17
0.0
0.0
Naïve
IFNγ
C
CD8
CD4
*
*
N.S.
N.S.
Percent of IFNγ+ Vβ3+ T cells
Mean Fluorescence Intensity
60
40
20
0
30000
20000
10000
0
WT Naive
WT SEA-SEA
RKIP-/- Naive
RKIP-/- SEA-SEA
WT
RKIP-/-

Figure 3-6: Tregs from RKIP$^{-/-}$ mice during SIRS show reduced IL-10 production. (A) Splenocytes were harvested as outline in Figure 3-1A and restimulated *in vitro* with PMA + ionomycin including Brefeldin A for 4 h. After restimulation, cells were surfaced phenotyped with antibodies against CD3, CD4, and Foxp3, stained intracellularly for IL-10 production, and cells were then analyzed by flow cytometry. Data are from 2 independent experiments, N=5-6/group. (B) Splenocytes were harvested from 4 week and 11 week old naïve RKIP$^{-/-}$ mice or wild type littermates (see Fig. 3-2). 5 x 10^5 cells/well were stimulated *in vitro* with PMA + ionomycin including Brefeldin A for 4 h then surface phenotyped with antibodies specific to CD3, CD4, and Foxp3, and stained intracellularly for IL-10 production. Data are from 3 independent experiments, N=10/group. (C) Supernatants from Figure 3-1 were analyzed for IL-10 production by ELISA. Data are expressed as a percentage change from naïve splenocytes cultured and stimulated similarly. As in Figure 3-1, data are from 5 independent experiments, N=10-13/group. Error bars represent SEM and *P* values determined by unpaired *t* test between groups *$P<0.05$.

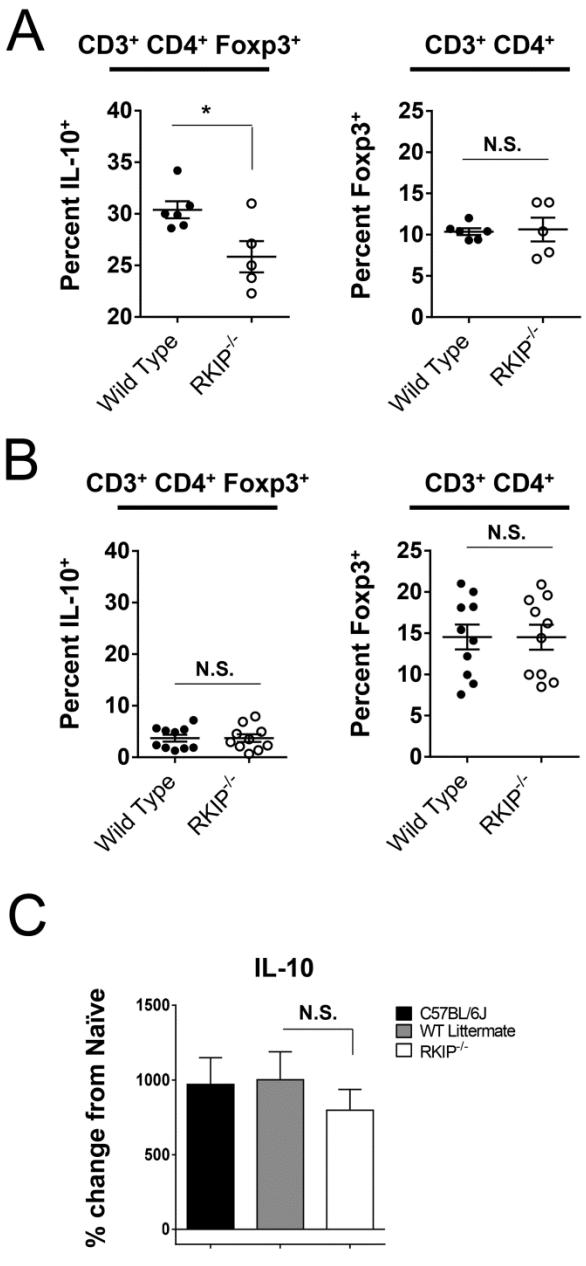
A
CD3+ CD4+ Foxp3+
CD3+ CD4+
Percent IL-10+
Percent Foxp3+
*
N.S.
40
35
30
25
20
25
20
15
10
5
0
Wild Type
RKIP-/-
B
CD3+ CD4+ Foxp3+
CD3+ CD4+
Percent IL-10+
Percent Foxp3+
N.S.
N.S.
40
30
20
10
0
25
20
15
10
5
0
Wild Type
RKIP-/-
C
IL-10
% change from Naïve
N.S.
1500
1000
500
0
C57BL/6J
WT Littermate
RKIP-/-

Figure 3-7: SEA-specific $CD8^+$ effector T cells lacking RKIP have an intrinsic signaling defect that lies downstream of the T cell receptor. (A) Splenocytes from Figure 3-5 were restimulated *in vitro* for 4 h with PMA + ionomycin including brefeldin A and then stained with antibodies against CD3, CD4, CD8, Vβ3, and IFNγ, followed by flow cytometric analysis. Data are from 3 independent experiments, N=8/group. (B) Splenocytes were harvested as in Figure 3-7A and cultured overnight (5×10^5/well) with PMA + ionomycin. Subsequently, supernatants were collected and analyzed for IFNγ production by ELISA. Data are from 2 independent experiments, N=6/group. (C) 48 hr post-SIRS induction splenocytes from C57BL/6J mice were isolated and restimulated overnight with SEA or PMA + ionomycin in the presence of medium alone, vehicle alone (DMSO), or 5μM locostatin. The supernatants from these cultures were then analyzed for IFNγ production by ELISA. The grey dotted line represents SEA (or PMA + ionomycin) restimulation without locostatin or vehicle. Data are from 3 independent experiments, N=9/group. (D) Isolated and magnetic bead purified APC and $CD8^+$ T cell populations from C57BL/6J mice 48 hr after SIRS induction were treated separately with either 5μM locostatin or vehicle for 1 hr. Subsequently, cells were washed twice with medium to remove any residual locostatin or vehicle present, and then untreated APCs or CD8+ T cells (in a 1:1 ratio) were added to these cultures and restimulated overnight with 0.1μg SEA. As controls, cultures of untreated APCs and $CD8^+$ T cells containing locostatin or vehicle for the entire duration were stimulated in parallel. The supernatants of these overnight cultures were then assessed for IFNγ production by ELISA. The grey dotted line represents untreated APCs and $CD8^+$ T cells stimulated with SEA alone. Data are from 3 independent experiments, N=10-11/group. Error bars represent SEM and *P* values determined by unpaired *t* test between groups.

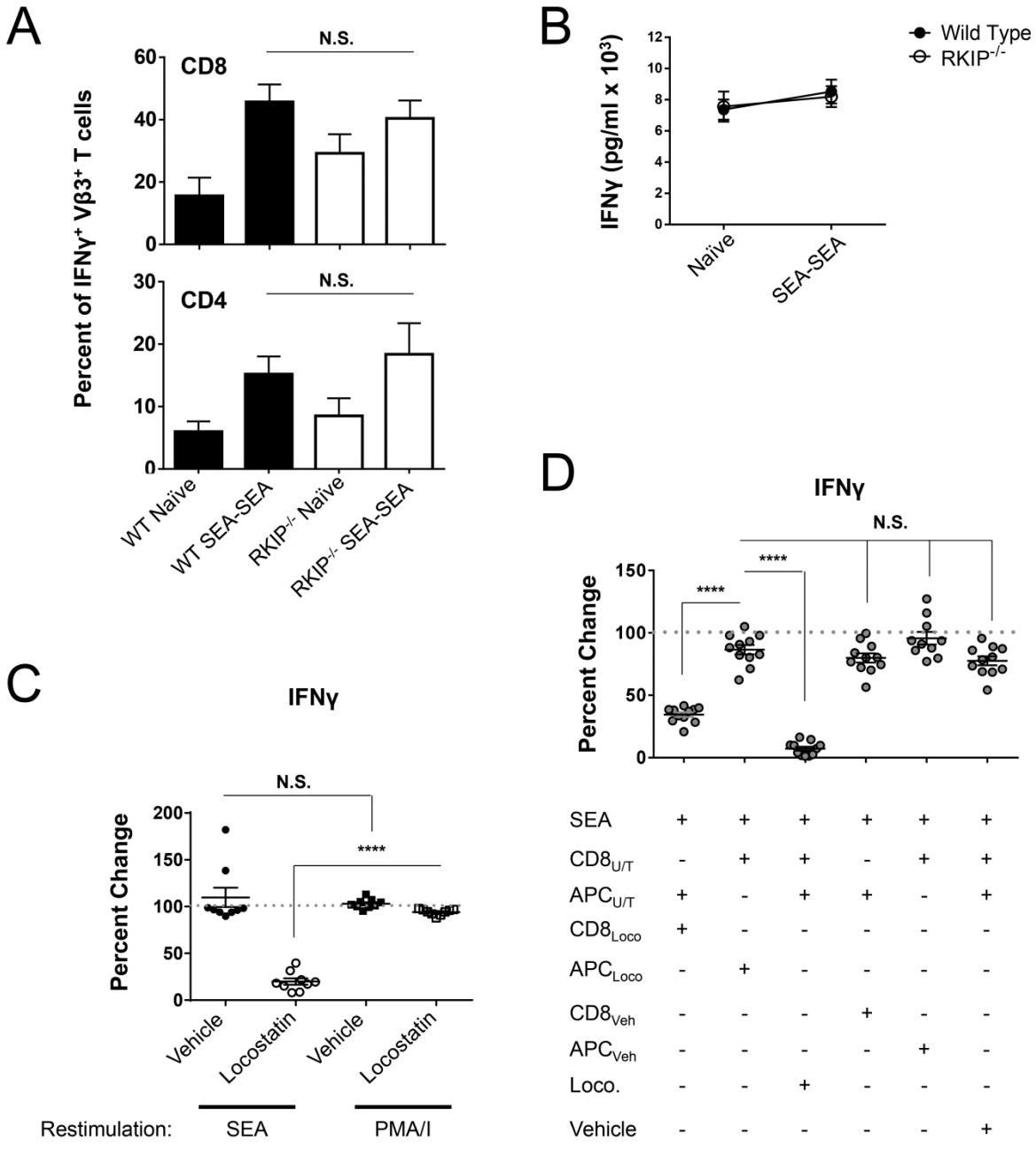
A
CD8
CD4
N.S.
Percent of IFNγ+ Vβ3+ T cells
WT Naïve
WT SEA-SEA
RKIP-/- Naïve
RKIP-/- SEA-SEA
B
Wild Type
RKIP-/-
IFNγ (pg/ml x 10³)
Naïve
SEA-SEA
C
IFNγ
Percent Change
Vehicle
Locostatin
Restimulation:
SEA
PMA/I
D
IFNγ
Percent Change
SEA
CD8U/T
APCU/T
CD8Loco
APCLoco
CD8Veh
APCVeh
Loco.
Vehicle

Figure 3-8: Blockade of RKIP with the small molecule inhibitor locostatin abates IFNγ production from SEA restimulated wild type SIRS splenocytes. (A) 48 h post-SIRS induction splenocytes from C57BL/6J mice were harvested as described in Figure 3-1A and restimulated them overnight with SEA or PMA + ionomycin in the presence of medium alone, vehicle alone (DMSO), or a titration of locostatin (0.5 - 50μM). The supernatants from these cultures were then analyzed for IFNγ production by ELISA. **Low dose locostatin (5μM) shows both a biological effect on IFNγ production while leaving the bulk of T cells viable, even after overnight stimulation.** (B) Splenocytes from cultures in Figure 3-8A were stained for CD3 and Annexin V in order to assess viability by flow cytometry.

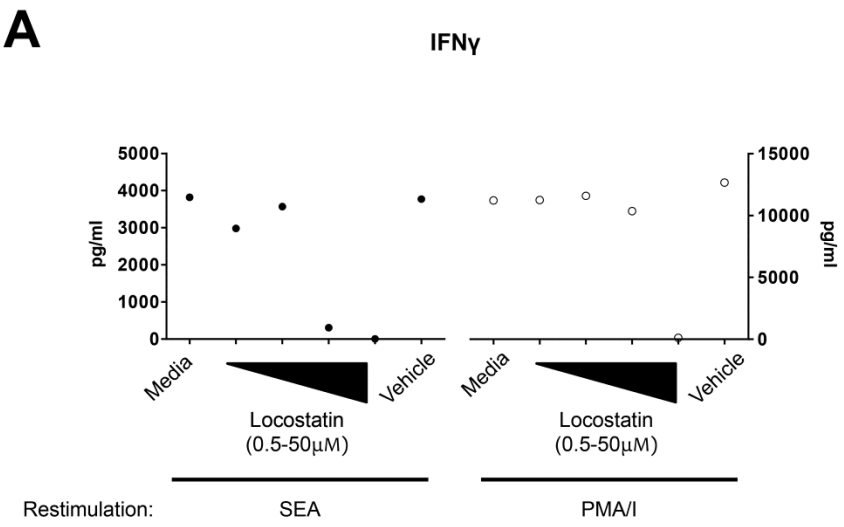
A
IFNγ
5000
4000
3000
2000
1000
0
pg/ml
15000
10000
5000
0
pg/ml
Media
Vehicle
Locostatin
(0.5-50μM)
Media
Vehicle
Locostatin
(0.5-50μM)
Restimulation:
SEA
PMA/I

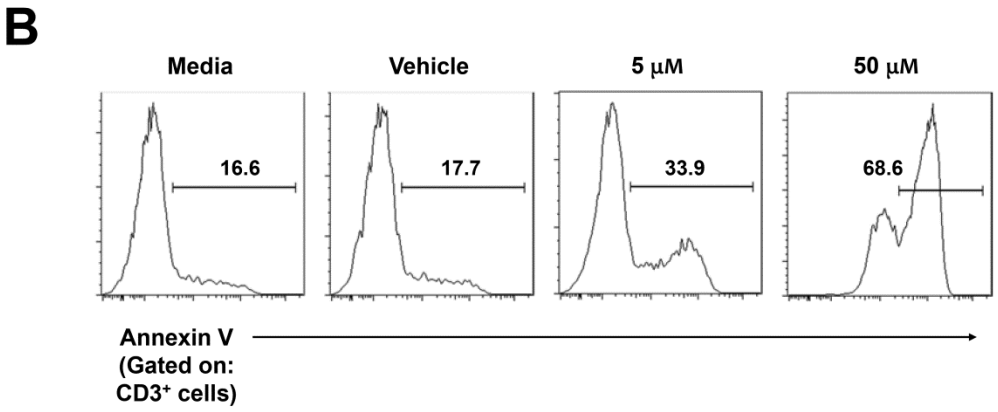
B
Media
Vehicle
5 μM
50 μM
16.6
17.7
33.9
68.6
Annexin V
(Gated on:
CD3+ cells)

Figure 3-9: RKIP-/- SIRS mice have no quantitative differences in splenic APC populations compared to wild type. (A) 48 h post-SIRS induction splenocytes were harvested from RKIP-/- and wild type littermates and stained for B cells (B220) and different macrophages and dendritic cells (CD11b, CD11c) populations. Error bars represent SEM (N=7-11, 3 independent experiments). **RKIP-/- splenic APC populations exhibit no differences in MHC-II expression, or the costimulatory molecules CD80/86 compared to wild type**. (B) APC populations from Figure 3-9A were stained and analyzed by flow cytometry for MHC-II (AF700), CD80 (PE), and CD86 (Biotin-PECy7) surface expression. Error bars represent SEM (N=7-11, 3 independent experiments).

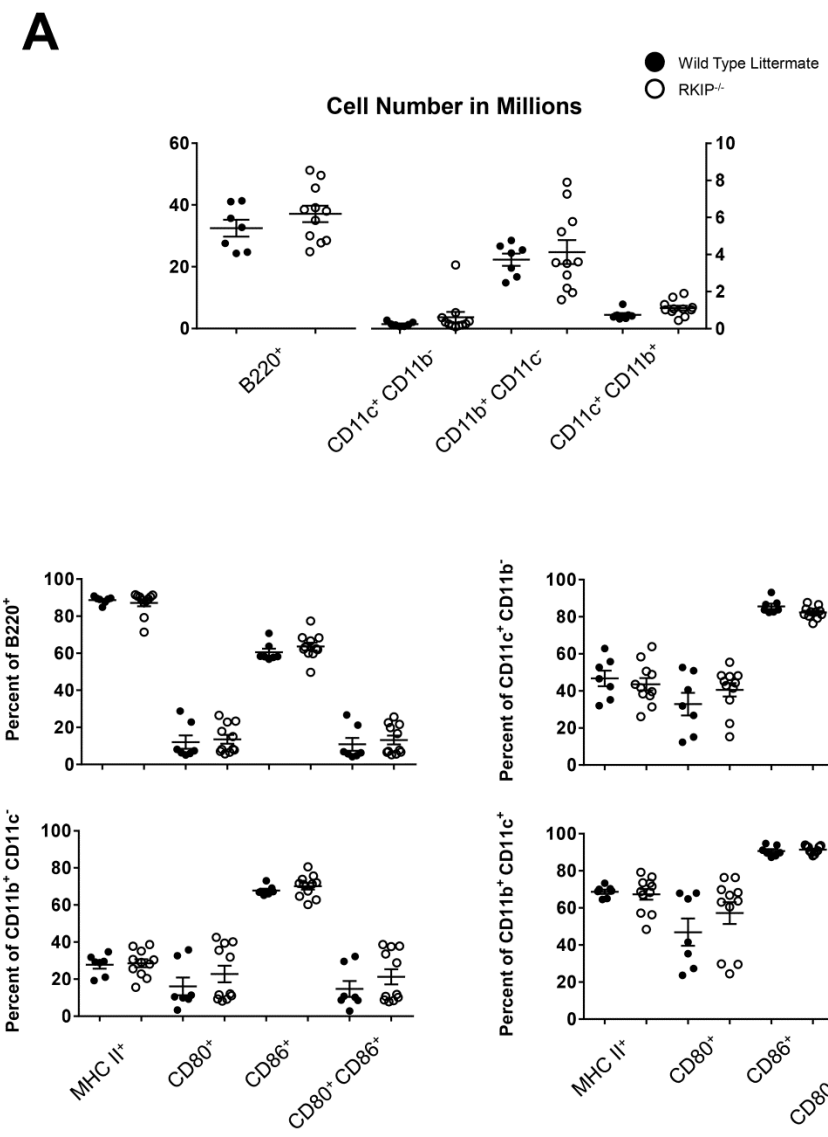
A
Wild Type Littermate
RKIP-/-
Cell Number in Millions
60
40
20
0
10
8
6
4
2
0
B220+
CD11c+ CD11b-
CD11b+ CD11c-
CD11c+ CD11b+
B
Percent of B220+
Percent of CD11c+ CD11b-
Percent of CD11b+ CD11c-
Percent of CD11b+ CD11c+
100
80
60
40
20
0
MHC II+
CD80+
CD86+
CD80+ CD86+

Figure 3-10: RKIP$^{-/-}$ T cells can expand, survive, and contribute to cytokine production in response to PAMP-TLR mediated stimuli. (A) Schematic representation of immunization protocol. (B) Splenocytes were harvested at 12 d post immunization with LPS as outlined in Figure 3-10A and stained directly *ex vivo* for SEA-specific (Vβ3^{+}) T cells as outlined in Figure 3-5A. Data are from 3 independent experiments, N=11-14/group. (C) Splenocytes were harvested as in Figure 3-10A and cultured (5 x 10^5/well) overnight with 0.1μg SEA. The next day, IFNγ and IL-2 levels in supernatants were measured by ELISA. Data are from 3 independent experiments, N=11-14/group. (D) Liver leukocytes were harvested, treated, and analyzed as in Figure 3-10B. (E) Liver leukocytes were harvested, treated, and analyzed as in Figure 3-10C. Error bars represent SEM and *P* values determined by unpaired *t* test between groups.

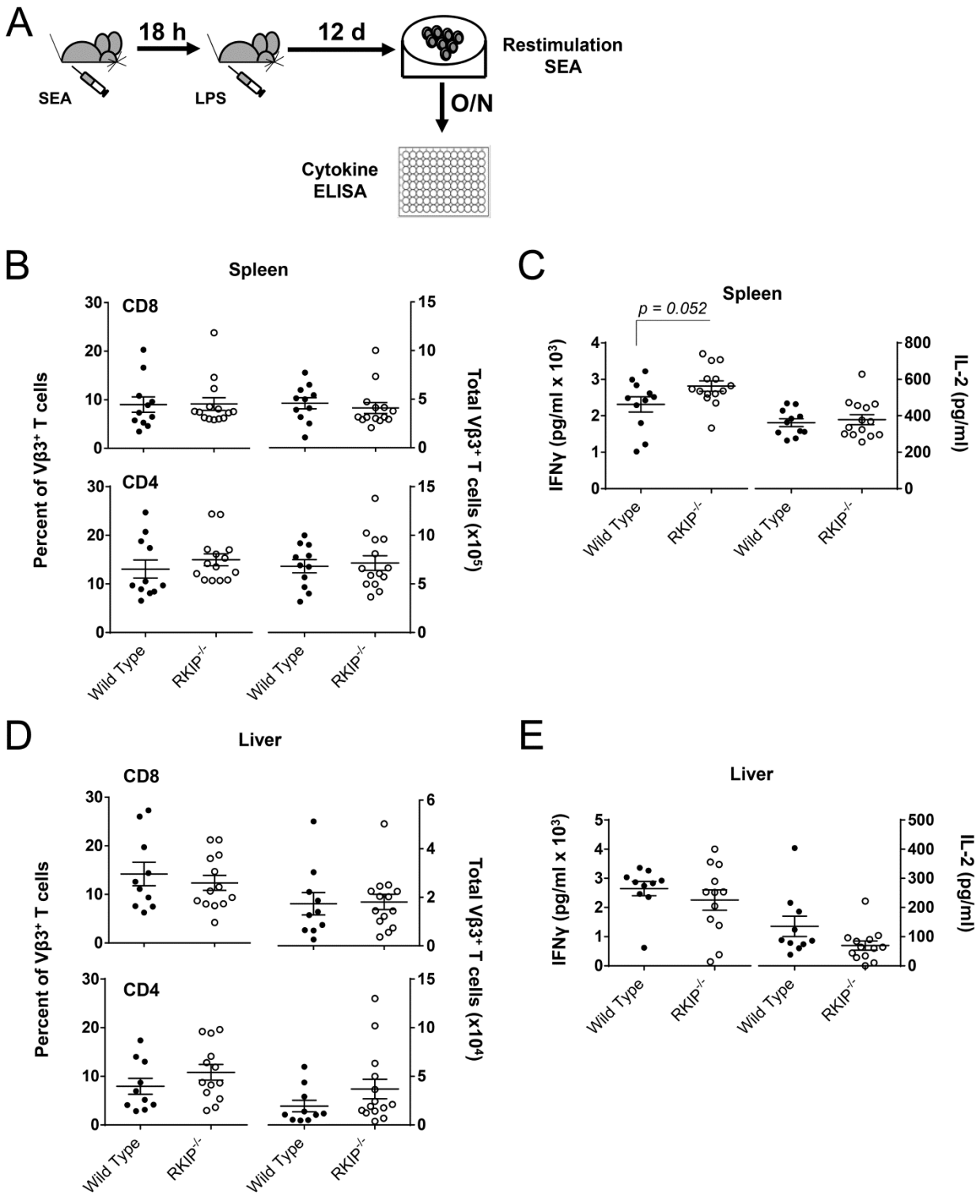
A
18 h
12 d
SEA
LPS
Restimulation
SEA
O/N
Cytokine
ELISA
B
Spleen
CD8
CD4
Percent of Vβ3+ T cells
Total Vβ3+ T cells (x10⁵)
Wild Type
RKIP-/-
C
Spleen
p = 0.052
IFNγ (pg/ml x 10³)
IL-2 (pg/ml)
D
Liver
CD8
CD4
Percent of Vβ3+ T cells
Total Vβ3+ T cells (x10⁴)
E
Liver
IFNγ (pg/ml x 10³)
IL-2 (pg/ml)

TABLE I: Normal clonal expansion, contraction, and survival in RKIP$^{-/-}$ mice after SEA-LPS Immunization

		pLN		Spleen		Liver	
		CD8*	CD4*	CD8	CD4	CD8	CD4
Naïve	Wild Type	2.61 ± 0.20	4.30 ± 0.31	2.99 ± 0.46	4.07 ± 0.18	2.44 ± 0.44	1.76 ± 0.57
	RKIP$^{-/-}$	2.32 ± 0.13	4.26 ± 0.12	2.80 ± 0.27	5.69 ± 0.93	2.38 ± 1.19	1.69 ± 0.46
LPS	Wild Type	2.70 ± 0.20	4.25 ± 0.13	3.20 ± 0.82	4.98 ± 0.72	2.17 ± 0.28	1.90 ± 0.88
	RKIP$^{-/-}$	2.29 ± 0.09	3.98 ± 0.60	3.27 ± 0.61	5.48 ± 0.52	2.25 ± 0.94	1.53 ± 0.13
SEA	Wild Type	1.14 ± 0.19	2.03 ± 0.13	2.78 ± 0.92	3.43 ± 0.25	1.59 ± 0.27	0.96 ± 0.15
	RKIP$^{-/-}$	1.44 ± 0.19	2.20 ± 0.17	2.03 ± 0.15	3.61 ± 0.31	1.75 ± 0.26	1.67 ± 0.29
SEA+LPS	Wild Type	5.36 ± 1.02	7.57 ± 1.04	9.00 ± 1.57	13.04 ± 1.86	14.18 ± 2.31	7.95 ± 1.55
	RKIP$^{-/-}$	5.87 ± 0.68	8.73 ± 0.78	9.13 ± 1.31	14.96 ± 1.23	12.37 ± 1.49	10.82 ± 1.55

* Percent of Vβ3^{+} T cells in various tissues on day 12 after no treatment, LPS, SEA, or Both

Data is a pooled analysis of all experiments in Figure 6. 3 independent experiments, N=11-14/group.

CHAPTER 4

RKIP IS INVOLVED IN DOWNSTREAM SIGNALING AFTER PATTERN RECOGNITION RECEPTOR ENGAGEMEMENT, IMPACTING CYTOKINE PRODUCTION

ABSTRACT

The ability to sense pathogen-associated molecular patterns (PAMPs) through pattern recognition receptors (PRRs) is a critical first step in our body's defense against pathogenic infection. Although much of the signaling mediators downstream of PRR ligation have been well established, new molecules continue to be discovered. Previous data from our laboratory and others suggest that one such molecule, Raf-1 kinase inhibitor protein (RKIP), which has been proposed to interact with several important signaling proteins in pathways typically activated after PRR ligation, may play an important role in PRR signaling events. However, RKIP's function within primary immune cells and specifically how RKIP effects normal PRR signaling is currently unknown. Herein, we suggest that RKIP may play a role in PAMP sensing by PRRs, specifically in Toll-like receptor (TLR) signaling, by forming an ordered signaling complex after TLR ligation. The functional significance of this phenomenon is a marked loss in pro-inflammatory cytokine production after PAMP sensing in the absence or blockade of RKIP, signifying that RKIP is necessary for the proper production of cytokines after TLR ligation. These data also mark RKIP as a potential druggable target in cytokine-based therapies for diseases related to pathogenic cytokine release.

INTRODUCTION

Our body's ability to detect foreign pathogens quickly and efficiently is key in mounting an effective immune response against them. PRRs are largely responsible for coupling PAMP sensing to the generation of pro-inflammatory cytokines, activation and maturation of antigen presenting cells, and subsequently effective adaptive responses of T and B cells. The importance of PRRs and host defense has been demonstrated in both mice and humans with defective PRR responses leading to an increased susceptibility to bacterial, viral, and fungal infections (13). Moreover, PRR responses that are excessively robust can lead to or potentiate inflammatory diseases including systemic inflammatory response syndrome (SIRS), inflammatory bowel disease (IBD), rheumatoid arthritis (RA), systemic lupus erythematosus (SLE), atherosclerosis, and others (36). On the other hand, because of their ability to induce potent inflammatory responses, PRR agonists are also promising molecules for raising the adjuvanticity of certain vaccine-based therapies (186).

The most widely studied, and best understood, family of PRRs are the TLRs, which are responsible for sensing many structural components of pathogens including nucleic acids, proteins, and lipoproteins. Once these patterns are sensed by TLR bearing cells, they transduce a pro-inflammatory genetic program to the nucleus through the utilization of either the MyD88 (all TLRs except TLR3) or TRIF (TLR3 & 4) adaptor molecules. Despite having exponentially increased our understanding of TLR function over the past 20 years, important signaling molecules within these pathways that modulate, potentiate, or regulate the TLR response are continuously being discovered. In 2010, Tang and colleagues showed that RKIP interacted with proteins downstream of MyD88 signaling in cancer cells including TRAF6, TAK-1, and IKKα/β (169). Additionally, our laboratory has shown that RKIP blockade, using the small molecule

inhibitor locostatin, decreased TNFα and IFNγ production from human peripheral blood mononuclear cells (PBMCs) stimulated with the TLR4 ligand LPS (140), and that administration of LPS helps RKIP$^{-/-}$ T cells overcome a deficit in IFNγ production in a mouse model of SIRS (Fig. 3-10). These data suggest that RKIP may be a potentially important player in TLR signaling dynamics; however, the exact nature of RKIP's role within these responses in unknown, especially in primary immune cells.

Through the following studies, we present data that demonstrate that RKIP is an active participant in the early signaling events of several TLRs. Our data are consistent with the working hypothesis that RKIP's role is most likely to facilitate the generation and stabilization of a membrane-associated protein complex involved with TLR signaling. The functional importance of these interactions is demonstrated by evidence that loss of RKIP through targeted-deletion or through exogenous blockade lead to a diminished cytokine profile. Thus, this study is the first to suggest that RKIP is not only involved in the ability of PRRs to transduce inflammatory signals properly after PAMP sensing, but also points to RKIP as a potential target for treating inflammatory diseases linked to inappropriate TLR responses or bolstering the adjuvanticity of vaccines that utilize TLR agonists.

RESULTS

Currently, exceptionally little is known regarding RKIP's role during PAMP sensing by immune cells. The data in Figure 3-10 show that in the context of T cell mediated inflammation, exposure to a PAMP after TCR ligation with SEA did not result in the same defect in IFNγ production seen after serial TCR triggering in $CD8^+$ T cells. Additionally, our laboratory has previously demonstrated that exposing human PBMCs to LPS during RKIP blockade with locostatin decreases TNFα and IFNγ production from these cells (140), although this effect was very dose dependent with low doses elevating IFNγ and higher locostatin inhibiting. Taken together, these data suggest that RKIP may or may not play a role in TLR signaling, and that this role may be fundamentally different than its established effect in IFNγ production from serially triggered $CD8^+$ T cells.

Stimulation of wild type splenocytes with LPS leads to a time and dose dependent disappearance of RKIP protein

In order to test the hypothesis that RKIP is indeed involved in TLR signaling, we first tested the response of bulk splenocytes from wild type C57BL/6J mice to the TLR4 agonist LPS and measured RKIP protein levels by immunoblot over time. This heterogeneous mixture of cells, which has been consistently characterized by many laboratories (14), contains a number of populations capable of sensing a wide complement of PAMPs and thus provided a very important tool for determining any generalizable effect on TLR ligation. We found that after stimulation of these splenocytes with LPS, RKIP became very difficult to detect by immunoblot as rapidly as 10 minutes after exposure (Fig. 4-1A/B). This effect was transient, and began around 5 minutes after stimulation, peaked between 10-30 minutes (data not shown), and was

nearly completely abrogated by 60-90 minutes (Fig. 4-1B and Fig. 4-2). This effect was highly reproducible over many experiments despite being conducted with different culture medium and varying doses of LPS. Additionally, treatment of bulk splenocytes with locostatin also impeded the detection of RKIP by immunoblot (Fig. 4-1A) and seemed to provide an additive effect in conjunction with LPS exposure. However, this phenomenon may be explained by masking of the epitope that the RKIP antibody used in these studies recognizes through steric hindrance or blockade. Unfortunately, this hypothesis cannot be tested until better site specific antibodies corresponding to regions outside of the locostatin binding area are commercially available and validated.

RKIP was originally characterized by its binding to, and functional inhibition of, Raf-1 kinase which subsequently resulted in a decrease in downstream MAPK phosphorylation of MEK and ERK (132). In order to validate that our decrease in RKIP detectability shown in Figures 4-1A/B impinged upon its previously characterized function, we stimulated bulk splenocytes again with a titration of LPS and measured both RKIP and phosphorylated-ERK protein levels 10 minutes after exposure. Consistent with these previously published results, we found an inverse relationship between RKIP protein detectability and ERK phosphorylation that was dose-dependent (Fig. 4-1C and Fig. 4-1D). Taken together, these data suggest that RKIP is involved in the early signaling events located downstream of TLR4 ligation in splenocytes, and that RKIP's previously characterized function (i.e. suppression of the Raf-MEK-ERK axis) may need to be transiently prohibited in order to allow for proper ERK phosphorylation to occur during PAMP sensing.

The inability to detect RKIP protein after PAMP stimulation is generalizable to multiple TLR ligands

Next, we wanted to determine if the disappearance of RKIP on immunoblot after TLR4 triggering was generalizable to multiple TLR ligands or whether it was an effect specific to LPS sensing by splenocytes. To test this question, we stimulated bulk splenocytes with titrations of several TLR ligands including: Pam_3Cys (TLR1/2), Poly I:C (TLR3), LPS (TLR4), CpG type A (TLR9), and CpG type B (TLR9), and then measured RKIP by immunoblot at 10 minutes, 30 minutes (data not shown), and 90 minutes after TLR ligation. These agonists were chosen in order to stimulate both of the different signaling pathways downstream of TLRs (i.e. MyD88 and TRIF) independently (e.g. TLR3 vs. TLR9) or cooperatively (TLR4). We found that each of the TLR ligands tested exhibited the same phenomenon observed in Figure 4-1; however, each did so with varying potencies and kinetics (Fig. 4-2A). Poly I:C and CpG-A seemed to have the most profound effect on RKIP detectability, with LPS and CpG-B affecting RKIP less robustly. Interestingly, TLR2 ligation with Pam_3Cys also led to a decrease in RKIP, but the effect was delayed until 30-90 minutes after stimulation. The stimuli also differed in the duration that RKIP remained less detectable. CpG-A and LPS affected RKIP at 10 minutes post stimulation but by 90 minutes the effect had ceased, whereas Poly I:C and CpG-B seemed to still have an effect on RKIP up to 90 minutes after TLR ligation (Fig. 4-1B). These data suggest that although RKIP may be involved in the signaling machinery of all TLRs tested here, the degree to which it is utilized, and the timing of its utilization, may vary depending on the nature of the stimulus.

Proteosomal degradation and *de novo* translation impart only minor contributions to the disappearance of RKIP

Next, we wanted to better understand the molecular mechanism of RKIP's disappearance after PAMP sensing in splenocytes. Based on our previous findings, two hypotheses emerged as potential possibilities to explain RKIP's disappearance: 1) proteosomal degradation with

subsequent *de novo* translation of RKIP protein and 2) sequestration of RKIP into a signaling complex, and/or altered subcellular localization, which rendered it insoluble during lysate generation. In order to test the former hypothesis, we cultured splenocytes again with LPS or medium alone in the presence of the translational inhibitor cyclohexamide. Also, based on the transient nature of LPS's effect on RKIP detectability, we suspected that the presence of pre-synthesized RKIP mRNA was highly likely given that *de novo* transcription and subsequent translation of new protein can take much longer than the 90 minutes it took for RKIP to reappear. Because of this, we also repeated our stimulation in the presence of the transcriptional inhibitor actinomycin D to determine whether or not *de novo* transcription was necessary for detection of RKIP at 90 minutes post TLR ligation. We found that after stimulating splenocytes with LPS in the presence of actinomycin D, there was no effect on the RKIP's disappearance at 10 minutes post TLR ligation and reappearance at 90 minutes, confirming our suspicion that *de novo* transcription of RKIP was likely not involved with this phenomenon (Figs. 4-3A/C). Additionally, stimulating in the presence of cyclohexamide only had minimal effects are preventing the re-detectability of RKIP at 90 minutes in one of two experiments, suggesting that *de novo* translation of RKIP protein also plays little to no role (Figs. 4-3A/C). Finally, we wanted to determine if degradation via the proteasome played a role in the rapid loss of RKIP detection. In order to test this, we repeated our LPS stimulation in splenocytes after a 10 minute pre-treatment with the pan-proteasome inhibitor lactacystin. Due to the rapidity of RKIP's disappearance, pre-treatment was required in order to assure that the majority of cellular proteasomes were blocked before stimulation commenced. The active β-lactone intermediate responsible for proteosomal inhibition has been shown to peak at 10 minutes and decay shortly thereafter with a half-life around 30 minutes (187). When comparing the amount of detectable

RKIP at 10 minutes after TLR4 ligation between splenocytes pre-treated or not with lactacystin, we found only a small increase in the amount of RKIP in the pre-treated group (Fig. 4-3B). There still remains a possibility that RKIP may be degraded by a non-proteosomal mechanism, such as cleavage via cellular caspases; however, after assessing RKIP's primary amino-acid sequence using the bioinformatics tool ExPASy Peptide Cutter, no cleavage sites for any non-proteosomal peptidases were found (Table II). Nevertheless, taken together these data suggest that the transient loss of RKIP detection after PAMP sensing may be impacted by proteosomal degradation and *de novo* protein synthesis.

The disappearance of RKIP protein after PAMP stimulation may be due to insoluble complex formation or altered subcellular localization

In order to test our second hypothesis regarding the disappearance of RKIP, we first looked at RKIP's cellular distribution in splenocytes after LPS stimulation by immunofluorescent microscopy. Interestingly, we observed that after TLR4 ligation with LPS, RKIP's pattern of staining changed drastically. Splenocytes cultured in medium alone had an RKIP staining pattern that was diffusely spread across the cytoplasm with a small increase in intensity at the cell membrane, but after LPS stimulation, this RKIP staining pattern became much more punctate in nature and seemed to be localized into a very small, clustered region within each cell that was in or near the nucleus (Fig. 4-4A). This finding gave credence to the idea that RKIP may be a member of a distinct signaling complex that forms after TLR ligation. To look at this further, we repeated our LPS stimulation and separated our lysates into "cytoplasmic" and "nuclear" fractions using a commercially available kit. After TLR4 ligation, RKIP could be seen within the "nuclear" fraction, but was absent in splenocytes that were cultured in medium alone (Fig. 4-4B). This nuclear RKIP band was much less intense, but still present at 90 minutes post LPS

stimulation. Also of note, the molecular weight of the nuclear RKIP band was slightly higher than that found within the cytoplasm, suggesting that the form of RKIP found within this fraction may very well be post-translationally modified in some way. There are numerous putative post translational modification sites contained within RKIP that could explain this shift; however, most of these sites still need validation (Table II). Finally, even though we were able to confirm that our commercial subcellular fractionation kit was able to prevent cytoplasmic protein contamination into our "nuclear" fractions (confirmed by the exclusivity of Hsp90, a purely cytoplasmic protein, within our cytoplasmic fractions), we still cannot rule out the possibility that RKIP may also be tethered to the cytoplasmic membrane or endoplasmic reticulum (ER) within these punctate regions of staining seen in Figure 4-4A, given that many studies have highlighted the problem of membrane and ER-associated protein contamination into "nuclear" fractions in commercial kits that utilize RIPA buffer (188). Nevertheless, these data suggest that after PAMP sensing in splenocytes, RKIP does not undergo substantial degradation, and its disappearance on immunoblot analysis is more consistent with its re-direction into an ordered signaling complex that becomes insoluble during our normal lysate generation, most likely due to its tethering to insoluble material such as membrane-associated lipid rafts.

Loss of RKIP by genetic knockout or exogenous blockade leads to altered cytokine and chemokine responses after TLR stimulation

In order to determine if loss of RKIP had any significant downstream functional effects after TLR ligation, we stimulated bulk mesenteric lymph node (MLN) cells from RKIP$^{-/-}$ mice and wild type littermates with the TLR9 ligand CpG-A overnight. The supernatants from these cultures were then subjected to multiplex cytokine analysis that measured the output of 32 distinct cytokines and chemokines from these cells. Many cytokines were found to be lower than

the lowest limit of assay detection in both RKIP$^{-/-}$ and wild type littermate bulk MLN cells after TLR9 ligation: G-CSF, IL-1β, IL-2, IL-3, IL-4, IL-7, IL-10, IL-15, IL-17A, CCL2, LIF, M-CSF, VEGF, and Eotaxin (data not shown). Of the cytokines and chemokines that were induced by CpG, the vast majority were generated in much smaller quantities in RKIP$^{-/-}$ MLN cells compared to wild type littermate: TNFα, GM-CSF, IL-5, IL-6, IL-9, IL-12, CXCL1, CXCL2, CXCL5, CCL3, CCL4, and CCL5 (Fig. 4-5A). This suggests that RKIP may be necessary for adequate production of some cytokines and chemokines following triggering of the MyD88 pathway. Also, consistent with our previous findings that SEA-LPS vaccination led to slightly higher IFNγ output in RKIP$^{-/-}$ mice (Fig. 3-10C) and previous data showing that low doses of locostatin increased IFNγ after LPS stimulation of human PBMCs (140), we also observed increased levels of IFNγ, as well as the interferon-stimulated genes CXCL9, and CXCL10 after CpG stimulation of RKIP$^{-/-}$ MLN cells (Fig. 4-5A). In order to validate the observation that loss of RKIP results in decreased cytokine output after TLR ligation, we treated wild type splenocytes with either LPS or CpG-A overnight in the presence of exogenous RKIP blockade using the small molecule inhibitor locostatin and measured IL-6 and TNFα production in the culture supernatants. Consistent with our findings in Figure 4-5A, splenocytes treated with locostatin had markedly lower production of both cytokines measured (Fig. 4-5B), once again suggesting that functional RKIP is necessary for appropriate cytokine production during TLR signaling in splenocytes.

DISCUSSION

Charles Janeway first hypothesized the existence of a group of receptors important for recognizing foreign pathogens and providing the initiating events in host defense in *Approaching the Asymptote? Evolution and Revolution in Immunology* during a Cold Spring Harbor symposia in 1989 (189). Since that time, a voluminous literature base has been developed supporting Janeway's theory, and currently we understand, in moderate detail, the existence, specificity, function, and importance of PRRs in host immunity and disease. After initially being discovered in plants in 1995 (190), groups shortly thereafter described their function in *Drosophila melongaster* (191), *Mus musculus* (192), and *Homo sapiens* (193). The first family of PRRs to be functionally described was the Toll-like receptors, named after their homology to a known *Drosophila* protein involved in embryonic polarity, *Toll*, initially discovered in 1985 (194). TLRs were found to recognize a number of different structural molecules found in bacteria, viruses, and fungi, including: LPS and lipopeptides, single and double-stranded RNA and DNA, flagellin, a protein involved in bacterial motility, and unmethylated CpG sites in DNA. Currently, it is known that many more families of PRRs exist in mice and humans including: C-type lectin receptors (CLRs) which respond to glycoproteins and glycolipids, NOD-like receptors (NLRs) which recognize structural components of peptidoglycan and are responsible for coupling other PRRs to the inflammasome, and RIG-I-like receptors (RLRs) which respond to intracellular nucleic acids.

Despite the immense collection of PAMPs that PRRs can recognize, the vast majority of signaling events after PRR ligation are restricted to two well-defined pathways named for the adapter molecule that initiates them: myeloid differentiation primary response gene 88 (MyD88) and TIR-domain-containing adapter-inducing interferon-β (TRIF)(195). All TLRs except for

TLR3 signal through MyD88 (196-198), while TLR3 and TLR4 can signal through TRIF (199, 200). MyD88 signaling leads to the induction of NF-κB through the canonical pathway, and subsequently, the production of many pro-inflammatory cytokines (through AP-1), as well as co-stimulatory molecules important for providing "signal 2" to T cells during activation (201). On the other hand, TRIF activation leads to a type I interferon dominated response (through IRF3/7) which is important for anti-viral immunity (202). Despite having some differences in upstream signaling molecules, ligation of CLRs, NLRs, and RLRs also lead to the activation of these downstream signaling molecules. Even though the MyD88 and TRIF pathways have been well defined, molecules that are important for proper transduction through these pathways are still being discovered on a regular basis, as exemplified by the recent discovery of STING as an alternative means of type I interferon generation (203).

Previously, our lab and others have suggested that RKIP may be another such molecule important for PRR signaling. This hypothesis was based on several lines of evidence including: the fact that RKIP binds several molecules upstream of NF-κB activation (TRAF6, IKKα/β and TAK1; (133)), that blockade of RKIP with low dose locostatin in human PBMCs leads to decreased TNFα production after LPS stimulation (140), and administration of LPS helps $RKIP^{-/-}$ T cells overcome a deficit in IFNγ production (204). Nevertheless, the exact nature of RKIP's role in primary cells remains unknown, and provides an important area for investigation.

Through our studies, we demonstrate that RKIP is markedly affected after stimulation of bulk splenocytes with the TLR4 ligand LPS. This is evidenced by the fact that RKIP becomes exceedingly difficult to detect by immunoblot shortly, but transiently, after TLR ligation (Fig. 4-1A/B), the mechanism of which we still do not understand completely. This "disappearance" begins as early as 5 minutes after stimulation, peaks at 10-30 minutes, and is almost completely

resolved 60-90 min later. Importantly, this phenomenon was generalizable to stimulation through TLRs that activate My88 alone, TRIF alone, or both together, suggesting that RKIP probably plays a role in both pathways (Fig. 4-2), albeit with different potency and kinetics. Although, the relative impact of RKIP on each pathway individually, and whether or not this is an effect of a specific lesion that lessens heterologous pathway activation, requires additional study. Interestingly, in these experiments it became clear that the RKIP inhibitor locostatin also leads to an inability to detect RKIP using this method (Fig. 4-1C/D). This finding could be due to several factors including epitope masking by steric hindrance of locostatin when bound within RKIP's ligand binding pocket, or increased proteosomal degradation when RKIP is pulled away from potential binding partners by locostatin.

Next, we sought to better understand RKIP function after PRR triggering. Based on previous work demonstrating the RKIP can act as a negative regulator of MAPK signaling *in vitro,* and given the rapidity of RKIP's "disappearance" seen in Figure 4-1, we hypothesized that perhaps it was essential for RKIP to be degraded in order to provide the release of inhibition necessary for TLR signaling to proceed. Additionally, because of the transient nature of this effect, we also hypothesized that pre-synthesized RKIP mRNA must be present within the cell in order to bypass *de novo* transcription, a process which typically requires at least several hours to generate a biologically observable effect (205). Our data show that RKIP's disappearance on immunoblot is not robustly affected by pre-treatment with the pan-proteosomal inhibitor lactacystin (Fig 4-3B). This does not rule out the possibility of another form of protein degradation with an endogenous peptidase; however, a bioinformatic analysis using ExPASy-peptide cutter exemplifies that RKIP lacks putative cleavage sites for caspases 1 through 10, factor Xa, thrombin, and granzyme B (Table II). RKIP detectability was also not robustly affected by pre-

treatment with either the transcriptional inhibitor actinomycin D or the translational inhibitor cyclohexamide (Fig. 4-3A) after TLR ligation. Additionally, we tested if RKIP was secreted after TLR ligation in splenocytes by immunoblotting for RKIP in the supernatants from these cultures and found that they were devoid of detectable RKIP (data not shown). Based on these data, we concluded that intracellular levels of RKIP were most likely staying relatively constant after PRR triggering. Given this, we next determined that it was necessary to investigate RKIP by utilizing immunofluorescence which would provide us the opportunity to visualize RKIP over the time of our stimulation, and could potentially corroborate our immunoblot findings. It is shown by immunofluorescence not only that RKIP was still observable after TLR4 ligation, but also that the staining pattern became very punctate in nature instead of cytoplasmically diffuse (Fig. 4-4A). This observation suggests that RKIP is more likely being recruited to a signaling complex after stimulation, rather than being degraded and resynthesized. Because RKIP has only been previously described as a negative signaling regulator, these data also imply a dual role for RKIP in that it may additionally act in a positive manner to promote signal transduction, perhaps as a scaffold protein. Furthermore, after utilizing a subcellular fractionation method in place of traditional whole cell lysis, we were able to find RKIP within “nuclear” fractions after LPS stimulation (Fig. 4-4B). As aforementioned, these fractions are highly contaminated by proteins that are associated with cytoplasmic and organelle membranes, especially proteins contained in lipid rafts. This type of signaling architecture is exceptionally common for MAPK transduction, which recruits signaling complexes to the plasma membrane by KSR (206), endosomes via MP1 (207) and β-arrestin (208), endoplasmic reticulum by ERi1 (209), and to the golgi apparatus via Sef (210). This is especially significant given that RKIP also contains a pleckstrin homology domain, which is necessary for recruitment and binding to lipids (Table II). It is difficult to

determine at this time with absolute confidence whether RKIP is located within the nucleus or in one of these membrane-associated signaling complexes, given the fact that RKIP also has a putative nuclear localization sequence (Table II). Further studies using better imaging approaches such as confocal or two-photon microscopy are required to co-localize RKIP with proteins of known location and function.

RKIP has been previously described as a negative regulator of MAPK activation through the interaction with Raf-1, MEK, and ERK. This pathway is critical for generating pro-inflammatory cytokines through the induction of Elk-1 and the transcription of *Fos* which, when combined with the protein Jun, form the transcription factor AP-1 (211). By measuring phosphorylated-ERK (active) in our studies, we were able to demonstrate that RKIP and p-ERK are indeed inversely proportional to one another, giving weight to these prior studies (Fig. 4-1C/D). Surprisingly, even though pERK levels increase as RKIP decreases, a genetic deletion of RKIP or exogenous blockade did not translate into increased cytokine levels (Fig. 4-6). RKIP has previously been shown to modulate its substrate affinity after phosphorylation by PKC from Raf-1 to GRK2, thus allowing for the transduction of both the Raf-MEK-ERK axis and G-protein coupled receptors through disinhibition (212). Given this, it is possible that after TLR stimulation, RKIP also switches affinity away from Raf-MEK-ERK and to another (MyD88/TRIF) pathway allowing both to proceed simultaneously and cooperatively with subsequent cytokine production. However, if RKIP is lost completely or is prevented from functioning properly, this could result in an effect that only allows one of two pathways (ERK) to transduce a signal without the cooperation of the other. This could effectively override the high levels of p-ERK and lead to poor cytokine responses. In other words, it may “take two to tango” in regards to cytokine production, with the possibility that RKIP is utilized to assist in

pathway cooperativity. A bioinformatic analysis of putative post-translational modification sites revealed that RKIP has 2 glycosylation sites and at least 32 phosphorylation sites, 13 of which have higher predictability scores than the validated PKC Ser_{153} phosphorylation site (Table II). This suggests that there are numerous possibilities in terms of altered RKIP substrate affinity that have yet to be described. Another alternative explanation for the p-ERK-cytokine disconnect would be that exceedingly high levels of p-ERK transmits a negative, instead of a positive, signal to the cell through a negative feedback loop. This hypothesis is less likely because it would require the strength of this suppressive signal mediated by p-ERK to shut down normal pro-inflammatory cytokine production through MyD88 and TRIF signaling which prototypically does not involve the Raf-MEK-ERK axis, but rather the JNK and p38 MAPKs.

TLRs have been implicated in the pathogenesis of several human inflammatory diseases including: SIRS/sepsis (213), atherosclerosis (214), inflammatory bowel disease (215), rheumatoid arthritis (216), asthma (217), systemic lupus erythematosus (36), and ischemia/reperfusion injury (218). To this end, therapeutic agents have been developed to decrease the inflammation seen after TLR stimulation by exogenous or endogenous ligands, and several have been examined in human clinical trials. These include the TLR4-TIRAP small molecule inhibitor TAK-242 (resartorvid) for sepsis and SIRS (219, 220) and chaperonin-10 (Cpn-10) for RA (221) and SLE (currently recruiting). Many other pharmaceutical companies, such as Coley, Dynavax, and VentiRx, currently have TLR antagonists in their respective pre-clinical study pipelines as well (222). RKIP may represent a potential novel therapeutic target option for these diseases, given that its targeted inhibition using an already commercially available small molecule inhibitor leads to decreased cytokine responses are TLR stimulation. However, a more thorough understanding of RKIP's exact molecular mechanism for facilitating

PRR responses is needed in order to provide the amount of evidence necessary to proceed into human disease trials.

Figure 4-1: Stimulation of wild type splenocytes with LPS leads to a time and dose dependent disappearance of RKIP protein. (A) Representative immunoblots of bulk splenocyte lysates from wild type C57BL/6J mice kept either on ice in balanced salt solution (BSS) or cultured in BSS at 37°C & 5% CO_2 for 10 min. or 60 min. (data not shown) in the presence or absence of 10μg/ml LPS, 50μM of the RKIP inhibitor locostatin, or both. Dimethyl sulfoxide (DMSO) at the same percent (v/v) as locostatin (~0.1%) was utilized as a vehicle control. (B) Densitometric quantification of RKIP expression from 4 independent experiments conducted similarly to Figure 4-1A. RKIP expression was normalized to the loading control (Actin) to generate an RKIP/Actin ratio, and then the relative quantity of RKIP protein was determined by setting the ratio of each medium control to 100. Error bars represent SEM and *P* values determined by unpaired *t* test between groups $*P<0.05$. (C) Immunoblots for RKIP and phosphorylated ERK-1/2 from lysates of wild type bulk splenocytes that were cultured as in Figure 4-1A for 10 min. in the presence of various quantities of LPS (range: 1.56-50μg/ml) or medium alone. (D) Densitometric quantification of RKIP and p-ERK expression from immunoblot in Figure 4-1C. Data are represented as relative abundance between pERK and RKIP protein levels.

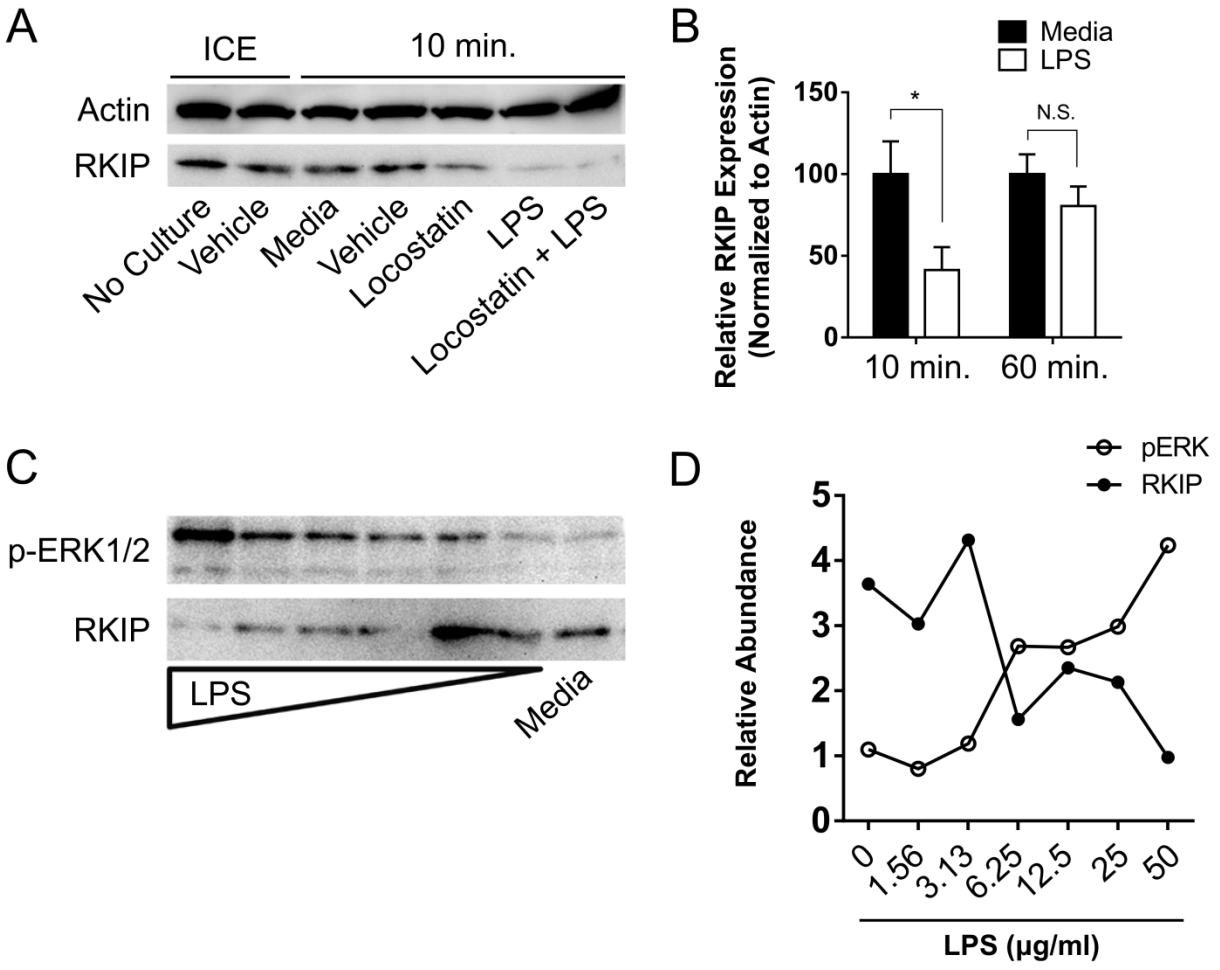
A
ICE
10 min.
Actin
RKIP
No Culture
Vehicle
Media
Vehicle
Locostatin
LPS
Locostatin + LPS
B
Media
LPS
Relative RKIP Expression (Normalized to Actin)
150
100
50
0
*
N.S.
10 min.
60 min.
C
p-ERK1/2
RKIP
LPS
Media
D
pERK
RKIP
Relative Abundance
5
4
3
2
1
0
0
1.56
3.13
6.25
12.5
25
50
LPS (µg/ml)

Figure 4-2: The inability to detect RKIP protein after PAMP stimulation is generalizable to multiple TLR ligands. (A) Representative immunoblots of RKIP and Actin protein from lysates of wild type splenocytes stimulated for 10 min. or 90 min. with titrations of the following TLR ligands: TLR9- CpG type A (0.33-27μg/ml), TLR9- CpG type B (0.33-27μg/ml), TLR3- Poly I:C (0.33-81μg/ml), TLR4- LPS (0.33-81μg/ml), and TLR1/2- Pam_3CSK4 (0.33-81μg/ml). Medium controls (M) were utilized for Poly I:C, LPS, and Pam_3CSK4 stimulations, and ODNs containing GpC dinucleotides (**) were used as negative controls for CpG-A, and CpG-B stimulations. (B) Densitometric quantification of RKIP protein levels from 10 min. (closed circles) and 90 min. (open circles) stimulations in Figure 4-2A. Data are presented as relative RKIP expression normalized to actin as described in Figure 4-1B.

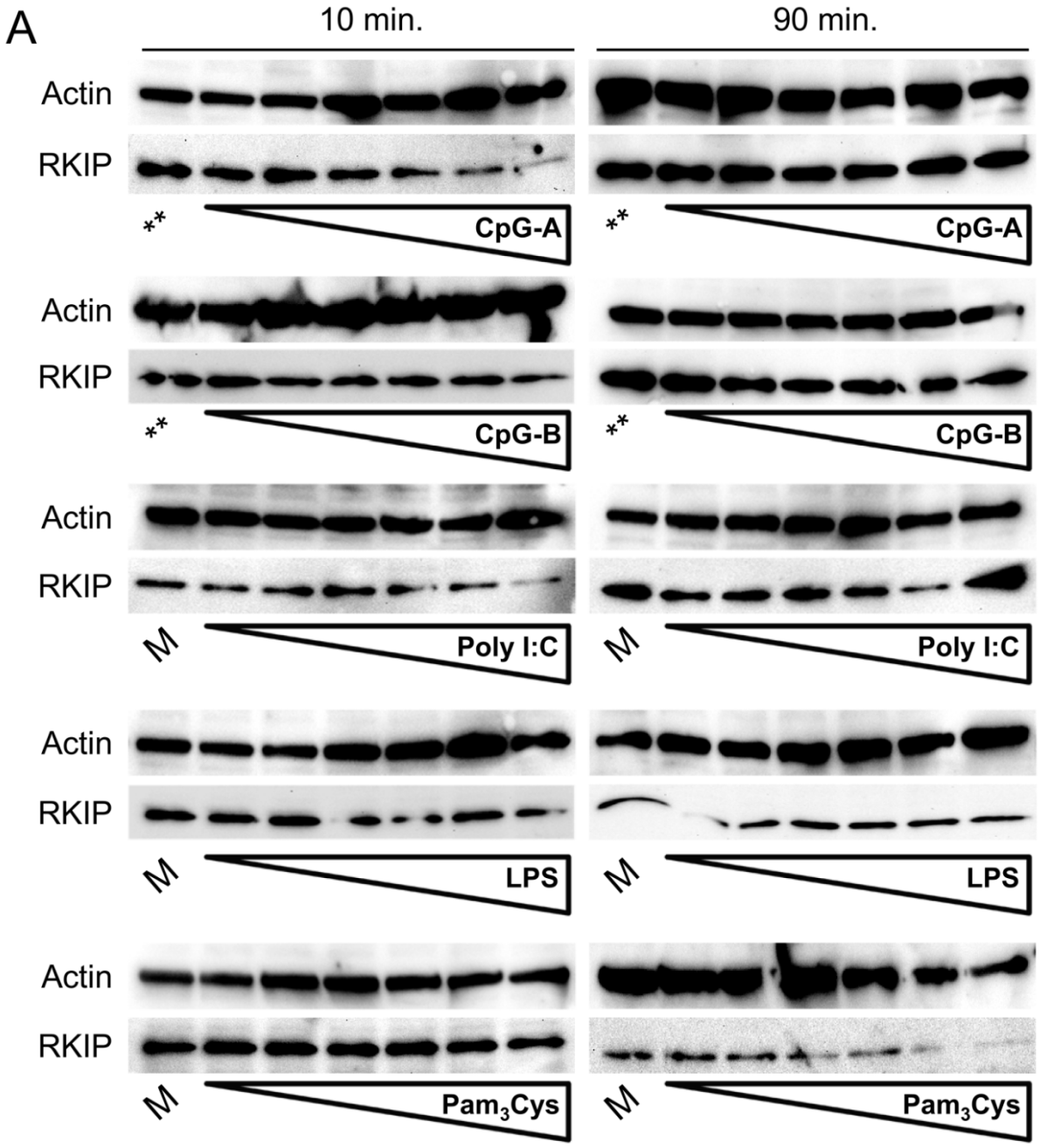
A
10 min.
90 min.
Actin
RKIP
**
CpG-A
CpG-B
M
Poly I:C
LPS
Pam3Cys

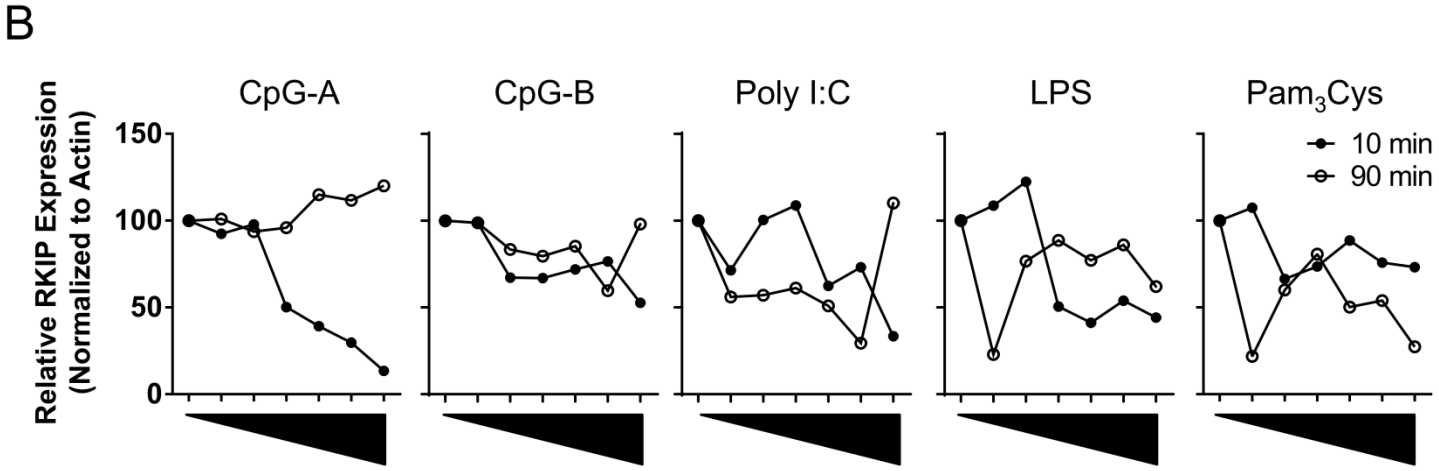
B
CpG-A
CpG-B
Poly I:C
LPS
Pam3Cys
Relative RKIP Expression
(Normalized to Actin)
150
100
50
0
10 min
90 min

Figure 4-3: Proteosomal degradation and *de novo* translation impart only minor contributions to the disappearance of RKIP. (A) Representative immunoblots of wild type bulk splenocytes stimulated with LPS (50μg/ml) or medium alone for 10 min. or 90 min. in the presence of the transcriptional inhibitor actinomycin D (100ng/ml) or the translational inhibitor cyclohexamide (10μg/ml). (B) Immunoblot of bulk wild type splenocytes treated similarly to Figure 4-3A in the presence or absence of the proteosomal inhibitor lactacystin (2μM). (C) Densitometric quantification of RKIP protein levels from experiments outlined in Figures 4-3A/B. Data are presented as relative RKIP expression normalized to actin as described in Figure 4-1B.

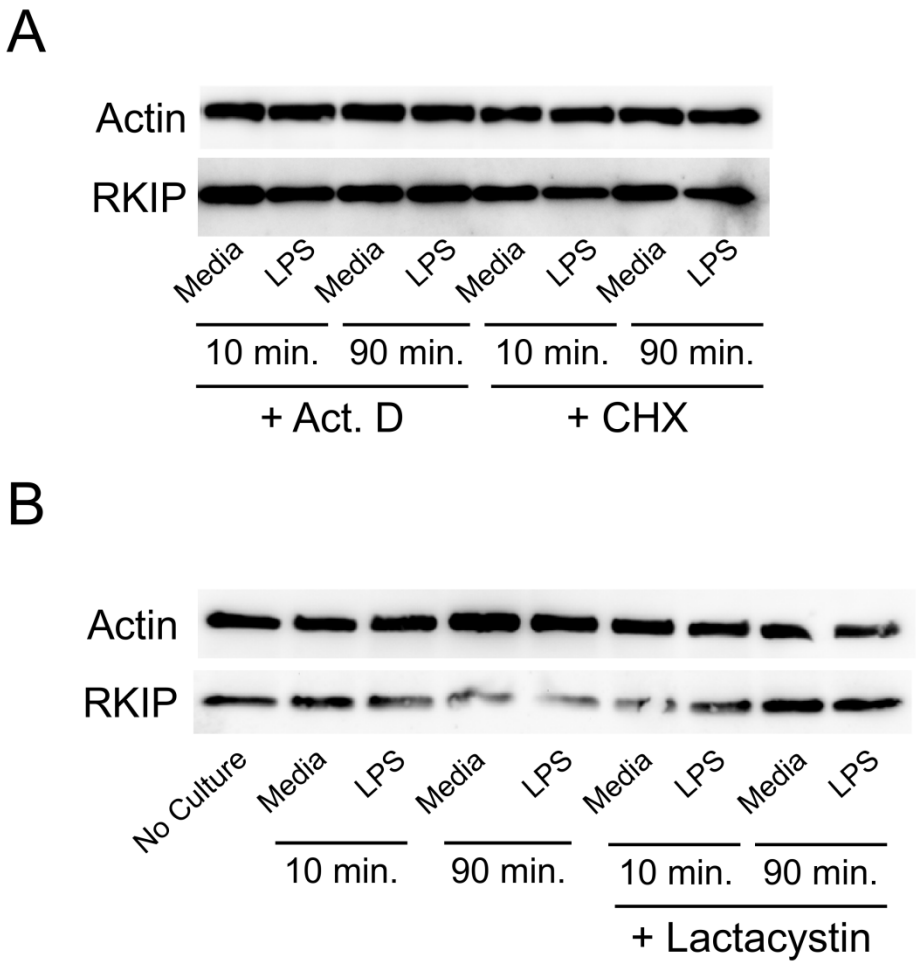
A
Actin
RKIP
Media
LPS
Media
LPS
Media
LPS
Media
LPS
10 min.
90 min.
10 min.
90 min.
+ Act. D
+ CHX
B
Actin
RKIP
No Culture
Media
LPS
Media
LPS
Media
LPS
Media
LPS
10 min.
90 min.
10 min.
90 min.
+ Lactacystin
C
Relative RKIP Expression (Normalized to Actin)
Exp. 1
Exp. 2
Exp. 1
Exp. 2
Media
LPS
150
100
50
0
250
200
150
100
50
0
10 min
90 min
Nothing
+ Actinomycin D
+ Cyclohexamide
+ Lactacystin

Figure 4-4: The disappearance of RKIP protein after PAMP stimulation may be due to insoluble complex formation or altered subcellular localization. (A) Immunofluorescent images of RKIP (green) from wild type bulk splenocytes cultured with either medium or LPS (50μg/ml) for 10 min. Data are from 2 independent experiments. (B) Wild Type bulk splenocytes were stimulated for 10 min. or 90 min. in the presence or absence of LPS (25μg/ml). Lysates from these cultures were generated using the NE-PER subcellular fractionation kit (Thermo Pierce) which separates cellular protein content into "cytoplasmic" and "nuclear" fractions. These lysates were immunoblotted for RKIP protein or Hsp90 as a cytoplasmic protein control. Data are representative images of 5 independent experiments.

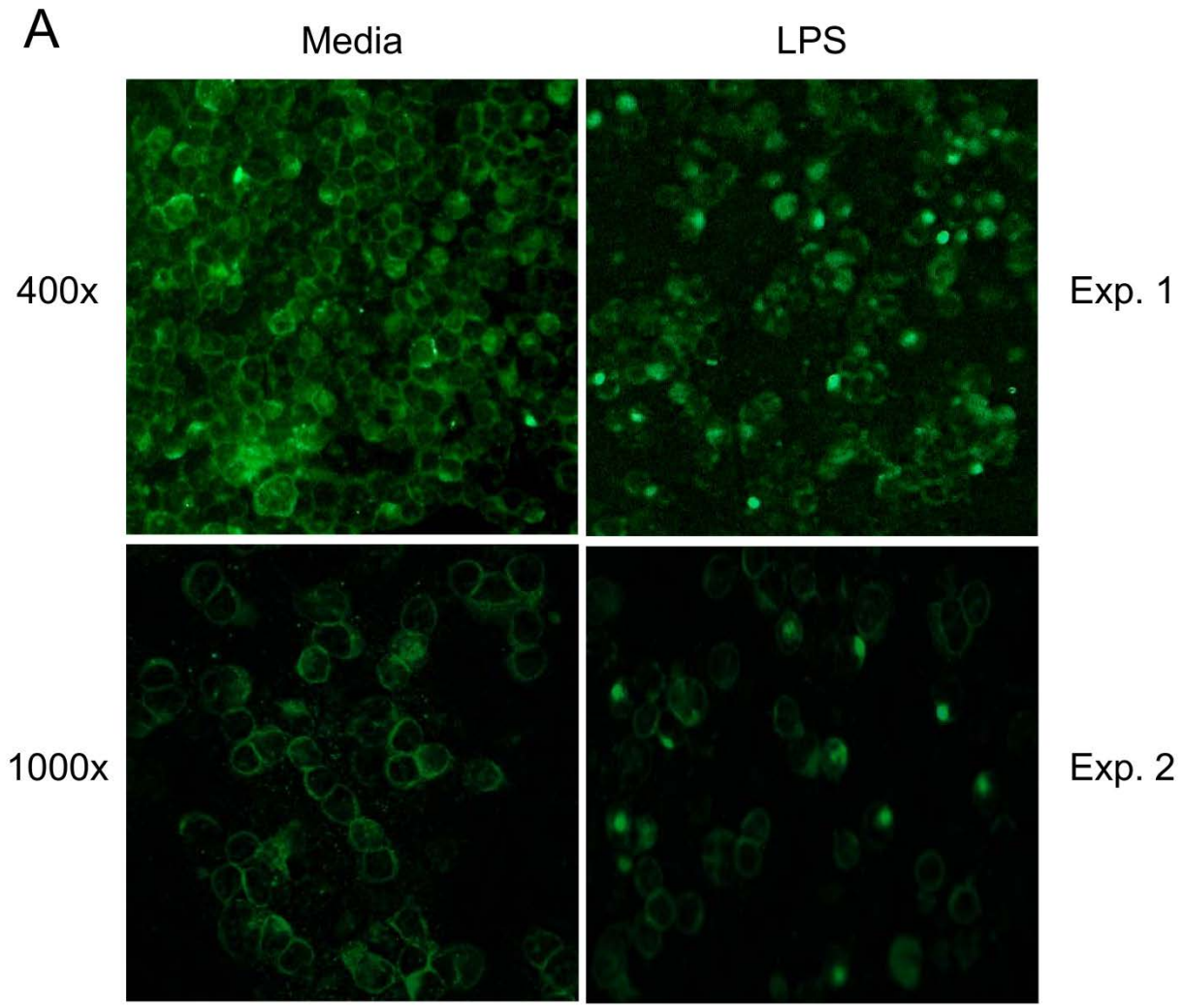
A
Media
LPS
400x
Exp. 1
1000x
Exp. 2

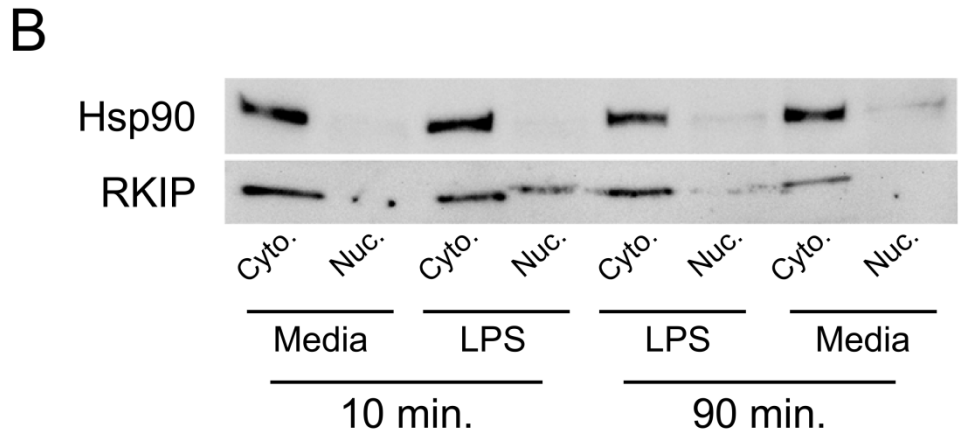
B
Hsp90
RKIP
Cyto.
Nuc.
Cyto.
Nuc.
Cyto.
Nuc.
Cyto.
Nuc.
Media
LPS
LPS
Media
10 min.
90 min.

Figure 4-5: Loss of RKIP by genetic knockout or exogenous blockade leads to altered cytokine and chemokine responses after TLR stimulation. (A) Multiplex cytokine analysis of bulk mesenteric lymph node (MLN) cells from $RKIP^{-/-}$ or wild type littermate mice stimulated with CpG-A (9μg/ml) overnight *in vitro*. Data are represented as relative abundance with the value of each analyte in wild type littermate stimulations being normalized to 100. (B) ELISA for IL-6 and TNFα protein in culture supernatants from wild type bulk splenocytes treated overnight with medium, LPS (50μg/ml), or CpG-A (9μg/ml) in the presence of vehicle (DMSO) or locostatin (50μM). Error bars represent SEM and *P* values determined by unpaired *t* test between groups using Welch's correction for variable standard deviations $*P<0.05$, $**P<0.01$. Data are from 2 independent experiments; N=4/group total.

A

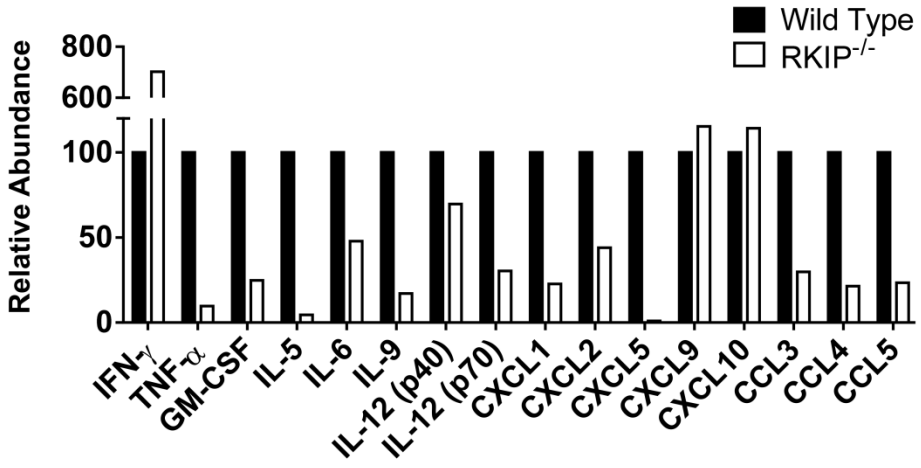
Wild Type
RKIP-/-
Relative Abundance
800
600
100
50
0
IFN-γ
TNF-α
GM-CSF
IL-5
IL-6
IL-9
IL-12 (p40)
IL-12 (p70)
CXCL1
CXCL2
CXCL5
CXCL9
CXCL10
CCL3
CCL4
CCL5

B

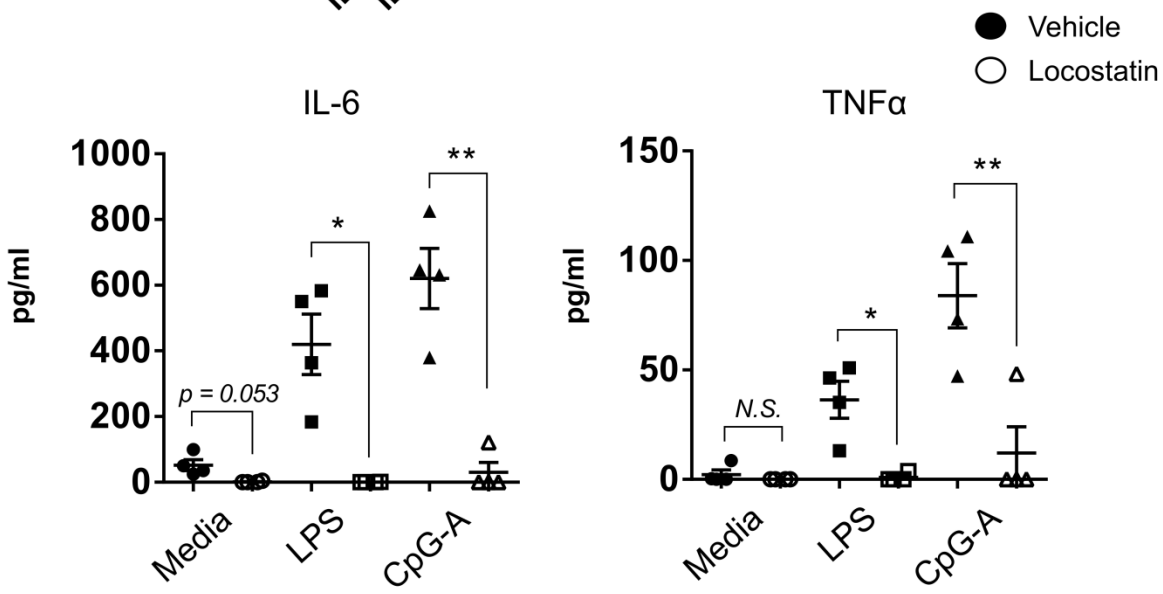
Vehicle
Locostatin
IL-6
TNFα
pg/ml
1000
800
600
400
200
0
150
100
50
p = 0.053
N.S.
*
**
Media
LPS
CpG-A

TABLE II: Bioinformatic Analysis of RKIP in *Mus musculus*

Prediction	Sequence (Site)	Score	Algorithm	Reference
PBP Family Sig.	YTLVLTDPSRKDPKF REWHH (64)	N.A.	Predict Protein	Rost et. al. Nucleic Acids Research. W321-326 (2004)
Localization	Cytoplasmic	N.A.	LOCkey	
Nuclear Localization Sequence	RGKFKVETFRKK	N.A.	PredictNLS	Nair. et al. EMBO Reports. 1(5): 411-415 (2000)
Peptidase Cleavage	No Caspase (1-10), Factor Xa, Thrombin, or GzB sites found	N.A.	ExPASy-Peptide Cutter	Gasteiger et. al. The Proteomics Protocols Handbook, Humana Press. (2005)
Asn (N)-Glycosylation	NKSG (140)	0.6721 (>0.5 confidence threshold)	NetNGlyc v1.0	Gupta et. al. Pacific Symposium on Biocomputing 7:310-322 (2002)
O-Glycosylation	None	N.A.	NetOGlyc v3.1	Steentoft et. al. EMBO 32(10):1478-88 (2013).
PKCα/β/γ Phosphorylation	RGKVE**T**FRKKYNL* (153)	0.114% (<0.2% high confidence)	Scansite v2.0 Motif Scan	John et. al. Nucleic Acid Res. 31(13):3656-3641 (2003).
PKCζ Phosphorylation	RGKVE**T**FRKKYNL* (153)	0.003% (<0.2% high confidence)		
PIP3-binding domain (PH)	GKFKVET**F**RKKYNL (154)	0.112% (<0.2% high confidence)		
Serine Phosphorylation**	MNRPSSISW (51)	0.849	NetPhos v2.0	Blom et. al. J. Mol. Biol. 294(5):1351-1362 (1999)
	NRPSSISWD (52)	0.995		
	PSSISWDGL (54)	0.984		
	PDAPSRKDP (75)	0.998		
	SGPPSGTGL (113)	0.891		
	EQPLSCDEP (132)	0.780		
	EPILSNKSG (139)	0.958		
	LSNKSGDNR (142)	0.734		
	YEQLSGK (185)	0.813		
		(>0.5 confidence threshold)		
Threonine Phosphorylation†	YAGVTVDEL (33)	0.846		
	GKVLTPTQV (42)	0.702		
	FKVETFRKK (153)*	0.724		
	PVAGTCYQA (167)	0.515		
		(>0.5 confidence threshold)		
Tyrosine Phosphorylation‡	VLSDYVGSG (106)	0.624		
	EWDDYVPKL (176)	0.979		
		(>0.5 confidence threshold)		

* Thr (Ser) 153 phosphorylation site validated in: Lorenz et. al. *Nature* 426, 574-579 (2003).
** 14 Predicted p-Ser sites; (9/14 have higher predictability than Thr/Ser_{153})
† 9 Predicted p-Thr sites; (2/9 have higher predictability than Thr/Ser_{153})
‡ 9 Predicted p-Tyr sites; (2/9 have higher predictability than Thr/Ser_{153})
N.A. = not acquired

CHAPTER 5

RKIP IS NECESSARY FOR THE GENERATION OF OPTIMAL TYPE I INTERFERON RESPONSES DURING B CELL ACTIVATION BY TLR LIGANDS

ABSTRACT

The activation of APCs by TLR ligands is critical for the host's initial response to pathogenic invasion, and the robust inflammatory response generated by these interactions has been harnessed as a means to enhance the adjuvanticity and effectiveness of vaccine-based therapies. However, if these responses are directed against endogenous ligands, such as host nucleic acid, autoimmunity can result, leading to significant morbidity in patients. B lymphocytes play an underappreciated role in facilitating both advantageous adjuvant responses and deleterious autoimmunity through the production of protective or destructive antibodies. Interventions that can affect the response of B cells to TLR ligands could provide a useful therapeutic tool for autoimmune diseases, or provide valuable insight into B cell adjuvant reactions. Previous data from our laboratory suggest that RKIP may play an important role in the generation of cytokines after TLR ligation in splenocytes; nevertheless, RKIP's functional impact on B cell responses to PAMPs has not been studied. Here we demonstrate that loss of RKIP results in an attenuated TRIF-type I IFN transcriptome signature in steady state B cells. This leads to a deficiency in the generation of IFNα and the interferon-stimulated chemokine CXCL10 in response to TLR3 stimulation with Poly I:C, despite the normalization of many transcripts after TLR-triggering. Additionally, by blocking RKIP with the small molecule inhibitor locostatin, type-I interferon responses could also be significantly diminished in wild type B cells, providing evidence that RKIP may prove to be a valuable therapeutic target for inflammatory diseases potentiated by B cells and type-I IFNs.

INTRODUCTION

The largest constituency capable of acting as APCs within the spleen are B lymphocytes. B cells are responsible for the production of antibodies that help to protect the host eliminate invading pathogens, but if directed against inappropriate self or innocuous targets, these autoantibodies can initiate both systemic and localized inflammatory reactions through antibody-dependent cellular cytotoxicity or immune complex deposition (223). B cell antibody production is also critical for prophylactic vaccination against many viral and bacterial pathogens (224), and more recently even parasitic infections and certain cancers (225, 226). Besides the generation of both protective and destructive adaptive antibody responses, B cells are also important in pathogen recognition through innate PRRs, antigen presentation and activation of cognate T cells, and even the production of many pro-inflammatory cytokines and chemokines (IL-6, TNF, Type I IFNs, CCL2,3,4,5, CXCL10, etc.) that bolster immune responses (227). Thus B cells intersect adaptive and innate immune pathways.

Because of the pleiotropic effects that B lymphocytes exert on the overall immune response, having the ability to therapeutically target RKIP in B cells and decrease cytokine production during auto-inflammatory diseases may provide a useful alternative to direct B cell ablation with traditional anti-CD20 therapies like rituximab (228). This therapeutic approach can lead to significantly adverse events including tumor lysis syndrome, cardiac arrest, renal failure, and progressive multifocal leukoencephalopathy (229). Previous data from our laboratory demonstrate that RKIP may play an important role in the generation of cytokines during serial TCR engagement in T cells and after TLR ligation in splenocytes; however, RKIP's functional impact on B cell responses, and specifically to PAMPs, is currently unknown.

It is shown that RKIP is utilized downstream of TLR signaling in B cells, and that it is necessary for the maintenance of TRIF-Type-I IFN transcriptomic gene signature. Specifically, through genetic disruption of the RKIP gene in B cells, and through its exogenous inhibition using the small molecule inhibitor locostatin, we demonstrate that the proper function of RKIP is necessary for optimal production of IFNα and the interferon stimulated chemokine CXCL10 after exposure to the nucleic acid adjuvant Poly I:C. Due to the critical nature of Type-I IFN responses in anti-viral immunity, augmentation of Th1 and CTL reactions, contextual immune suppression, and enhancement of B cell function after PAMP sensing, the ability to therapeutically inhibit these responses affords a unique opportunity to help control inappropriate immune reactions that lead to human disease. Finally, these studies provide new insight into the basic mechanisms of nucleic acid adjuvant usage by B cells, and how RKIP may be important for the maintenance of these responses during vaccination.

RESULTS

Since RKIP was involved in the TLR4 response (chapter 4), we hypothesized that after TLR ligation, RKIP is transiently recruited to a membrane-associated signaling complex. The functional significance of this interaction was decreased cytokine output after loss of RKIP through genetic interruption or by therapeutic blockade. In light of these findings, we next sought to determine the specific nature of the lesion that exists in the absence of RKIP in the context of TLR ligation. Clinically, this is a very important question given RKIP's impact on cytokine production during PRR ligation because it could potentially open the door to both a novel therapeutic strategy for inflammatory diseases and could shed light on the importance of RKIP during vaccine-adjuvant based interventions.

Loss of B cells abrogates the disappearance of RKIP after LPS stimulation

In order to choose a model to best study the effects of RKIP loss during TLR responses, we established four major criteria: 1) select a cell population that played an important and established role in human inflammatory diseases, 2) test cells that were important for vaccine-adjuvant based therapies, 3) study a population that feasibly allowed testing of enough cells to undertake a systems approach to examine the role of RKIP, and 4) the cells chosen must also exhibit the same phenomenon of RKIP disappearance after TLR ligation seen in the chapter 4 data set. B lymphocytes were best suited to satisfy these criteria because they are known to be critical players in many auto-inflammatory conditions such as RA and SLE, they are critical for the production of protective antibodies during vaccine-based therapies by responding to adjuvants like monophosphoryl lipid A (MPL), and they make up 40-50% of the splenocytes cell mass thus providing a feasible number of cells for various experimental techniques (230-235).

Finally, we stimulated bulk splenocytes from wild type, TCR-$\beta\delta^{-/-}$ (no T cells), and RAG-$1^{-/-}$ mice (no B or T cells) and found that the RKIP disappearance after TLR4 ligation with LPS was greatly diminished when B cells were absent ($RAG^{-/-}$) but was retained when only T cells were depleted ($\beta\delta^{-/-}$), suggesting that B cells were a major contributor to the phenomena outlined in chapter 4 (Figure 5-1A; compare 0 to 50μg LPS).

$RKIP^{-/-}$ B cells have higher basal levels of phosphorylated-ERK and TLR4/TLR9 engagement leads to transient disappearance of RKIP protein and reciprocal increases in p-ERK in B cell enriched populations

In order to test the role that RKIP plays in TLR responses in B cells, we began by purifying naïve "untouched" steady state splenic B cells by magnetic bead negative selection against CD4, CD43, and Ter119 (B cell isolation kit, Miltenyi Biotec). This method results in a highly enriched B cell population (~95 ± 2% by CD19 and CD45R expression) that is largely devoid of NK cells (data not shown), CD8 and CD4 T cells, $CD11b^{+}$ monocytes (Figure 5-1B). After purification, approximately 1-2% of the remaining cells are $CD11c^{+}$, so we cannot rule out the possibility that some plasmacytoid and other dendritic cell populations may still be contributing to any effect seen, but they are massively outnumbered by B cells. Using this B cell enriched population we determined whether p-ERK aberrations existed when RKIP was knocked out. We examined B cells directly *ex vivo* from wild type or $RKIP^{-/-}$ mice and found that there were higher amounts of basal p-ERK levels in B cells devoid of RKIP by immunoblot (Figure 5-2A). Next, we wanted to determine if this B cell enriched population behaved similarly to bulk splenocytes in response to TLR ligation. To test this, we treated wild type B cells with 9μg/ml CpG-B, 50μg/ml LPS, or vehicle alone and harvested cells 10 min, 1 h, 2 h, 4 h, or overnight after stimulation. We observed that B cells, after stimulation with CpG-B, a TLR ligand with a

penchant for B cells, begin to have significant amounts of p-ERK after about 1 h and these levels increase to a maximum at 4 h post stimulation (Figure 5-2B). This maximum p-ERK is preceded by a moderate decrease in RKIP at 2 h post stimulation, which is consistent with the data in Figure 4-2A/B. After TLR4 ligation with LPS, however, p-ERK is maximally induced at 1 h after stimulation and decreased thereafter. Consistent with our findings in bulk splenocytes presented in chapter 4, this high p-ERK is preceded by a transient disappearance of RKIP 10 min after TLR4 ligation (Figure 5-2C). Taken together, these data show these splenic B cell enriched populations perform similarly to bulk splenocytes in the context of RKIP's behavior after TLR ligation.

LPS and CpG-B drive divergent B cell cytokine programs partially controlled by RKIP

Next, we wanted to test whether RKIP was necessary for cytokine production in response to LPS and CpG-B in our enriched B cell population. Therefore, we treated wild type and RKIP$^{-/-}$ B cells with medium (data not shown), LPS, or CpG-B overnight, and subjected the supernatants from these cultures to multiplex cytokine array analysis. The vast majority of cytokines were made similarly between wild type and RKIP$^{-/-}$ (Figure 5-3A), and some were not produced in response to either CpG-B or LPS including: IL-3, IL-4, IL-5, IL-7, IL-12, IL-13, IL-17, IFNγ, M-CSF, Eotaxin, CXCL5, and LIF (data not shown). Of the cytokines that were different, most were decreased in RKIP$^{-/-}$ B cells compared to wild type, except for CCL5 in response to CpG-B, and IL-2 in response to LPS (Figure 5-3B). Also, we observed that the cytokine programs that were generated in response to LPS and CpG-B varied from one another. For example, CpG-B, which has previously been described as a strong stimulator of B cell responses (236), was much more potent at inducing pro-inflammatory cytokines such as: IL-1α/β, IL-6, TNFα, GM-CSF, and IL-9. Also, CpG-B induced high quantities of CCL2, CCL3, and CCL4 chemokines compared to

LPS (Figure 5-3C). In contrast, LPS was able to potently stimulate CXCL10 and CCL5 chemokines more than CpG-B, which implies that these chemokines are more likely to be associated with TRIF stimulation rather than MyD88. Given the vastly different cytokine profiles in response to stimulation through MyD88 alone or in conjunction with TRIF, we next tried to validate these findings by conventional ELISA by testing Poly I:C in order to examine TRIF stimulation. We stimulated our naïve splenic B cell enriched populations with medium, LPS, Poly I:C, or CpG-B overnight and measured IL-1β, CCL2, CCL3, CCL5, and CXCL10 in the culture supernatants. We also measured the type I interferons IFNα, and IFNβ, given that our multiplex array suggested a potential effect in the TRIF pathway. We found that several cytokines were lower than the lowest limit of detection by conventional ELISA after TLR ligation including IL-1β, CCL2, and IFNβ (data not shown). CCL3, which had no genotype effect in our multiplex array, also showed no difference by ELISA (Figure 5-3D). When testing for CCL5, CXCL10, and IFNα, we found that RKIP$^{-/-}$ B cells made less of these cytokines compared to wild type (Figure 5-3D & Figure 5-8B), but only when the TRIF signaling pathway was driven alone with Poly I:C. Taken together, these data suggest that RKIP may be necessary for TRIF-dependent cytokine production.

Naïve RKIP$^{-/-}$ B cells have an attenuate transcriptome which normalizes rapidly after TLR ligation with LPS or CpG-B

In order to better understand the altered cytokine responses in B cells devoid of RKIP, we isolated total mRNA from wild type and RKIP$^{-/-}$ B cells that were naïve or stimulated for 1 h *in vitro* with either LPS or CpG-B for RNA sequencing. Interestingly we found that in naïve B cells, 884 genes (3.7% of total) were significantly different in RKIP$^{-/-}$ compared to wild type (Figure 5-4C). Of these 884 genes that were significantly different, 870 were reduced in the

RKIP$^{-/-}$ B cells compared to wild type, suggesting that in the absence of RKIP, these cells have a transcriptome that is attenuated at baseline (Figure 5-4A). However, when RKIP$^{-/-}$ B cells were stimulated with either LPS or CpG for just 1 h, their transcriptomes became largely normalized compared to wild type (Figure 5-4B). LPS seems to have a slightly stronger effect on transcriptome normalization compared to CpG-B, most likely because of its ability to trigger both the MyD88 and TRIF pathways simultaneously. In fact, after stimulation, the majority of significantly altered genes in RKIP$^{-/-}$ B cells were increased rather than decreased, suggesting that even though RKIP$^{-/-}$ B cells may start at a disadvantage at the mRNA level, the transcriptome can be rapidly normalized, or even exhibit slightly higher induction of some genes after TLR ligation (Figure 5-4C).

Pathway analysis of altered genes in RKIP$^{-/-}$ B cells reveals an enrichment of pathways involved in mitochondrial function, TLR signaling, and cytokine responses

Next, we wanted to determine whether the genes that were significantly different in untouched RKIP$^{-/-}$ B cells were restricted to specific pathway alterations, or if the transcriptome attenuation was a global effect on all pathways. In order to test this, we subjected all of the genes that were statistically significantly different between wild type and RKIP$^{-/-}$ and had a $\log_2$ (fold change) greater than ± 1.2 (absolute fold change greater than ± 2.3) to pathway analysis using the Ingenuity Pathway Analysis (IPA) software algorithm. IPA identified 371 pathways that contained at least one of our genes of interest, of those 371, 98 had enrichment not due to chance (Table III). The most significantly enriched pathways in RKIP$^{-/-}$ B cells were those that were important for mitochondrial function, TLR signaling, and cytokine responses (Figure 5-5A). Additionally, pathways important for proliferation, apoptosis, and co-stimulation were also

enriched, but to a lesser degree. Most of these canonical pathways share important genes between them, which could explain why they showed similar enrichment.

RKIP$^{-/-}$ B cells do not have significantly altered basal or maximal mitochondrial respiration before or after stimulation with TLR ligands

Our IPA analysis determined that the most significantly enriched pathway in RKIP$^{-/-}$ B cells was composed of 22 different genes important for mitochondrial function. These genes were comprised of components of each of the major complexes involved in the electron transport chain, as well as, several associated kinases known to modulate their function (Table IV). Because all of the identified genes were decreased in B cells devoid of RKIP, we hypothesized that oxidative phosphorylation may also be diminished, and may be a contributing factor to decreased cytokine output. Also, given recent evidence that metabolic products can post-transcriptionally regulate cytokine translation (237), we thought it necessary to test the mitochondrial function of RKIP$^{-/-}$ B cells. In order to determine if loss of RKIP played a role in oxidative phosphorylation, we stimulated B cells from wild type (C57BL/6J), RKIP$^{-/-}$, RKIP$^{+/-}$, and RKIP$^{+/+}$ mice with LPS, CpG-B, Poly I:C, PMA + ionomycin, or medium alone for 1 h, and then analyzed their rate of oxygen consumption (OCR) on the Seahorse XF96 extracellular flux analyzer which measures several parameters of mitochondrial function (Figure 5-6A). We observed no significant differences in either the basal OCR (Figure 5-6B) or maximum OCR (Figure 5-6C) between groups regardless of stimulation. Thus, 1 h after TLR stimulation no difference was seen but it is possible that during the stimulation metabolic differences occurred, but this was not tested. It remains open that early during stimulation, metabolic changes may occur, but if so, this did not last past 1 h.

Steady state RKIP$^{-/-}$ B cells have an attenuated TRIF-Type I Interferon transcriptome signature

After demonstrating that mitochondrial function was relatively normal in RKIP$^{-/-}$ B cells, we next re-examined the RNA sequencing data and IPA pathway analysis to assess the TLR signaling pathways. We observed by RNAseq that untouched naïve RKIP$^{-/-}$ B cells exhibited a decreased TRIF-type I interferon gene signature that included significant reductions in upstream mediators of type I interferon generation including: *Ticam1* (TRIF), *Traf3, Irf3, Irf5, Irf7, Ikbke* (IKKε), as well as a subunit of the type I interferon receptor (*Ifnar1*). Other pathway members including: *Tmem173* (STING), *Tram, Tank, Tbk1*, and *Mavs* (IPS-1) were also reduced, but not significantly so (Figure 5-7A, left panel). Naïve B cells devoid of RKIP also had significant reductions in *Tlr3* and *Tlr9* transcript levels, but the rest of their PRRs were, for the most part, intact (Figure 5-7A, right panel). Additionally, the MyD88 and NF-κB signaling pathways were also somewhat decreased, but this was less robust compared to the TRIF-type I interferon pathway (Table V). Importantly, after stimulation with either LPS or CpG-B for 1 h, we discovered that the vast majority of gene transcripts that were affected at baseline had normalized to wild type levels, with the exception of *Irf7* after CpG-B stimulation (Table VI). To avoid the complication of using disadvantaged RKIP$^{-/-}$ B cells, we employed locostatin to test RKIP inhibition in wild type cells. We found that after 2 h of Poly I:C stimulation in wild type B cells, in the presence of absence of the RKIP inhibitor locostatin, there was no significant difference in the transcript levels of *Irf3, Irf5, Irf7, Traf3, Tbk1, Ikbke,* or *Ifnar1* between B cells with RKIP inhibition or none (Figure 5-7B). Nevertheless, RKIP inhibition had an effect on *Ifna* transcription when wild type B cells were pretreated with locostatin prior to Poly I:C stimulation. The amount of *Ifna* mRNA was significantly reduced 1-2 h after stimulation compared to vehicle

pre-treated B cells (Figure 5-7C). However, after approximately 6 h post stimulation, the transcript levels of *Ifna* were indistinguishable between groups. Taken together these data suggest that RKIP may be important for the early induction of *Ifna*, but there are mechanisms in place that allow the transcript levels of this gene to approximate normal with a sustained stimulus.

RKIP optimizes IFNα synthesis and the Type I IFN stimulated chemokine CXCL10 following TLR3 ligation

In order to determine whether the perturbations in TRIF-type I interferon seen in RKIP$^{-/-}$ B cells, or RKIP blockade, had any functional consequences, we tested cytokine output from these pathways. First, enriched B cells populations from wild type and RKIP$^{-/-}$ mice were stimulated with Poly I:C with or without RKIP blockade for 6 h (data not shown) or overnight and CXCL10 and CCL5 were measured in the culture supernatants. Consistent with findings in Figure 5-7, we found a severely diminished (~30% of wild type) amount of the interferon-stimulated chemokine CXCL10 in RKIP$^{-/-}$ B cells after stimulation (Figure 5-8A). In contrast, CCL5, a chemokine only partially dependent upon TRIF signaling, was slightly decreased (~70% of wild type). Importantly, RKIP blockade in wild type B cells mirrored CXCL10 output from RKIP$^{-/-}$ B cells. Nevertheless, locostatin had little to no effect on RKIP$^{-/-}$ B cells, suggesting a moderate degree of specificity (Figure 5-8A).

To test the therapeutic relevance of these findings, we repeated the experiment described in Figure 5-8A in wild type B cells alone in the context of type I interferon receptor blockade (anti-IFNAR1) or isotype control. First, RKIP blockade potently inhibited IFNα production at 6 h in culture and during its feed-forward enhancement after overnight (Figure 5-8B). In fact, the

reduction IFNα was even greater after overnight culture, suggesting the RKIP may play a role in both the initial production of type I interferons, but also in their ability to enhance their own production through a feed-forward loop. Consistent with our findings in Figure 5-8A, we also found a significant decrease in CXCL10 production from wild type B cells after RKIP inhibition, and to a lesser degree CCL5 (Figure 5-8B). Importantly, in the presence of type-I interferon receptor blockade CXCL10 production was abolished, demonstrating its dependence on type-I interferon signaling. In contrast, CCL5 production was independent of IFNAR blockade. Taken together, these data suggest that RKIP may be a valuable therapeutic target to inhibit the production of type I interferons and their associated downstream effectors during TLR responses in APCs.

DISCUSSION

B cells are well known to impact vaccine development due to their antibody producing capacity, they are nevertheless understudied cytokine producing cells that may contribute to vaccine adjuvanticity and the potentiation of autoimmune diseases (238-241). One way B cells can contribute to adjuvant responses is by producing cytokines in response to PAMPs (121, 238, 242, 243). Through these interactions, B cells can be significant producers of both cytokines and chemokines which contribute to the establishment of the inflammatory milieu and chemotactic locomotor gradients (244, 245). Recently, there have been renewed efforts to better utilize B cell responses to nucleic acid adjuvants to foster vaccine development for HIV, malaria, intracellular pathogens, and other emerging infections (238, 246, 247). A successful application of this strategy has been the mechanistic reexamination of the YF-17D vaccine against yellow fever causing *Flaviviridae* which provides protection through TLR7 ligation and Type-I IFN production (248-250). Analogously, B cell depleting agents such as Rituximab (anti-CD20 mAb) have been utilized as a successful treatment modality for autoimmune diseases such as rheumatoid arthritis, multiple sclerosis, systemic lupus erythematosus and many others (233, 251). What both of these reactions have in common is the necessity of B cells to respond to initial triggering through their PRRs in order to produce productive reactions *in vitro* and *in vivo* (252).

Previous data from our laboratory implicated RKIP as an important molecule for productive cytokine responses after TLR signaling in splenocytes, yet the role that RKIP plays in these critical initiating events of PRR ligation in B cells is unknown and provides a fertile area of study. We initially observed that depleting B cells from our bulk splenocyte populations using $RAG^{-/-}$ mice abrogated our central finding in chapter 4 (i.e. the “disappearance” of RKIP shortly

after TLR ligation), while losing only T cells ($\beta\delta^{-/-}$ mice) kept this phenomenon intact (Fig. 5-1A). The fact that B cells exhibited similar responses to bulk splenocytes, in terms of RKIP after LPS and CpG stimulation and high basal p-ERK levels when lacking RKIP, verified that this cell population was at least a significant contributor to our findings in chapter 4 (Fig. 5-2A-C). However, because our method to enrich naïve splenic B cell populations does not robustly deplete $CD11c^{+}$ cells (Fig. 5-1B), it prevents us from ruling out the possibility that conventional and plasmacytoid dendritic cells might also play a role in our studies. Although the likelihood of pDC effects may be marginal given that they do not express TLR3 (253) and that TLR9 ligation leads to IFNα production through IKKα and IRF7 (42), which was not seen in our studies (Fig. 5-3D).

Upon investigation of the cytokine milieu driven by either LPS or CpG-B in B cells, we observed vastly divergent outputs depending on the nature of the ligand. CpG-B was much more potent than LPS in inducing pro-inflammatory cytokine production including IL-1, IL-6, TNF, GM-CSF, and others. However, LPS stimulated B cells were more efficiently able to produce factors normally associated with TRIF, namely CXCL10 and CCL5 (Fig. 5-3C). Interestingly, RKIP seemed to be more important for the cytokine output in response to CpG-B, rather than LPS, in B cells (Fig. 5-3B). This could be due to several factors including the ability of LPS to signal through both MyD88 and TRIF, potentially giving this stimulus a way to circumvent small signaling lesions due to heterologous pathway activation. Consistent with this hypothesis, when inducing the TRIF pathway alone with the dsRNA Poly I:C, we observed attenuated production of several TRIF-associated cytokines including IFNα, CXCL10, and CCL5, but not CCL3 which is made indiscriminately in response to NF-κB activation (Fig 5-3D). Nevertheless, consistent with Figure 4-5A, $RKIP^{-/-}$ cells were altered in their output of some cytokines but not others.

Because the generation of many cytokines is dependent on the cooperative nature of several pathways, it becomes very difficult to pinpoint the exact location of RKIP function.

In order to better understand the molecular mechanisms of these differential adjuvant responses, as well as to garner new insights into how RKIP affects cytokine production from B cells, we utilized total transcriptome RNA sequencing of naïve, LPS, and CpG-B stimulated B cells from wild type and RKIP$^{-/-}$ mice. This approach has, to our knowledge, not been previously utilized to interrogate the RKIP pathway during TLR signaling. Through RNAseq, we discovered that the vast majority (~96.2%) of mRNAs were unaffected in RKIP$^{-/-}$ B cells. However, there were 884 mRNAs that had significantly different expression levels in naïve RKIP$^{-/-}$ B cells compared to wild type, and interestingly, of these mRNAs, 870 (98.4%) were decreased in RKIP deficient cells (Fig. 5-4A). Importantly, we also observed that within 1 hour of TLR ligation with either LPS or CpG-B many of these transcripts normalize to wild type levels, or in some cases, are induced even higher than wild type (Fig. 5-4B/C). This suggests that RKIP$^{-/-}$ B cells, may start off at a signaling disadvantage due to their partially attenuated transcriptome, but may catch up, at least at the level of transcription, over time. This is an excellent example of why it is difficult to compare a knockout mouse to wild type due to a disadvantage in the steady state, even though there is no obvious phenotypic defect.

In order to determine if the affected transcripts from our RNA sequencing analysis were evidence of specific pathway alterations or stochastic changes within the transcriptome, we used Ingenuity's pathway analysis (IPA) in conjunction with the Database for Annotation, Visualization and Integrated Discovery (DAVID) to mine for enrichment of particular pathways based on our list of altered genes. We discovered that although many canonical signaling pathways were affected, there was a significant enrichment in pathways involved in

mitochondrial function, TLR signaling, cytokine responses, co-stimulation, and survival (Fig. 5-5A, Table III).

Recent findings from Dr. Pearce's laboratory and others have implicated products involved in cellular metabolism as regulators of cytokine production post-transcriptionally (237), as well as, from an energetics standpoint (254). Because genes involved in mitochondrial function were the most highly enriched pathway within RKIP$^{-/-}$ B cells, we tested the capacity of these cells to properly undergo oxidative phosphorylation *ex vivo* and after stimulation with TLR ligands. Despite the fact that loss of RKIP led to a number of decreased transcripts involved in the oxidative phosphorylation machinery (Table IV), RKIP$^{-/-}$ B cells had no significant difference in their oxygen consumption rates, and thus their ability to undergo oxidative phosphorylation, before or after stimulation with LPS, CpG-B, or Poly I:C compared to wild type (Fig. 5-6A/B).

With mitochondrial dysfunction providing little evidence to explain the aberrations in cytokine production, we next turned our attention to evaluating mRNAs involved in TLR signaling. Upon examination, we observed that naïve RKIP$^{-/-}$ B cells had a greatly attenuated "Type-I IFN gene signature", previously described by others (255), that included significantly decreased levels of *Ticam1, Traf3, Irf3, Irf5, Irf7, Ifnar1, Ikbke,* and others (Fig. 5-7A). RKIP$^{-/-}$ B cells also had lower expression levels of some genes involved MyD88 and NF-κB signaling as well, but to a lesser degree (Table V). Interestingly, these cells also had lower basal expression of *Cd40,* which could suggest that in addition to having an attenuated TLR signaling apparatus, these B cells may have trouble accepting help from cognate T helper cells through CD40L-CD40 interaction. Because it is still unknown exactly how B cells integrate the initial activation events of PRR ligation with recognition of antigen through the BCR and T cell help via CD40L, it is unclear exactly how large of a disadvantage diminution of two critical signaling events would place

RKIP$^{-/-}$ B cells at. Future studies looking at CD40L-mediated help, as well as BCR crosslinking effects in the context of these attenuated pathways in RKIP$^{-/-}$ mice should be conducted before conclusions can be made regarding effects on the entirety of the B cell response.

However, as with the broad overview of transcriptomic changes between naïve and TLR triggered B cells, most of these deficits in transcript levels are normalized after stimulation, with the exception of *Irf7* after TLR9 ligation (Table VI). This normalization was confirmed independently of RNA seq by qPCR analysis of several genes associated with the Type-I IFN signature after Poly I:C stimulation with or without RKIP blockade (Fig 5-7B). Nevertheless, despite the correction of genes involved in the Type-I IFN generating signaling machinery, transcript levels of *Ifna* were still decreased until about 6 hours post TLR3 ligation with Poly I:C in the presence of RKIP blockade in wild type B cells (Fig. 5-7C). The functional effect of this was a significant reduction in both IFNα protein and the interferon-dependent chemokine CXCL10 (Fig. 5-8B). The abatement of these two important molecules was also confirmed in RKIP$^{-/-}$ B cells (Fig. 5-8A, Fig 5-3D). Additionally, we have observed that after adoptive transfer of wild type TCR transgenic T cells into RKIP deficient hosts, these T cells have a decreased migratory capacity to peripheral tissues, especially to the liver (data not shown). This migration into the hepatic circulation has been shown to be dependent on the generation of chemotactic gradients involving CXCL9 and CXCL10 and their interaction with the CXCR3 receptor on circulating T cells (256), and thus is consistent with the notion that RKIP$^{-/-}$ mice have deficits in the production of these cytokines. Finally, CCL5 was also decreased in the presence of RKIP blockade; however, unlike CXCL10, CCL5 is not dependent on type-I IFN signaling and is only partially dependent on downstream TRIF signaling (Fig.5-8B). Currently, it is still unclear whether or not the role that RKIP plays in the generation of IFNα and its sequelae and the

production of CCL5 are one in the same. Given that the MyD88 and NF-κB signaling pathways also were affected in RKIP$^{-/-}$ B cells, and that they also contribute to the production of CCL5, it is conceivable that RKIP's role in CCL5 generation may be independent of its effects on the TRIF-Type-I IFN pathway.

Previous work from other laboratories have established that productive B cell responses to nucleic acid PRR ligands are dependent upon the fidelity of the Type-I IFN positive feed forward loop (257). This is due in part to the up-regulation of TLR3 and TLR7 expression which provide more robust reactions to occur following initial activation (258), and the increase production of B cell survival factors, such as BAFF (259). This feed-forward loop is exemplified by the increase in IFNα production between 6 hours after Poly I:C stimulation and overnight (Fig. 5-8B, left panel). Interestingly, RKIP blockade reduced both the initial production of IFNα (6 h) and its enhanced feed-forward production (O/N), perhaps even to a larger extent. These data suggest that RKIP may play a role in facilitating the Type-I IFN response both before and after the generation of IFNα *per se*. The mechanism by which RKIP mediates these effects requires more study, however we hypothesize that RKIP may act by stabilizing signaling complexes upstream of Type-I IFN production (most likely at the level of TRAF3, TBK-1, and IKKε) and/or coupling the Type-I IFN receptor to its downstream machinery which would facilitate proper feed-forward signaling. This hypothesis will be expanded upon in chapter 6.

Irrespective of the exact molecular role that RKIP plays in generation of Type-I IFNs, the fact that its functional blockade is druggable and can essentially attenuate production of IFNα, and its related effectors, provides a novel target for therapeutic intervention in auto-inflammatory diseases that are predominated or potentiated by Type-I IFNs, such as SLE.

Figure 5-1: Loss of B cells abrogates the disappearance of RKIP after LPS stimulation

(A) Representative immunoblot of RKIP in bulk splenocyte lysates from wild type C57BL/6J mice, T cell deficient TCR-$\beta\delta^{-/-}$ mice, or T and B cell deficient RAG-$1^{-/-}$ mice stimulated for 10 min with either 10μg/ml or 50μg/ml of LPS. Balanced slat solution (BSS) was used as the vehicle control (0μg/ml LPS). N.A. = not acquired. (B) Representative flow cytometry plots illustrating the gating strategy for B cell enrichment before and after magnetic bead purification. Naïve "untouched" B cells were isolated by negative selection after incubation with anti-CD4, anti-Ter119 (expressed on all leukocytes except B cells) (260), and anti-CD43 (expressed on all T and B cells that have previously been activated) (261) antibody-magnetic bead complexes. The average purity of B cell enriched populations is 95 ± 2% (N>50 mice).

A

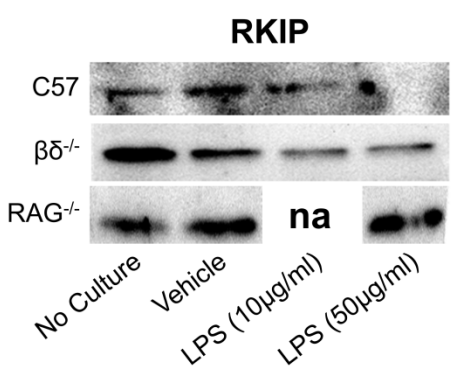
RKIP
C57
βδ-/-
RAG-/-
na
No Culture
Vehicle
LPS (10μg/ml)
LPS (50μg/ml)

B

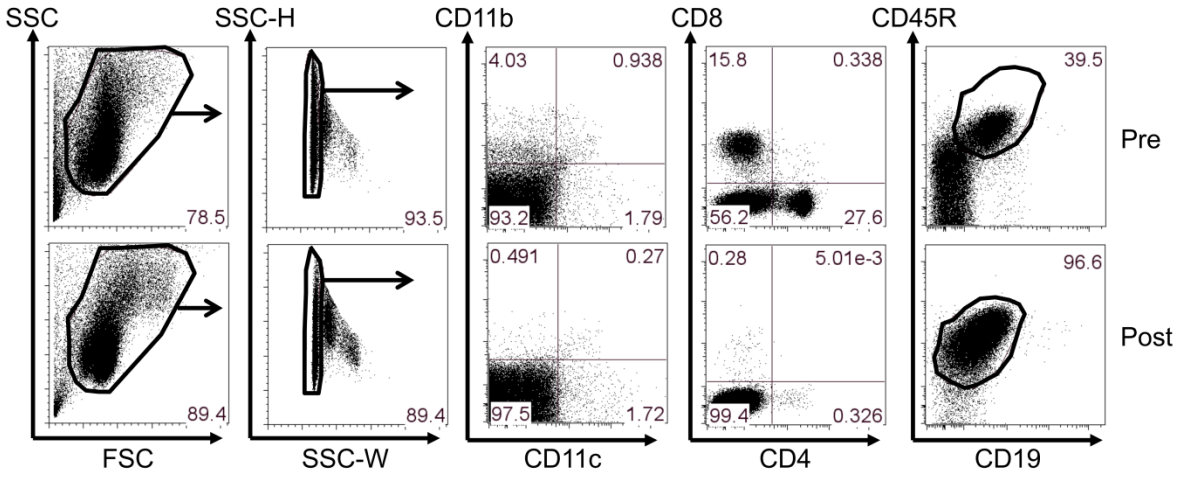
SSC
SSC-H
CD11b
CD8
CD45R
78.5
93.5
4.03
0.938
93.2
1.79
15.8
0.338
56.2
27.6
39.5
Pre
89.4
89.4
0.491
0.27
97.5
1.72
0.28
5.01e-3
99.4
0.326
96.6
Post
FSC
SSC-W
CD11c
CD4
CD19

Figure 5-2: RKIP$^{-/-}$ B cells have higher basal levels of phosphorylated-ERK (A) phosphorylated-ERK/ERK-1 ratios determined by densitometric analysis of lysates from unstimulated splenic B cell enriched populations. **TLR4 and TLR9 ligation leads to transient disappearance of RKIP protein and reciprocal increases in p-ERK in B cell enriched populations** (B) Immunoblots of RKIP, pERK-1/2, and ERK-1 in splenic B cell enriched populations from wild type mice stimulated with either media, 50μg/ml LPS, or 9μg/ml CpG-B for 10 min, 1 h, 2 h, 4 h, or overnight. Data are representative of 3 independent experiments.

A

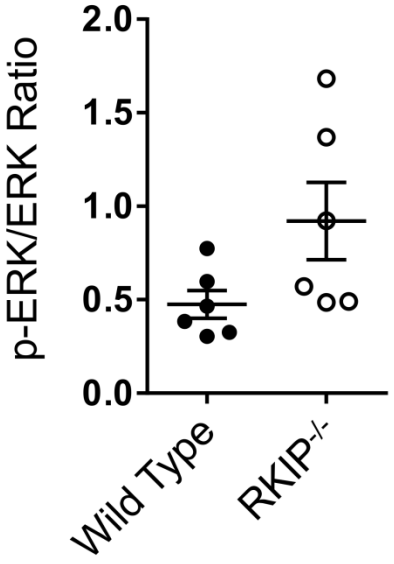
p-ERK/ERK Ratio
2.0
1.5
1.0
0.5
0.0
Wild Type
RKIP-/-

B

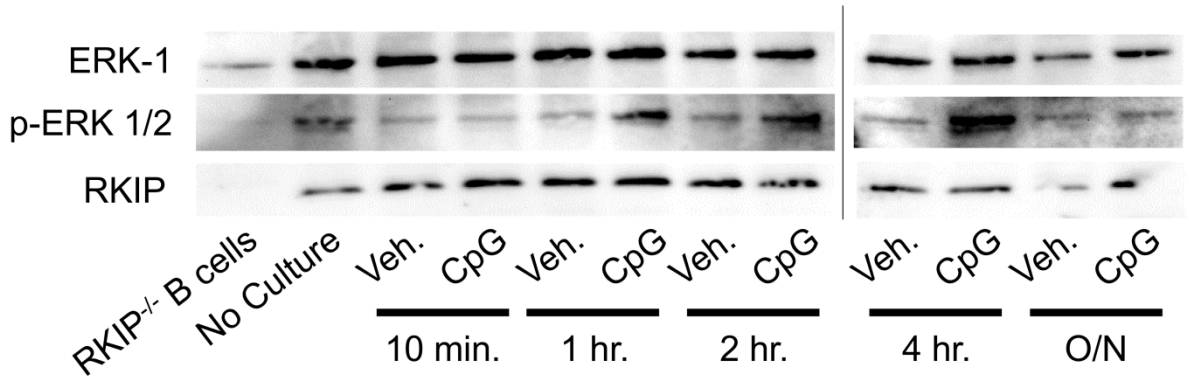
ERK-1
p-ERK 1/2
RKIP
RKIP-/- B cells
No Culture
Veh.
CpG
Veh.
CpG
Veh.
CpG
Veh.
CpG
Veh.
CpG
10 min.
1 hr.
2 hr.
4 hr.
O/N

C

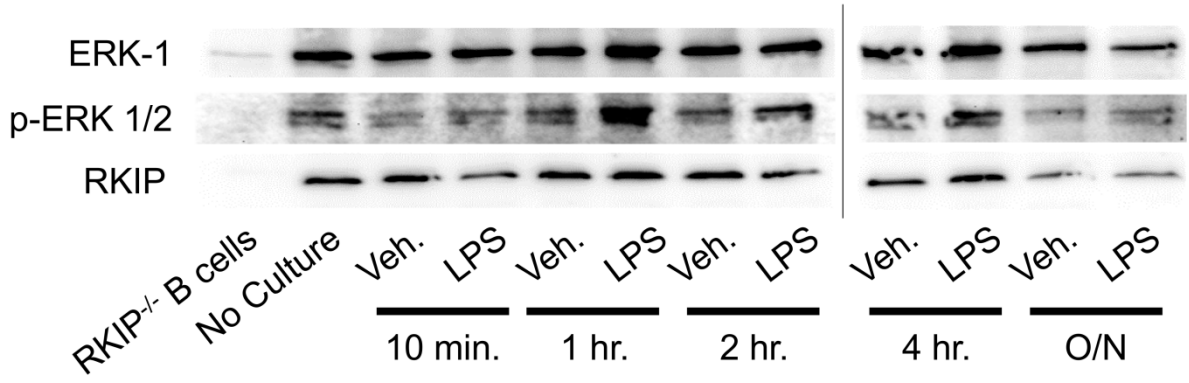
ERK-1
p-ERK 1/2
RKIP
RKIP-/- B cells
No Culture
Veh.
LPS
Veh.
LPS
Veh.
LPS
Veh.
LPS
Veh.
LPS
10 min.
1 hr.
2 hr.
4 hr.
O/N

Figure 5-3: LPS and CpG-B drive divergent B cell cytokine programs partially controlled by RKIP (A-C) Multiplex cytokine array of naïve splenic B cells stimulated with either medium (data not shown), 50μg/ml LPS, or 9μg/ml CpG-B overnight. Data are presented as $RKIP^{-/-}$ quantities or each cytokine normalized to wild type (set to 100). Error bars represent mean ± SEM, and data are from 3 independent experiments; N=6/group. P values determined using *t* tests between 2 groups, using Welch's correction where necessary; **p*<0.05, ***p*<0.01, ****p*<0.001, *****p*<0.0001. (D) Naïve splenic B cells stimulated as in Figure 5-3A with the addition of 50μg/ml Poly I:C overnight. Supernatants from these cultures were used to determine quantities of CCL5, CXCL10, CCL3, and IFNα by ELISA. Error bars represent mean ± SEM, and data are from 3 independent experiments; N=6-9/group. P values determined using *t* tests between 2 groups, using Welch's correction where necessary; **p*<0.05, ***p*<0.01.

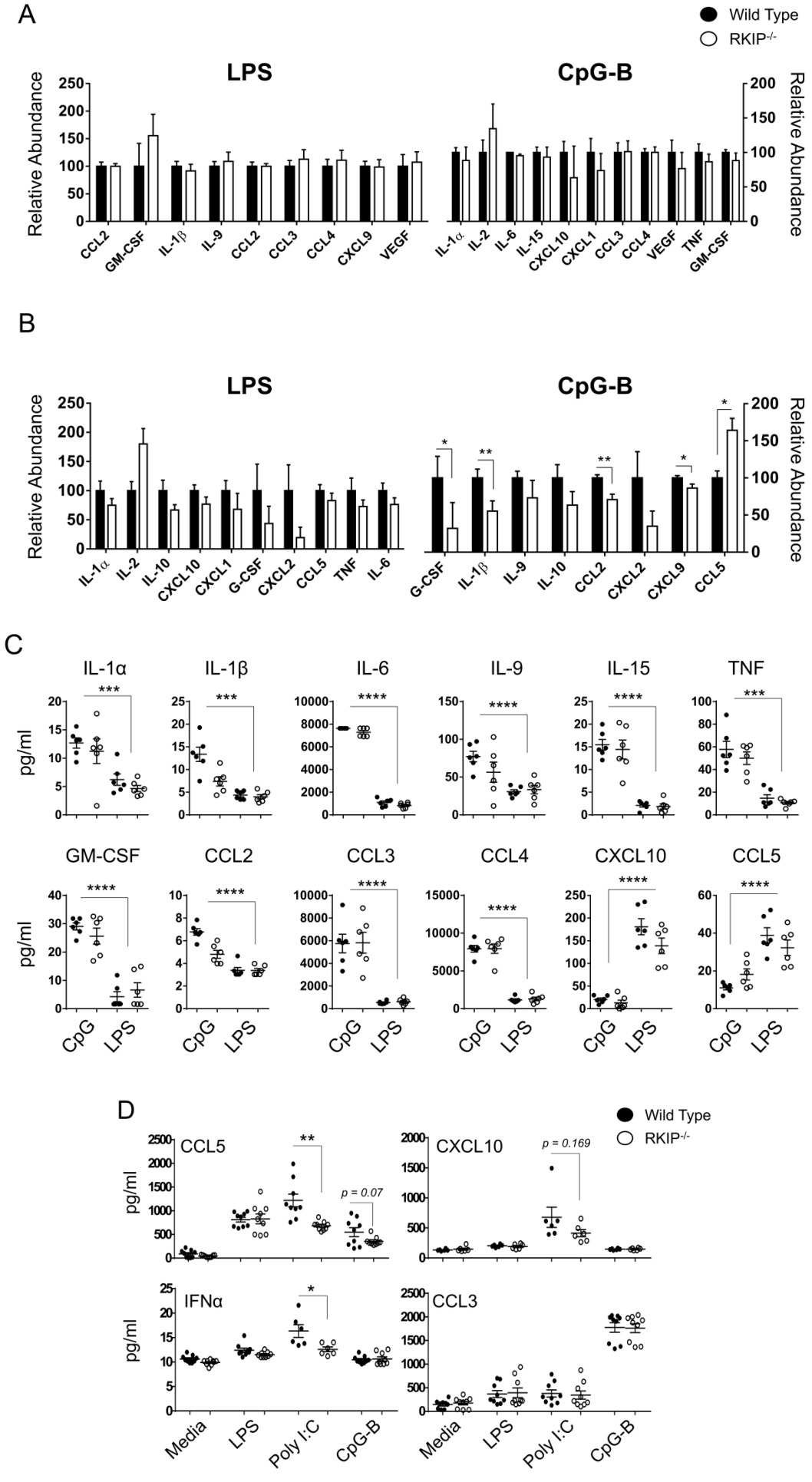
A
Wild Type
RKIP-/-
LPS
CpG-B
Relative Abundance
CCL2
GM-CSF
IL-1β
IL-9
CCL2
CCL3
CCL4
CXCL9
VEGF
IL-1α
IL-2
IL-6
IL-15
CXCL10
CXCL1
CCL3
CCL4
VEGF
TNF
GM-CSF
B
LPS
CpG-B
Relative Abundance
IL-1α
IL-2
IL-10
CXCL10
CXCL1
G-CSF
CXCL2
CCL5
TNF
IL-6
G-CSF
IL-1β
IL-9
IL-10
CCL2
CXCL2
CXCL9
CCL5
C
IL-1α
IL-1β
IL-6
IL-9
IL-15
TNF
GM-CSF
CCL2
CCL3
CCL4
CXCL10
CCL5
pg/ml
CpG
LPS
D
Wild Type
RKIP-/-
CCL5
CXCL10
IFNα
CCL3
pg/ml
p = 0.07
p = 0.169
Media
LPS
Poly I:C
CpG-B

Figure 5-4: Naïve RKIP$^{-/-}$ B cells have an attenuated transcriptome which normalizes rapidly after TLR ligation with LPS or CpG-B (A) Heat map representing the expression of the top 400 altered genes between wild type and RKIP$^{-/-}$ naïve B cell transcriptomes. Color intensity represents relative expression of gene transcripts (0 = min, 100 = max). Total mRNA sent for RNA sequencing was pooled from 3 individual mice in each group. (B) Volcano plots showing significantly increased and decreased genes from naïve splenic B cell enriched populations, or after 1 h stimulation with 50μg/ml LPS or 9μg/ml CpG-B. Numbers represent percentages of all genes analyzed (23,235). (C) Table showing the number of genes that were statistically significantly up-regulated or down-regulated between naïve, LPS stimulated, or CPG-B stimulated wild type and RKIP$^{-/-}$ B cells.

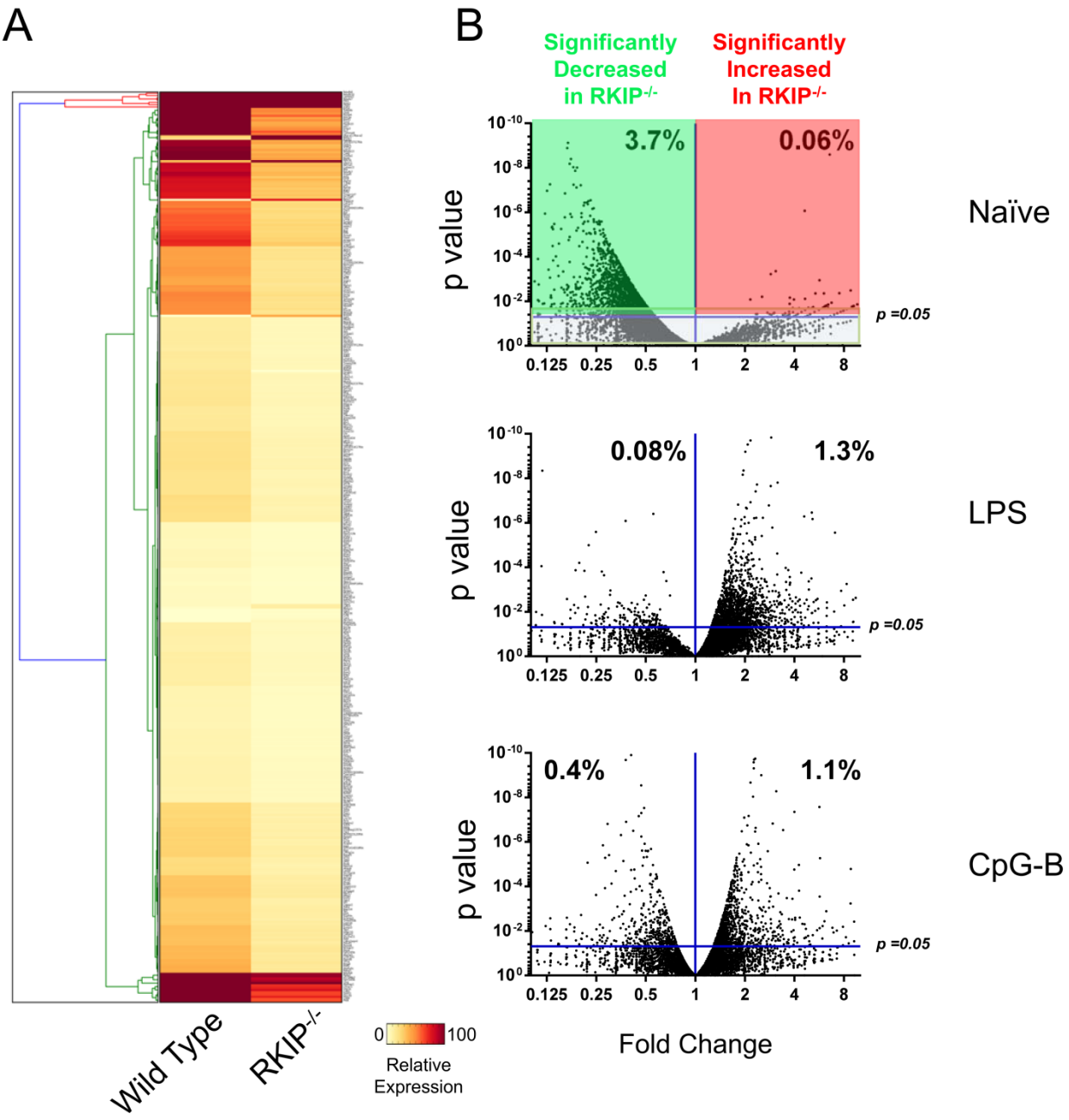

C

	Statistically Significant		± >1.2 Fold Change	
	↑	↓	↑	↓
Naïve	14	870	14	830
LPS	305	19	66	14
CpG-B	265	98	52	35

# of genes with higher (or lower) expression in RKIP-/- vs. Wild Type B cells

Figure 5-5: Pathway analysis of altered genes in RKIP$^{-/-}$ B cells reveals an enrichment of pathways involved in mitochondrial function, TLR signaling, and cytokine responses (A) Top 30 most enriched pathways in naïve RKIP$^{-/-}$ B cells graphically represented as $-\log_{10}$(p-value). Briefly, genes of interest were identified by taking all genes that were found to be statistically significantly different between experimental groups and had a relative fold change of > ±1.2, and subjected to functional pathway analysis using the IPA knowledge database (Ingenuity Systems; Redwood City, CA, USA). IPA cross-references a user's list of genes of interest to known canonical signaling pathways and determines the level of enrichment of a given pathway using the user's gene list and fold changes. IPA then calculates a *P* value based on this enrichment using Fisher's exact test.

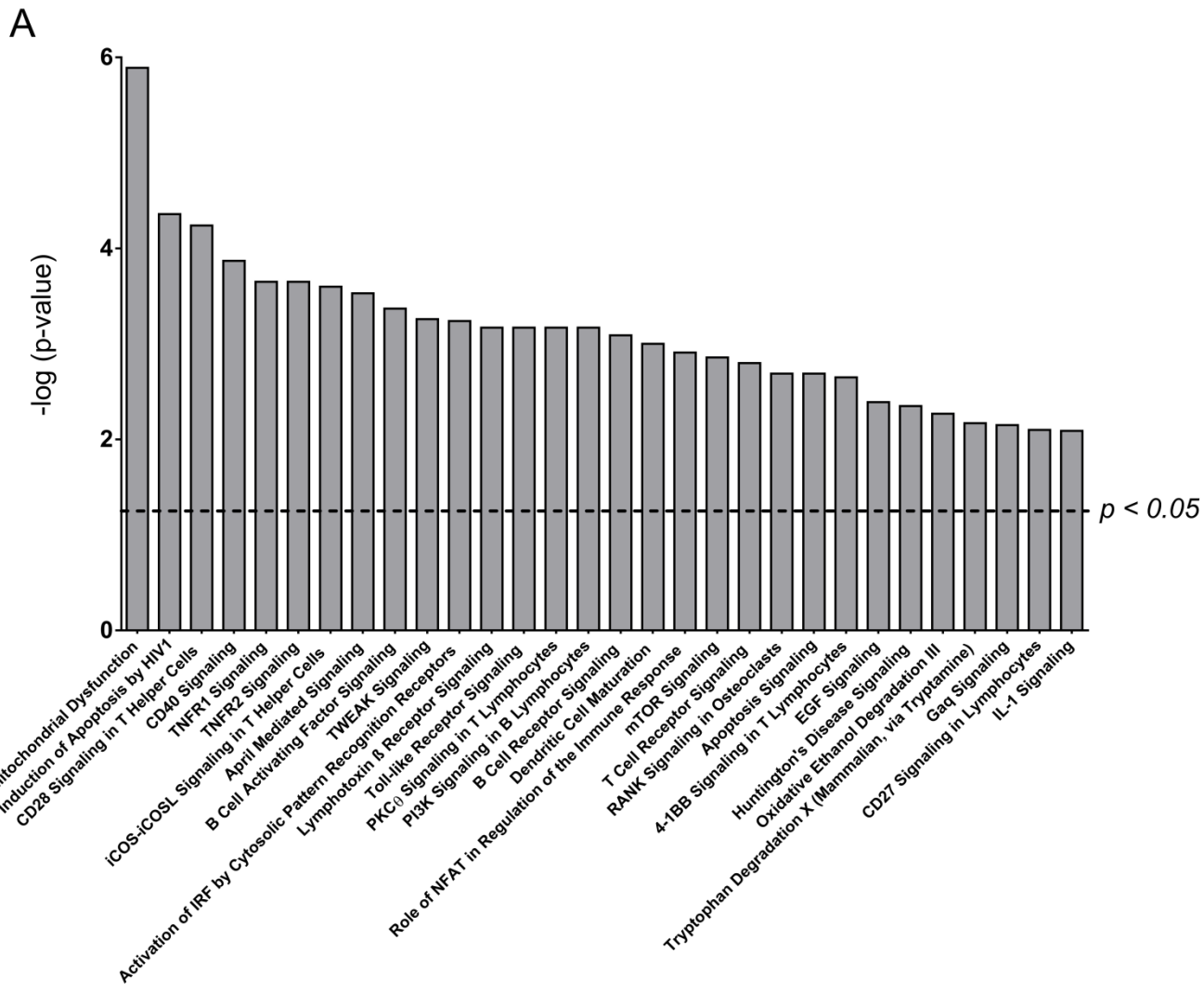
A
-log (p-value)
6
4
2
0
p < 0.05
Mitochondrial Dysfunction
Induction of Apoptosis by HIV1
CD28 Signaling in T Helper Cells
CD40 Signaling
TNFR1 Signaling
TNFR2 Signaling
iCOS-iCOSL Signaling in T Helper Cells
April Mediated Signaling
B Cell Activating Factor Signaling
TWEAK Signaling
Activation of IRF by Cytosolic Pattern Recognition Receptors
Lymphotoxin ß Receptor Signaling
Toll-like Receptor Signaling
PKCθ Signaling in T Lymphocytes
PI3K Signaling in B Lymphocytes
B Cell Receptor Signaling
Role of NFAT in Regulation of the Immune Response
Dendritic Cell Maturation
mTOR Signaling
T Cell Receptor Signaling
RANK Signaling in Osteoclasts
4-1BB Signaling in T Lymphocytes
Apoptosis Signaling
EGF Signaling
Huntington's Disease Signaling
Oxidative Ethanol Degradation III
Tryptophan Degradation X (Mammalian, via Tryptamine)
Gaq Signaling
CD27 Signaling in Lymphocytes
IL-1 Signaling

Figure 5-6: RKIP$^{-/-}$ B cells do not have significantly altered basal or maximal mitochondrial respiration before or after stimulation with TLR ligands (A) Technical diagram showing normal oxygen consumption rate curves and different measurable parameters by Seahorse extracellular flux analysis. Oligomycin is used to inhibit ATP synthase and inhibit mitochondrial respiration, FCCP uncouples the electron transport chain (ETC) allowing for maximal respiration capacity, and antimycin A/rotenone disrupt the ETC preventing oxygen utilization. (B-C) Splenic B cell enriched populations from C57BL/6J, RKIP$^{-/-}$, RKIP$^{+/-}$, and wild type littermates were cultured for 1 h with medium, 50μg/ml LPS, 50μg/ml Poly I:C, 9μg/ml CpG-B, or PMA + ionomycin and subsequently mitochondrial function was assessed by measuring oxygen consumption rates (OCR) expressed as pMoles/min. Basal mitochondrial rates (B) were determined by averaging OCRs at 0, 6, and 12 min (before oligomycin administration) for each mouse. Maximal mitochondrial rates (C) were determined by averaging OCRs at 33 and 40 min (4 min after FCCP administration). N=9 for C57BL6J and RKIP$^{-/-}$ groups from 3 independent experiments, and N=3 for RKIP$^{+/-}$ and RKIP$^{+/+}$ groups from 1 experiment.

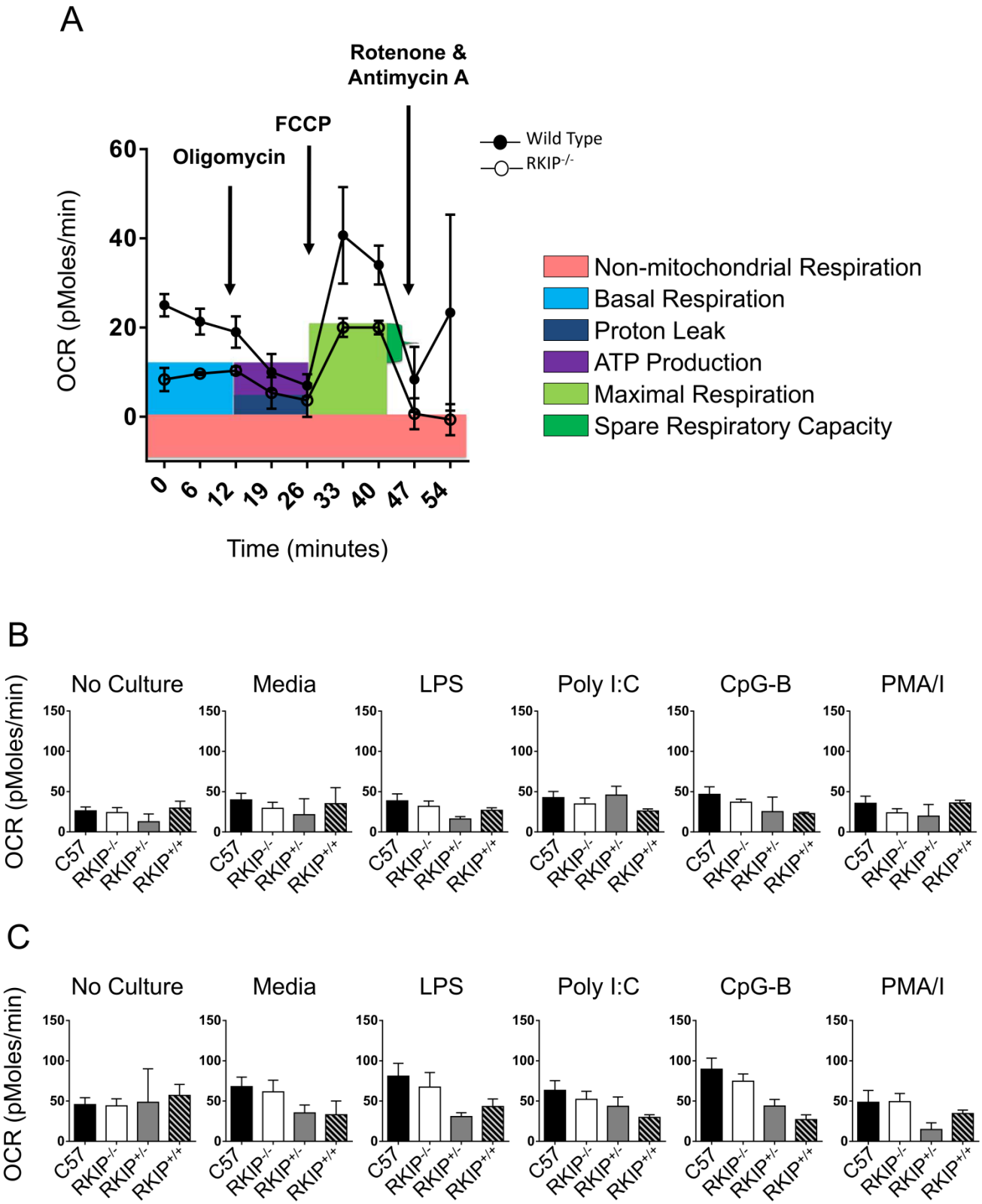
A
Rotenone &
Antimycin A
FCCP
Oligomycin
Wild Type
RKIP-/-
OCR (pMoles/min)
60
40
20
0
0
6
12
19
26
33
40
47
54
Time (minutes)
Non-mitochondrial Respiration
Basal Respiration
Proton Leak
ATP Production
Maximal Respiration
Spare Respiratory Capacity
B
No Culture
Media
LPS
Poly I:C
CpG-B
PMA/I
OCR (pMoles/min)
150
100
50
0
C57
RKIP-/-
RKIP+/-
RKIP+/+
C
No Culture
Media
LPS
Poly I:C
CpG-B
PMA/I
OCR (pMoles/min)
C57
RKIP-/-
RKIP+/-
RKIP+/+

Figure 5-7: Steady state RKIP$^{-/-}$ B cells have an attenuated TRIF-Type I Interferon transcriptome signature (A) Comparison of genes important for TRIF-type I interferon signaling (left panel) and pattern recognition receptor genes (right panel) in naïve wild type and RKIP$^{-/-}$ B cells from RNA sequencing data in Figure 5-4. Data are represented as relative abundance normalized to wild type quantities of each gene (set to 100). P-values calculated by Otogenetics normalized to FPKM using cufflinks software; *p<0.05, **p<0.01, ***p<0.001. (B) qPCR analysis of important TRIF-type I interferon genes from wild type and RKIP$^{-/-}$ B cells stimulated *in vitro* with 50μg/ml Poly I:C and 5μM locostatin or vehicle control (DMSO at same (v/v) percent) for 2 h. Data are expressed as fold change ($2^{-\Delta\Delta Ct}$), error bars represent mean ± SEM, data are from 1 experiment, N=3/group. (C) qPCR analysis of IFNα transcript levels from wild type B cells stimulated with 50μg/ml Poly I:C and 5μM locostatin or vehicle control (DMSO at same (v/v) percent) for 1, 2, 4, or 8 h. In 2 of 3 experiments, locostatin was given concomitantly with Poly I:C, and in 1 of 3 experiments, locostatin was given 10 min prior to Poly I:C stimulation. Error bars represent mean ± SEM, data are from 3 independent experiments N=3 (1 h), 9 (2 h, 4 h), or 6 (8 h); **p<0.01.

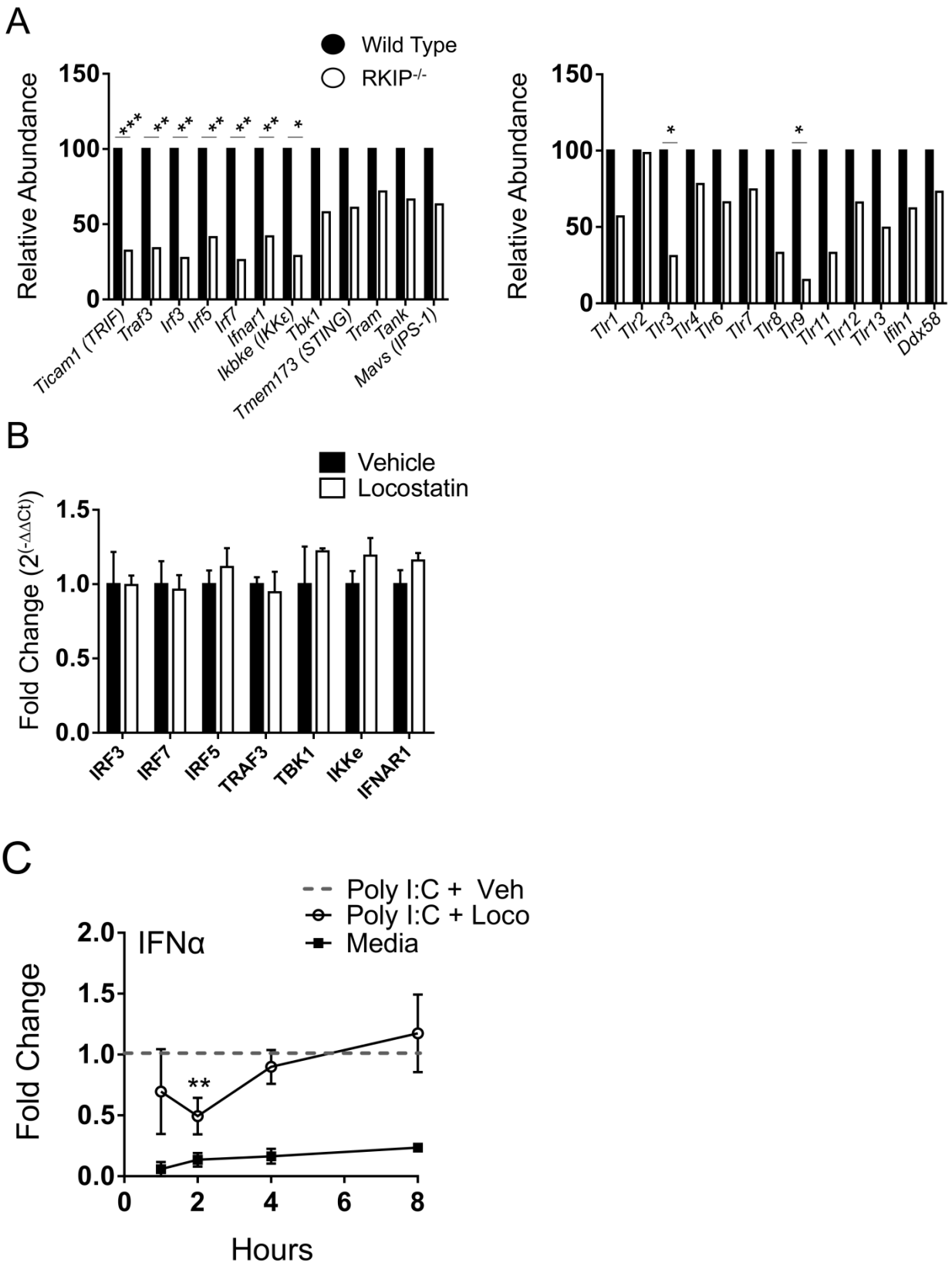
A
Wild Type
RKIP-/-
Relative Abundance
150
100
50
0
***
**
**
**
**
**
*
Ticam1 (TRIF)
Traf3
Irf3
Irf5
Irf7
Ifnar1
Ikbke (IKKε)
Tbk1
Tmem173 (STING)
Tram
Tank
Mavs (IPS-1)
Relative Abundance
150
100
50
0
*
*
Tlr1
Tlr2
Tlr3
Tlr4
Tlr6
Tlr7
Tlr8
Tlr9
Tlr11
Tlr12
Tlr13
Ifih1
Ddx58
B
Vehicle
Locostatin
Fold Change (2(-ΔΔCt))
1.5
1.0
0.5
0.0
IRF3
IRF7
IRF5
TRAF3
TBK1
IKKe
IFNAR1
C
Poly I:C + Veh
Poly I:C + Loco
Media
IFNα
Fold Change
2.0
1.5
1.0
0.5
0.0
**
0
2
4
6
8
Hours

Figure 5-8: RKIP optimizes IFNα synthesis and the Type I IFN stimulated chemokine CXCL10 following TLR3 ligation (A) ELISA for CXCL10 and CCL5 from culture supernatants of wild type and $RKIP^{-/-}$ B cells stimulated *in vitro* with 50μg/ml Poly I:C and 5μM locostatin or vehicle control (DMSO at same (v/v) percent) overnight. Error bars represent mean ± SEM, data are from 1 experiment, N=3/group; $^{**}p<0.01$, $^{****}p<0.0001$. (B) ELISA for CXCL10, CCL5, and IFNα from culture supernatants treated similarly as described in Figure 5-8A for 6h or overnight in the presence of anti-IFNAR1 blocking antibody (10μg/well) or isotype control (10μg/well). Error bars represent mean ± SEM data are from 3 independent experiments, N=6/group (6 h) and N=9/group (O/N); $^{*}p<0.05$, $^{**}p<0.01$, $^{***}p<0.001$, $^{****}p<0.0001$.

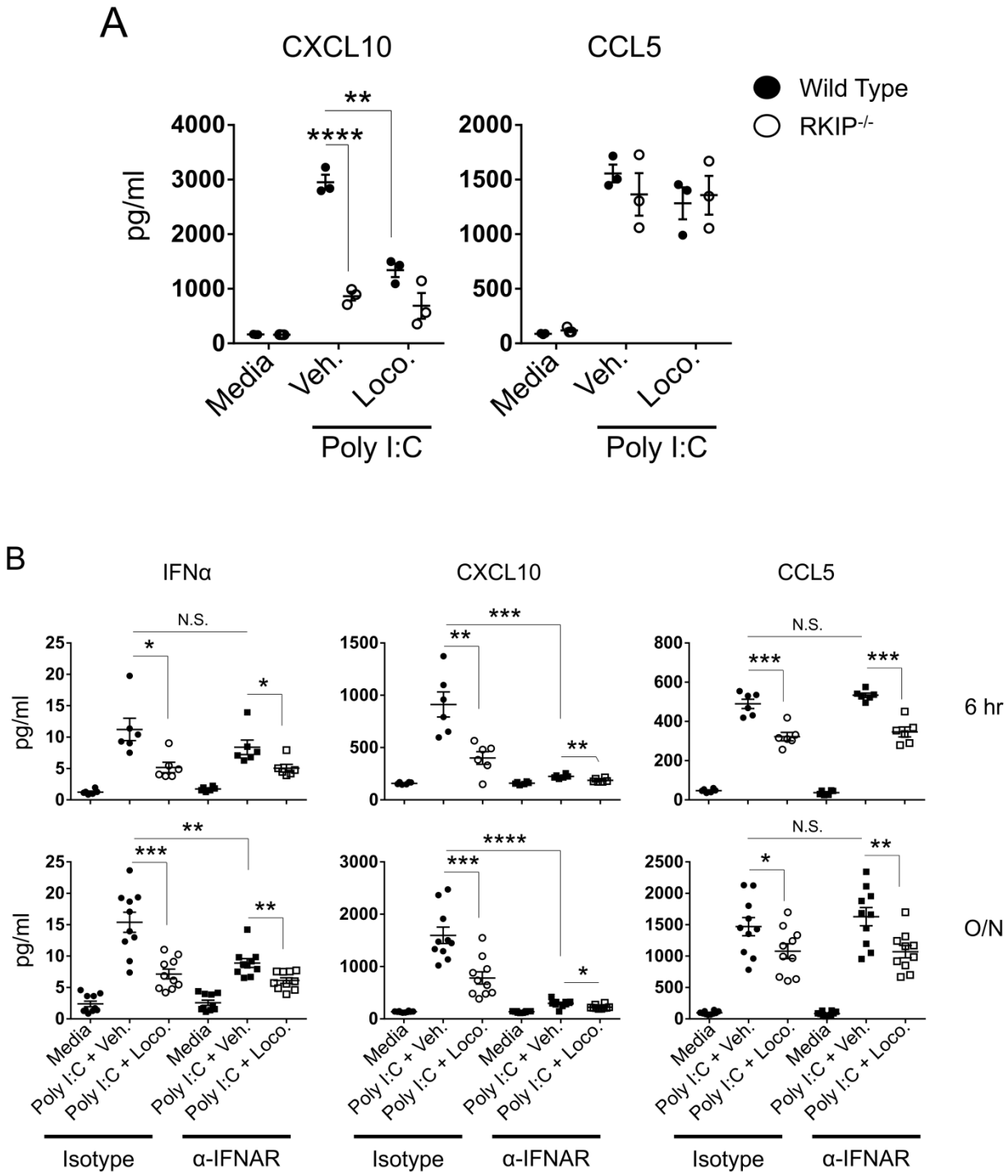
A
CXCL10
CCL5
Wild Type
RKIP-/-
pg/ml
4000
3000
2000
1000
0
2000
1500
1000
500
0
**
****
Media
Veh.
Loco.
Poly I:C
B
IFNα
CXCL10
CCL5
6 hr
O/N
pg/ml
N.S.
*
***
****
Media
Poly I:C + Veh.
Poly I:C + Loco.
Isotype
α-IFNAR

TABLE III: Ingenuity Analysis of Pathways Enriched in RKIP$^{-/-}$ B Cells

Pathway	*p-value*	-log (p-value)
Mitochondrial Dysfunction	1.28825E-06	5.89
Induction of Apoptosis by HIV1	4.36516E-05	4.36
CD28 Signaling in T Helper Cells	5.7544E-05	4.24
CD40 Signaling	0.000134896	3.87
TNFR1 Signaling	0.000223872	3.65
TNFR2 Signaling	0.000223872	3.65
iCOS-iCOSL Signaling in T Helper Cells	0.000251189	3.6
April Mediated Signaling	0.000295121	3.53
B Cell Activating Factor Signaling	0.00042658	3.37
TWEAK Signaling	0.000549541	3.26
Activation of IRF by Cytosolic Pattern Recognition Receptors	0.00057544	3.24
Lymphotoxin β Receptor Signaling	0.000676083	3.17
Toll-like Receptor Signaling	0.000676083	3.17
PKCθ Signaling in T Lymphocytes	0.000676083	3.17
PI3K Signaling in B Lymphocytes	0.000676083	3.17
B Cell Receptor Signaling	0.000812831	3.09
Dendritic Cell Maturation	0.001	3
Role of NFAT in Regulation of the Immune Response	0.001230269	2.91
mTOR Signaling	0.001380384	2.86
T Cell Receptor Signaling	0.001584893	2.8
RANK Signaling in Osteoclasts	0.002041738	2.69
Apoptosis Signaling	0.002041738	2.69
4-1BB Signaling in T Lymphocytes	0.002238721	2.65
EGF Signaling	0.004073803	2.39
Huntington's Disease Signaling	0.004466836	2.35
Oxidative Ethanol Degradation III	0.005370318	2.27
Tryptophan Degradation X (Mammalian, via Tryptamine)	0.00676083	2.17
Gαq Signaling	0.007079458	2.15
CD27 Signaling in Lymphocytes	0.007943282	2.1
IL-1 Signaling	0.008128305	2.09
Type I Diabetes Mellitus Signaling	0.008128305	2.09
Ethanol Degradation IV	0.008317638	2.08
Ethanol Degradation II	0.00851138	2.07
Antigen Presentation Pathway	0.00851138	2.07
Ceramide Signaling	0.009120108	2.04
CCR5 Signaling in Macrophages	0.009120108	2.04
SAPK/JNK Signaling	0.009332543	2.03
Regulation of IL-2 Expression in Activated and Anergic T Lymphocytes	0.01	2.00
Interferon Signaling	0.01	2.00
IL-10 Signaling	0.01	2.00
Non-Small Cell Lung Cancer Signaling	0.01	2.00
Androgen Signaling	0.01	2.00
NGF Signaling	0.01	2.00
Regulation of eIF4 and p70S6K Signaling	0.010715193	1.97
FcγRIIB Signaling in B Lymphocytes	0.010964782	1.96
CREB Signaling in Neurons	0.010964782	1.96
EIF2 Signaling	0.011481536	1.94
Phenylethylamine Degradation I	0.012022644	1.92
α-tocopherol Degradation	0.012022644	1.92
Estrogen Receptor Signaling	0.012589254	1.9
CTLA4 Signaling in Cytotoxic T Lymphocytes	0.013489629	1.87
Role of NFAT in Cardiac Hypertrophy	0.014125375	1.85
α-Adrenergic Signaling	0.014454398	1.84
Caveolar-mediated Endocytosis Signaling	0.015488166	1.81
Small Cell Lung Cancer Signaling	0.015488166	1.81
Calcium-induced T Lymphocyte Apoptosis	0.015848932	1.8
IL-4 Signaling	0.016595869	1.78
Role of RIG1-like Receptors in Antiviral Innate Immunity	0.016982437	1.77
14-3-3-mediated Signaling	0.017782794	1.75
IL-12 Signaling and Production in Macrophages	0.019054607	1.72
Systemic Lupus Erythematosus Signaling	0.019498446	1.71
Histamine Degradation	0.019952623	1.7

TABLE III: Ingenuity Analysis of Pathways Enriched in RKIP$^{-/-}$ B Cells (cont.)

Pathway	*p-value*	-log (p-value)
Tumoricidal Function of Hepatic Natural Killer Cells	0.019952623	1.7
IL-17A Signaling in Gastric Cells	0.019952623	1.7
Fc Epsilon RI Signaling	0.023988329	1.62
Fatty Acid α-oxidation	0.024547089	1.61
Renin-Angiotensin Signaling	0.025118864	1.6
PDGF Signaling	0.025703958	1.59
Chronic Myeloid Leukemia Signaling	0.026915348	1.57
GNRH Signaling	0.029512092	1.53
NF-κB Signaling	0.029512092	1.53
Granzyme B Signaling	0.029512092	1.53
CDP-diacylglycerol Biosynthesis I	0.029512092	1.53
NRF2-mediated Oxidative Stress Response	0.030902954	1.51
Protein Kinase A Signaling	0.031622777	1.5
Role of PI3K/AKT Signaling in the Pathogenesis of Influenza	0.032359366	1.49
UVB-Induced MAPK Signaling	0.032359366	1.49
Role of PKR in Interferon Induction and Antiviral Response	0.033113112	1.48
Altered T Cell and B Cell Signaling in Rheumatoid Arthritis	0.033884416	1.47
TREM1 Signaling	0.035481339	1.45
Integrin Signaling	0.035481339	1.45
Putrescine Degradation III	0.035481339	1.45
IL-8 Signaling	0.036307805	1.44
Superpathway of Inositol Phosphate Compounds	0.036307805	1.44
GDNF Family Ligand-Receptor Interactions	0.03801894	1.42
Death Receptor Signaling	0.040738028	1.39
Phosphatidylglycerol Biosynthesis II (Non-plastidic)	0.041686938	1.38
Noradrenaline and Adrenaline Degradation	0.043651583	1.36
Aryl Hydrocarbon Receptor Signaling	0.044668359	1.35
Virus Entry via Endocytic Pathways	0.045708819	1.34
FAK Signaling	0.045708819	1.34
UVA-Induced MAPK Signaling	0.045708819	1.34
Glucocorticoid Receptor Signaling	0.046773514	1.33
Acetyl-CoA Biosynthesis III (from Citrate)	0.046773514	1.33
Gap Junction Signaling	0.046773514	1.33
iNOS Signaling	0.047863009	1.32
Myc Mediated Apoptosis Signaling	0.047863009	1.32
D-myo-inositol (1,4,5)-trisphosphate Degradation	0.047863009	1.32

TABLE IV: Altered Genes Important for Mitochondrial Function in RKIP$^{-/-}$ B Cells

Gene	Relative Expression		Function
	Wild Type	RKIP$^{-/-}$	
Map2k4	6.02709	2.18678	JNK-K
Ndufv1	49.028	18.897	NADH dehydrogenase (Complex I) subunit
Atp5d	79.958	32.0431	ATP Synthase Delta (Complex V) subunit
Cox6a1	101.328	39.5858	Cytochrome C Oxidase (Complex IV) subunit
Ndufs7	183.742	55.3997	NADH dehydrogenase (Complex I) subunit
Cox8a	89.4472	25.6215	Cytochrome C Oxidase (Complex IV)subunit
Ndufa7	389.806	175.586	NADH dehydrogenase (Complex I) subunit
Ndufb8	333.707	120.657	NADH dehydrogenase (Complex I) subunit
Dhodh	6.02206	1.70485	Quinone dehydrogenase (Complex II) subunit
Ndufa1	207.983	65.7994	NADH dehydrogenase (Complex I) subunit
Ndufa2	628.054	215.532	NADH dehydrogenase (Complex I) subunit
Ndufa13	105.126	36.7641	NADH dehydrogenase (Complex I) subunit
Ndufb10	360.958	143.939	NADH dehydrogenase (Complex I) subunit
Fis1	142.321	60.9672	Mitochondrial fission 1 protein
Ndufs8	221.571	94.443	NADH dehydrogenase (Complex I) subunit
Txn2	113.475	39.5416	Thioredoxin-2
Ndufb7	89.5458	36.1698	NADH dehydrogenase (Complex I) subunit
Cyc1	15.5698	4.84798	Cytochrome C1
Cyb5r3	10.2153	2.45583	Cytochrome B5R3
Uqcrc1	84.7091	33.7325	Cytochrome b-c1 complex subunit 1
Uqcrq	185.161	79.4686	Cytochrome b-c1 complex subunit 1
Pink1	5.79479	1.79302	Ser/Thr kinase (Mito. Clearance-Autophagy)

TABLE V: Altered Genes Important for TLR-Type I IFN Signaling in Naïve RKIP$^{-/-}$ B Cells

Gene	Location	Relative Expression		$\log_2$ (Fold Change)	*p-value*
		Wild Type	RKIP$^{-/-}$		
Pattern Recognition Receptors					
Tlr1	Chr. 5	16.27	9.27	-0.811	0.0514
Tlr2	Chr. 3	1.16	1.00	-0.022	0.7594
Tlr3	Chr. 8	0.80	0.25	-1.691	0.0478*
Tlr4	Chr. 4	1.70	1.33	-0.355	0.5374
Tlr5	Chr. 1	0	0.02	N.A.	0.2244
Tlr6	Chr. 5	1.29	0.85	-0.595	0.4243
Tlr7	Chr. X	3.61	2.69	-0.423	0.3728
Tlr8	Chr. X	0.63	0.21	-1.597	0.1165
Tlr9	Chr. 9	0.82	0.13	-2.71	0.0121*
Tlr11	Chr. 14	0.28	0.09	-1.597	0.2275
Tlr12	Chr. 4	1.04	0.69	-0.597	0.4232
Tlr13	Chr. X	0.11	0.05	-1.013	0.5050
Ddx58 (RIG-I)	Chr. 4	7.50	4.66	-0.685	0.1002
Ifih1 (MDA-5)	Chr. 2	1.16	0.85	-0.453	0.4220
Type I IFN Generation					
Mavs (IPS-1)	Chr. 2	13.95	8.81	-0.663	0.1293
Tmem173 (STING)	Chr. 18	52.65	32.02	-0.714	0.0771
Ticam1 (TRIF)	Chr. 17	7.68	2.49	-1.626	0.0009***
Tram	Chr. 1	21.09	15.14	-0.478	0.2392
Tank	Chr. 2	28.27	18.77	-0.591	0.2103
Ikbke (IKKε)	Chr. 1	1.64	0.48	-1.789	0.0180*
Traf3	Chr. 12	2.29	0.78	-1.562	0.0026**
Tbk1	Chr. 10	9.40	5.45	-0.787	0.0675
Irf3	Chr. 7	5.27	1.45	-1.862	0.0027**
Irf7	Chr. 6	7.48	1.96	-1.925	0.0018**
Type I IFN Signaling					
Ifnar1	Chr. 16	5.86	2.46	-1.256	0.0030**
Ifnar2	Chr. 16	3.78	2.03	-0.899	0.2210
Stat1	Chr. 1	35.29	33.29	-0.084	0.8486
Stat2	Chr. 10	3.99	3.16	-0.338	0.4458
Stat3	Chr. 11	10.97	6.52	-0.751	0.1160
Irf9	Chr. 14	24.59	20.98	-0.229	0.5877
Cxcl9	Chr. 5	0.69	1.71	1.321	0.0669
Cxcl10	Chr. 5	0.23	1.21	2.419	0.2228
Cxcl11	Chr. 5	0.30	0	N.A.	0.1349

TABLE V: Altered Genes Important for TLR-Type I IFN Signaling in Naïve RKIP$^{-/-}$ B Cells

Gene	Location	Relative Expression		$\log_2$ (Fold Change)	*p-value*
		Wild Type	RKIP$^{-/-}$		
Type I Interferons					
Ifna4	Chr. 4	0	0.22	N.A.	0.1421
Ifna5	Chr. 4	0.53	0.18	-1.556	0.4870
Ifna13	Chr. 4	0.45	0.61	0.436	0.7858
Ifna14	Chr. 4	0.53	0.18	-1.556	0.4870
† *Ifna1,2,6,7,9,11,12 Ifnb, Ifne, Ifnk, Ifnz* – Not Detectable					
MyD88 & NF-κB Signaling					
Myd88	Chr. 9	10.39	4.39	-1.237	0.0100**
Cd14	Chr.18	0.63	0.58	-0.130	0.9053
Ly96 (MD-2)	Chr. 1	9.34	3.67	-1.349	0.0813
Tollip	Chr. 7	6.72	3.50	-0.939	0.0330*
Tirap	Chr. 9	1.99	1.24	-0.685	0.2038
Irak1	Chr. X	9.55	4.81	-0.989	0.0268*
Irak4	Chr. 15	8.32	4.52	-0.881	0.0479*
Irak3 (IRAK-M)	Chr. 10	2.75	1.40	-0.978	0.0956
Traf2	Chr. 2	31.54	14.50	-1.122	0.0058**
Traf6	Chr. 2	3.41	1.55	-1.135	0.0104*
Map3k7 (TAK-1)	Chr. 4	2.08	0.98	-1.095	0.0507*
Ripk1 (Rip1)	Chr. 13	3.32	1.84	-0.874	0.0742
Map3k8 (Tpl2)	Chr. 18	16.42	7.41	-1.147	0.0067**
Irf5	Chr. 6	78.11	32.38	-1.27	0.0017**
Chuk (IKKα)	Chr. 19	4.95	2.81	-0.814	0.1571
Ikbkb (IKKβ)	Chr. 8	21.97	8.03	-1.453	0.0011**
Ikbkg (IKKγ)	Chr. X	6.96	2.27	-1.615	0.0057**
Nfkbia (IκBα)	Chr. 12	73.79	38.71	-0.931	0.0217*
Rela	Chr. 9	25.45	8.12	-1.648	$7.37x10^{-5}$****
Relb	Chr. 7	9.15	2.35	-1.961	0.0002***
Nfkb1 (p105)	Chr. 3	19.88	12.63	-0.931	0.0217*
Mapk11 (p38)	Chr. 15	19.37	7.72	-1.327	0.0017**
Mapk8 (JNK)	Chr. 14	0.74	0.95	0.345	0.5689
Mapk1 (ERK)	Chr. 16	8.99	7.15	-0.329	0.4998
TLR Signaling Effector Molecules					
Tnf	Chr. 17	1.73	1.16	-0.652	0.8053
Il1b	Chr. 2	0.72	0.30	-1.265	0.354
Il6	Chr. 5	0	0.46	N.A.	0.0649
Il18	Chr. 9	4.24	2.74	-0.629	0.4125

TABLE V: Altered Genes Important for TLR-Type I IFN Signaling in Naïve RKIP$^{-/-}$ B Cells

Gene	Location	Relative Expression		$\log_2$ (Fold Change)	*p-value*
		Wild Type	RKIP$^{-/-}$		
TLR Signaling Effector Molecules (cont.)					
Ccl3	Chr. 11	0.34	0	N.A	0.1110
Ccl4	Chr. 11	4.76	1.76	-1.439	0.1234
Ccl5	Chr. 11	40.88	32.54	-0.329	0.4760
Cd40	Chr. 2	101.90	41.72	-1.29	0.0032**
Cd80	Chr. 16	0	0.14	N.A.	0.1122
Cd86	Chr. 16	12.41	8.89	-0.482	0.2510

TABLE VI: Normalization of TLR-Type I IFN Genes after TLR Stimulation in RKIP$^{-/-}$ B Cells

	Naïve		LPS		CpG-B	
Gene	Relative Expression†	*p-value*	Relative Expression	*p-value*	Relative Expression	*p-value*
TLR-Type I IFN Signaling Genes						
Ticam1 (TRIF)	0.3242	0.0009***	1.2291	0.4559	0.9894	0.9506
Traf3	0.3406	0.0026**	1.9121	0.0646	1.5892	0.02292*
Irf3	0.2751	0.0027**	1.1941	0.6824	0.8029	0.4315
Irf5	0.4145	0.0017**	1.7642	0.0020**	0.8705	0.3145
Irf7	0.2620	0.0018**	1.3720	0.4717	0.2994	$3.15x10^{-6}$****
Ifnar1	0.4198	0.0030**	1.3177	0.1425	0.9030	0.4149
Myd88	0.4225	0.0100**	1.7144	0.0497*	0.9104	0.5036
Irak1	0.5037	0.0268*	1.3225	0.1372	1.1498	0.3525
Irak4	0.5434	0.0479*	1.0666	0.7417	1.0336	0.8596
Tollip	0.5208	0.0330*	1.2484	0.3048	1.2885	0.0491*
Traf6	0.4545	0.0104*	0.9545	0.8360	1.0706	0.6418
Pattern Recognition Receptors						
Tlr1	0.5699	0.0514	1.2171	0.3111	0.9046	0.5155
Tlr2	0.9848	0.7594	0.6973	0.4475	0.7145	0.3626
Tlr3	0.3097	0.0478*	0.4643	0.2138	1.0053	0.2777
Tlr4	0.7818	0.5374	1.9635	0.1049	0.6574	0.4839
Tlr6	0.6620	0.4243	1.9506	0.3076	0.7490	0.3350
Tlr7	0.7458	0.3728	1.2270	0.5047	1.0651	0.7718
Tlr8	0.3305	0.1165	0.5362	0.2191	0.6558	0.7780
Tlr9	0.1528	0.0121*	0.2140	0.2839	1.3147	0.6933
Tlr11	0.3305	0.2275	1.1618	0.8494	2.3016	0.3307
Tlr12	0.6611	0.4232	0.4879	0.2162	1.0521	0.9385
Tlr13	0.4955	0.505	0.1019	0.9291	0.3042	0.2380
Ddx58 (RIG-I)	0.6220	0.1002	1.0943	0.6178	0.5187	0.1972
Ifih1 (MDA-5)	0.7305	0.422	0.7829	0.3916	0.8742	0.6581

†Relative expression of gene of interest in RKIP$^{-/-}$ B cells vs. Wild Type (WT = 1)

CHAPTER 6

DISCUSSION: RKIP IS AN IMPORTANT, CO-EVOLVED REGULATOR OF INTERFERON RESPONSES AND MAY PROVIDE A NOVEL TARGET FOR INTERVENTIONAL CYTOKINE-BASED THERAPY

INTRODUCTION

The preceding studies have defined, for the first time, important roles for RKIP within the immune system. RKIP's primary immunological function is to facilitate cytokine responses from T cells and APCs after stimulation through the TCR and PRRs respectively, and has a particularly important role in driving the production of Type-I and Type-II interferons. Additionally, we identify RKIP's requirement for the development of competent Tc1 effectors in a mouse model of systemic inflammatory response syndrome, as well as, its place in providing appropriate adjuvant responses in B cells, specifically to nucleic acids. Finally, we also establish that RKIP is a druggable protein, and through its targeted inhibition, cytokine responses can be greatly attenuated. This highlights locostatin as a new potential therapeutic intervention for inflammatory diseases that involve the overproduction of interferons, including SIRS, SLE, RA, and others. In this final chapter, I will discuss our current working molecular hypothesis for RKIP's role in Type-I IFN synthesis, as well as its impact in interferon signaling for the immune system at large. Also, I will outline a hypothesis for how RKIP came to be an important regulator of IFN signaling involving viral evasion and co-evolution. This will be followed by a discussion of the future directions that need to be accomplished in order to determine RKIP's exact molecular mechanism for its immunological function, and what disease models should be tested to provide the best evidence for future translational studies. Finally, I will finish with brief speculation on how locostatin may be used in the clinical setting as a novel treatment modality for cytokine-based therapeutic strategies.

RKIP DRIVES TYPE-I INTERFERON RESPONSES AFTER NUCLEIC ACID SENSING: A WORKING MODEL

Prior to TLR ligation, RKIP is most likely bound to Raf-1 preventing the downstream signaling of the Raf-MEK-ERK axis. This was the initially defined by Yeung. et. al. in 1999, that RKIP interacted with Raf-1 as evidenced by their co-immunoprecipitation and co-localization with one another by confocal microscopy. This interaction is fairly high affinity (~K_D= 11±3 μM in humans (262) and ~K_D=20μM in rats (263); however, no studies to our knowledge have been done *in vivo* to determine RKIP's relative affinity for Raf-1 versus other potential ligands. Additionally, it is not known if the default binding of RKIP to Raf-1 observed in cancer cell lines remains true for all cell types, or whether this translates *in vivo*. However, our studies do indicate that RKIP does inhibit the phosphorylation of ERK, evidenced by an increase in p-ERK when RKIP is knocked out or is inhibited with locostatin (Fig. 4-1C/D, 5-2A). This increases the likelihood of this RKIP-Raf interaction being the default state of the cell.

After B cells are exposed to Poly I:C, it is recognized by either endosomal TLR3 or cytosolic MDA-5, both of which are known to bind long dsRNA like Poly I:C (264, 265). It is unknown which of these is the predominantly activated pathway in B cells. TLR3 expression is very low in this population (and even lower in $RKIP^{-/-}$ B cells; Table V), even though it does retain its ability to signal (266). These pathways may be cooperatively activated (267), but would require mechanistic studies in *Tlr3*$^{-/-}$, *Ticam1*$^{-/-}$, or *Ifih1*$^{-/-}$ mice to determine definitively. Once Poly I:C ligates its corresponding PRR, downstream signaling results in the K-63 poly-ubiquitylation of TRAF3, which prevents its proteosomal degradation (268, 269). Subsequently, TRAF3 forms a critical signaling complex consisting of itself, TBK1, and IKKε which is responsible for

phosphorylation of IRF3 and IRF7 (270-272). These IRFs act as transcription factors (either homo- or heterodimers) that lead to Type-I IFN production (273).

Because inhibition or genetic loss of RKIP results in significantly attenuated levels of IFNα production after Poly I:C stimulation (Fig. 5-3D, 5-8A/B), one possibility is that RKIP acts to provide stability to this critical TRAF3/TBK1/IKKε complex, perhaps acting as a scaffold protein (Figure 6-1, (1)). The change in affinity away from Raf-1 and towards this complex, most likely requires a post-translational modification. Protein kinase C is known to phosphorylate RKIP which causes an affinity shift from Raf-1 to GRK2 (212). There is additional evidence that RKIP phosphorylation results in dimer formation which may also be responsible for alterations in affinity (274) towards non-Raf targets. Irrespective of the mechanism by which RKIP gains affinity for the TRAF3/TBK1/IKKε complex, a critical RKIP-mediated effect on this complex is a very plausible hypothesis given that locostatin can inhibit both early transcription and translation of the *Ifna* gene.

RKIP inhibition also leads to an even more pronounced reduction in IFNα during the feed-forward phase of the reaction. This phase is critical for mediating robust immune responses to viruses and vaccine adjuvants (275), as well as resultant pathology in systemic autoimmunity (276, 277). The mechanism that mediates this enhancement is typically through increased coupling of the receptor to downstream signaling molecules. This usually occurs at the level of increased recruitment of small molecule adaptors, such as TYK2 or JAK1 in the case of IFNAR, to the receptor. These facts give way to another possibility that could account for the decreased IFNα production in the response to Poly I:C, namely that RKIP could be responsible for maintenance of the feed-forward phase of the response by facilitating the recruitment of these adaptor molecules to IFNAR (Figure 6-1, (2)). This hypothesis doesn't account for decreased

IFNα production in the early phase; however, this may also be explained by the need for functional RKIP in the maintenance of appropriate basal circulating levels of TRIF-Type-I IFN signature transcripts (Fig. 5-7A).

Based on the two working hypotheses presented above, the mechanism for locostatin inhibition of IFNα production in wild type B cells may be through the destabilization of the TRAF3/TBK1/IKKε complex as RKIP is prevented from binding, or through abolishment of the ability of IFNα to feed-forward through IFNAR ligation (Figure 6-1, right panel). The exact mechanism of this inhibition will require identification if locostatin is to be used clinically.

ESTABLISHING RKIP'S ROLE WITHIN THE IMMUNE RESPONSE

Type-I IFNs can elicit pleiotropic effects after ligation of their receptor, IFNAR (Figure 6-2). IFNAR is expressed on nearly every cell in the body at different levels, and the response that is generated after Type-I IFN signaling depends on the cell's identity, as well as the relative expression of different STAT proteins within the cell (278). This makes the true nature of the Type-I IFN response within the immune system, and the body at large, exceedingly complex. Through RKIP's ability to facilitate Type-I IFN production, it is able to affect many different areas of both the innate and adaptive immune response. First, after stimulation with nucleic acid patterns, APCs respond to Type-I IFNs through autocrine or paracrine signaling which leads to an up-regulation of PRRs, including TLR3 and TLR7, as well as increases in anti-viral response genes (279) and APC maturation (280) through the phosphorylation of STAT-1/2 heterodimers. Also, in B cells specifically, Type-I IFNs can elicit increases in survival due to up-regulation of BAFF and APRIL (281, 282), as well as promote antibody production of T cell-independent antigens (283). Because nearly every successful vaccine used in clinical medicine utilizes the

production of antibody, RKIP may be an essential player in this process, especially with the use of nucleic acid adjuvants on the rise.

RKIP may also impact the ability to establish proper chemokine gradients, which are driven by Type-I IFN autocrine signaling to APCs and paracrine signaling on tissue mesenchymal cells. This is driven by the p-STAT-1/2 and IRF9 (ISGF3) trimeric complex binding to interferon-sensitive response elements (ISREs) in the enhancer regions of *Cxcl9*/*10*/*11* which recruit activated neutrophils and T cells via CXCR3 (284, 285). This response is also enhanced by Type-I IFN mediated IFNγ production which can also drive CXCL9/10/11 synthesis by p-STAT-1/1 binding of IFNγ-activating (GAS) sites within the enhancer regions of these genes (286, 287). Type-I IFN can also drive production of CCL2/7 which induce recruitment and pro-inflammatory responses from macrophages and Tip-DCs (288, 289). In preliminary studies, we observed altered migration to liver of adoptively transferred TCR-transgenic T cells after immunization in $RKIP^{-/-}$ recipients, suggesting that RKIP may indeed be necessary for establishing specific chemotactic gradients.

Through the studies presented in chapter 3, we established the importance of RKIP for the proper differentiation of Tc1 effector CTLs, as well as their ability to produce the effector cytokine, IFNγ, after TCR triggering (Fig. 3-1, 3-5). We determined that this was due, at least in part to an intrinsic defect downstream of the TCR signaling apparatus in Tc1 T cells devoid of RKIP (Fig. 3-7). However, Type-I IFNs have been shown to directly affect the production of Type-II IFN, IFNγ, through the phosphorylation of STAT-4 homodimers after IFNAR ligation in Th1 and Tc1 T cells, as well as natural killer (NK) cells (290-293). Type-I IFNs can also drive IFNγ production through the IL-12 independent differentiation of $CD4^+$ Th1 T cells, which provide help to developing $CD8^+$ Tc1 effectors (294-296), in addition to augmenting proliferation and

memory formation (297) of $CD8^+$ T cell directly (298-300). To sum, the data in this thesis imply that RKIP may be responsible for coupling the cooperative generation of Type I and Type II IFNs during the immune response. The importance of this RKIP-mediated regulation is evidenced by the fact that RKIP seems to control the production of IFNγ at several different levels of the reaction including: the synthesis of Type-I IFN, the skewing of Th1 helper T cells, the differentiation of Tc1 effectors *per se*, and the direct control over IFNγ after TCR triggering in these cells.

Finally, RKIP may be involved in several suppressive immunoregulatory effects of Type-I IFNs. Previously, Type-I IFN signaling has been shown to cause phosphorylation of STAT-3 homodimers in certain cell types, such as T regulatory cells (Tregs) and anti-inflammatory macrophages (301, 302). Also, LPS can drive the production of IL-10 from both mouse (303) and human (304) PBMCs through a mechanism that is dependent on Type-I IFN. A controversy still remains to whether the exact signaling machinery required for this effect is direct transcription of the *Il10* gene by p-STAT-3 (46), or through indirect activation of the PI3K-Akt-mTOR axis by JAK1 after IFNAR ligation (305). Recently, a new subtype of T regulatory cell, characterized by the transcription factor FoxA1, has been implicated in relapsing-remitting multiple sclerosis patients and in experimental autoimmune encephalomyelitis as a mechanism for symptom abatement after IFNβ administration. These Tregs were shown to suppress by p-STAT3 mediated up-regulation of programmed cell death ligand 1 (PD-L1), which was driven by exposure to Type-I IFN (306, 307). Because RKIP may be involved in both pro-inflammatory and anti-inflammatory processes through the actions of Type-I IFN, it will require significant future studies in order to determine the exact balance of these facets in different clinical contexts.

Only through these studies will it be possible to accurately predict which clinical scenarios would potentially benefit from inhibition of RKIP function.

THE GREAT ARMS RACE: VIRAL EVASION, INTERFERONS, AND RKIP CO-EVOLUTION

Darwinian evolution is the ultimate driving force behind biological diversity, fitness, and survival. Nothing exemplifies this concept better that the ongoing evolutionary "arms race" between pathogens and their hosts. The immune system has evolved numerous mechanisms, both specific and redundant, that aim to prevent, control, and eliminate infection by pathogens. Analogously, pathogens utilize inefficient genomic replication systems to allow evolution, through enhanced mutation rates, to happen on an abbreviated time scale. The outcome of this process, in many cases, is an increased level of fitness and survivability through the development of mechanisms that allow for immune system subversion or circumvention.

Viruses, because of their significant diversity and ability to rapidly evolve, present a unique challenge to the host's immune system (308). One of the most evolutionarily conserved mechanisms for eliciting anti-viral control is the Type-I IFN response. They were initially discovered by work done in the 1950s from Nagano and Kojima (309-311), and later Isaacs and Lindenmann (312), which described novel molecules that inhibited the replication of smallpox and influenza virus respectively. The exact molecular mechanisms by which IFNs elicit anti-viral immunity have been reviewed in depth previously (313), and seem to be conserved in most vertebrates (314) including humans (315), as far back as bony fish (*Osteichthyes*) (316). However, they have not yet been detected in invertebrate species. The importance of type-I IFN

mediated control of viral pathogens is illustrated by two critical facts: 1) mice and humans that have deficiencies in IFN production or signaling have increased morbidity and mortality to viruses (317), and 2) viruses have evolved mechanisms to subvert the IFN response at nearly every level (308). These viral subversion techniques include sequestration of viral dsRNA from nucleic acid sensing PRRs by Ebola virus-VP35 (318), Vaccinia virus-E3L (319), and Influenza A virus-NS1 (320), degradation or cleavage of TRIF and IPS-1 by Hepatitis C virus-NS3-4A (321), or disruption of signaling machinery through direct inhibition (e.g. Hepatitis C virus-NS5A (322, 323) and NS3-4A (324), Ebola viru-VP35 (318), Vaccinia virus-E3L (325) and A52R (326), and Influenza A virus-NS1 (327). These methods to circumvent viral immunity are just a few examples to highlight how extensively the IFN pathway can be attenuated by viral proteins.

By analyzing which host proteins are targeted by viral factors, new innate immunological functions can be ascribed to poorly-defined host proteins, or can even lead to the discovery of new proteins. In 2011, Folly and colleagues demonstrated by two-hybrid technology that the PrM structural protein from the human pathogen Dengue-2 virus physically interacted with the human form of RKIP (PEBP-1) (328). The authors go on to posit: “As induction of [the] IFN-alpha gene family is dependent on IRF7, it is formally possible that the PrM-RKIP (PEBP) complex might be inhibiting TAK1/IKK-dependent phosphorylation of the TLR3/7 receptors, negating the expression of IFN-alpha and therefore, IFN-alpha dependent genes.” To the best of our knowledge, our studies involving RKIP are the first to demonstrate experimentally that this hypothesis may have a high likelihood of being correct. Although future studies are required to determine the exact mechanism by which RKIP facilitates IFNα production, after these data are obtained, the purpose of PrM’s interaction with RKIP in humans should be easily extrapolated.

These findings, in the context of our work, strongly implicate RKIP as molecule that has co-evolved alongside IFNs and nucleic acid sensors in order to mediate these interferon responses and facilitate anti-viral immunity.

FUTURE DIRECTIONS

The current studies described herein have begun to highlight the role that RKIP plays in mediating interferon responses within the immune system. Although our knowledge of RKIP's function in the context of *in vitro* and *in vivo* immunity have grown exponentially through this work, there are still significant strides to be made in terms of establishing both the exact molecular mechanism by which it functions in these responses, as well as if or how these findings translate into a broader range of *in vivo* disease models and human immunity.

Currently, in order to better elucidate a molecular mechanism for how RKIP drives Type-I IFN production in APCs, we plan to explore what proteins RKIP co-localizes with after Poly I:C stimulation by confocal microscopy. Based on our cytokine and transcriptome studies, the list of potential RKIP binding partners is small enough to utilize this approach. We already have a commercially available FITC conjugated anti-RKIP antibody that works well for indirect immunofluorescence (Fig. 4-4A) which should be applicable for confocal microscopy as well. Also, antibodies for microscopy are commercially available for nearly all of our potential target proteins including TRAF3, TBK1, IKKε, IFNAR, JAK1, and TYK2. Unfortunately conventional co-immunoprecipitation of RKIP from primary cells is currently hampered by a lack of reagents that can bind RKIP for immunoprecipitation. RKIP can be immunoprecipitated from cell lines

after transfection of tagged-RKIP; however, the relevancy of this approach is unclear, given our interest in RKIP's interaction *in vivo*, or at the very least, in primary immune cells.

After we establish the binding partners of RKIP in our model, the next question we will seek to answer is whether or not these interactions can be destabilized by the irreversible inhibition of RKIP by locostatin. Because RKIP is covalently modified by locostatin within its ligand binding pocket (172), theoretically this should prevent RKIP from interacting with other proteins. An observable destabilization of the RKIP containing complex could then be linked to decreased IFNα production after RKIP blockade. This could be accomplished experimentally, once again through imaging by confocal microscopy, or by gel filtration. Additionally, we will seek to confirm our attenuated TRIF-Type-I IFN transcriptomic signature at the protein level by mining of the wild type and $RKIP^{-/-}$ proteomes by PF-2D proteomics (Figure 6-3). Through this approach we can not only confirm the identity of altered proteins within these specific signaling pathways, but also uncover new putative targets affected by RKIP during PRR signaling in APCs.

Finally, the breadth of potential clinical applicability of RKIP inhibition can be tested by locostatin therapy in different disease models. This allows for the circumvention of caveats that arise when using knockout mouse models. We have already established a potential role for RKIP modulating IFNγ production from Tc1 effectors in a mouse model of SIRS; however, given the evidence presented in chapter 5, we must now expand to models that are affected by altered production of Type-I IFN including: SLE, IBD, Psoriasis, MS, viral infection, and hematologic malignancy. The rationale for studying these diseases will be discussed at length in the next section.

LOCOSTATIN: A NEW CYTOKINE-BASED THERAPEUTIC INTERVENTION?

The clinical relevancy of these studies centers on the ability to utilize RKIP-inhibition by the small molecule inhibitor locostatin as a potential therapeutic intervention to treat human inflammatory diseases which consist of dysregulated interferon responses as part of their pathogenesis. Locostatin has the potential to provide therapeutic benefits over many current forms of treatment. First, because locostatin is a small organic molecule, it has the potential to be formulated for use *per os*, as most oxazolidinones have adequate oral bioavailability (329). This would provide a tremendous advantage to conventional monoclonal antibody biologics which are given by intravenous infusion or subcutaneous injection (330). Second, based on our studies of locostatin, it seems that it would fall in the middle of the spectrum in terms of immunosuppressive potency, of which either extreme could be disadvantageous. For example, the most common treatment for intense inflammatory reactions is corticosteroids which cause very robust immunosuppression, leaving the patient susceptible to opportunistic infections. In chapter 3, we show that despite the defect seen in IFNγ from $CD8^+$ T cells, these cells were still able to respond with cytokine production in response to a TLR stimulus such as LPS (Fig. 3-10). This suggests that patients may still be able to respond normally to pathogenic invasion, even under RKIP-inhibition. On the other hand, in contrast to most modern anti-cytokine based interventions, locostatin may provide a slightly broader suppressive response compared to the inhibition of one particular cytokine, given its ability to affect Type-I and Type-II IFNs, as well as interferon-stimulated cytokines like CCL2 and CXCL10.

The most likely clinical scenarios where locostatin therapy would have potential benefits are diseases that have established pathogenic connections to dysregulated Type-I or Type-II interferon responses. These include: SIRS, which was discussed at length in chapter 3, systemic

lupus erythematosus (SLE), rheumatoid arthritis (RA), inflammatory bowel disease (IBD), psoriasis, coeliac disease, and multiple sclerosis (MS). In SLE, patients have abnormally high levels of IFNα in their serum (331, 332), as well as genes involved in the "Type-I IFN signature" (255, 333). Serum from these patients was able to induce APC maturation (increased MHC-II and the con-stimulatory molecules CD80/CD86) and differentiation of antibody secreting plasma cells (334). Additionally, some patients that have received recombinant IFNα therapy for hepatitis C infection have developed an SLE-like syndrome with the production of anti-nuclear antibodies (ANA) (335). Phase-I clinical trials have been conducted using anti-IFNα neutralizing antibodies which have shown some improvement in symptomology (334); however, it may prove to be more beneficial to block IFNα production rather than blocking its effects *post hoc*. Similarly, psoriasis and coeliac disease both exhibit exacerbation of symptomology in the presence of type-I IFN. In a xenograft model of psoriasis, development of skin lesions and activation of autoreactive T cells could be inhibited through the suppression of IFN signaling through IFNAR blockade (336) or anti-BDCA2 (337), which prevents IFNα production from pDCs. Th1 polarization, robust IFNγ synthesis and presentation of gluten specific peptides to autoreactive T cells is the main driving force behind the pathology seen in coeliac patients (338, 339). However, anti-IFNα treatment of biopsy specimens from coeliac patients was able to inhibit IFNγ production (340), the mechanism of which has been discussed previously.

On the other hand, diseases that have their pathology related to mixed Th1/Th17 responses, such as MS, RA, and IBD, are much more controversial in regard to their response to Type-I IFN inhibition. In MS, IFNβ (Betaseron) is prescribed as fairly efficacious therapeutic option (341), and in mouse models of MS such as EAE, IFNβ deficient mice develop worse disease (342), but can be improved with analogous IFNβ administration (343). Also, Type-I IFNs have been shown

to inhibit Th17-mediated inflammation in EAE (344), suggesting that the therapeutic action of IFNβ administration may be through both Th17 suppression and induction of FoxA1^{+} Tregs (Fig. 6-2). Similarly, treatment with interferons in both the collagen induced arthritis model of RA (345) and human IBD patients (346-348) have shown promising results. However, because each of these three diseases are also impacted by a significant Th1 component and Type-I IFNs are known to drive these responses, it remains an exceptionally complex system to treat, which may provide insight into why some recombinant IFN therapies have exhibited contradictory results (349-351). Irrespective of existing experimental evidence in humans and mouse disease models, locostatin-mediated inhibition of IFNα and IFN-stimulated genes must be tested individually in each disease model in order to determine experimentally the effectiveness of this therapeutic strategy.

CONCLUSIONS

The studies presented herein were designed to test if Raf-1 kinase inhibitor protein (RKIP) played any functionally significant role in immunity, and to interrogate its possibility of providing a novel therapeutic target for modulating inflammatory responses. Based on previous studies from other laboratories that attributed negative regulatory functions to RKIP in the context of MAPK and NF-κB signaling in cell lines, we set out with the hypothesis that its function was to suppress the production of pro-inflammatory cytokines, proliferation, and cell survival. However, after extensive investigation, our data clearly demonstrate that RKIP is actually necessary for the production of certain cytokines, namely Type-I and Type-II interferons, but was less involved in cell survivability and proliferation. Additionally, this work has established RKIP as an important contributor to the signaling machinery downstream of TCR triggering in CD8^{+} T cells and TLR ligation in APCs. Finally, these studies have shown that

RKIP is a druggable protein, and through its targeted inhibition, cytokine responses can be significantly diminished. Thus, this provides elementary rationale for its potential clinical applicability in therapeutic interventions for inflammatory diseases (Figure 6-4). Through this current work, we have provided a solid foundation for future studies that seek to investigate further the molecular mechanisms of RKIP function within the immune system, as well as its advancement into clinically relevant inflammatory disease models.

Figure 6-1: Working model of RKIP's functional role in mediating Type-I IFN production from APCs after Poly I:C stimulation (Left Panel) Prior to stimulation, RKIP is bound to Raf-1, thus preventing its phosphorylation of MEK and keeping MAPK activity suppressed. Signaling machinery for TRIF-TRAF3-IRF axis, NF-κB, and signaling through IFNAR is synthesized, but not held in a functional confirmation thus preventing the synthesis of cytokines. (Center Panel) After Poly I:C administration, the dsRNA is sensed either through ligation of TLR3 in endosomes, binding to MDA-5 in the cytosol, or through the production of cyclic-di-GMP and activation of ER-associated STING. These events (along with IL-1R signaling) lead to the K-63 mediated poly-ubiqutinylation of TRAF3 and prevents its proteasomal degradation. TRAF3 subsequently binds to IKKε and TBK-1 to facilitate phosphorylation of IRF3 and IRF7 which translocate to the nucleus driving the production of Type-I IFNs. These Type-I IFNs act in an autocrine (or paracrine) fashion through IFNAR ligation which leads to phosphorylation of STAT1/2 heterodimers, and with the aid of IRF9, drives the expression of IFN-responsive genes such as CXCL10 by binding interferon-stimulated response elements (ISRE). After exposure to Poly I:C, RKIP may become post-translationally modified, and lose affinity for Raf-1 while gaining affinity for other proteins, thus allowing the formation of the transcription factor AP-1, in concert with NF-κB signaling, which drives a pro-inflammatory and co-stimulatory genetic program. RKIP also facilitates the production of Type-I IFNs, perhaps through direct stabilization of complexes upstream of IRF phosphorylation (1), or aiding in receptor coupling of IFNAR to its downstream elements, thus enhancing the necessary IFN feed-forward loop (2). (Right Panel) Treatment with the RKIP inhibitor locostatin significantly attenuates the Type-I IFN response, potentially through the destabilization of upstream signaling complexes or uncoupling of the IFNAR receptor.

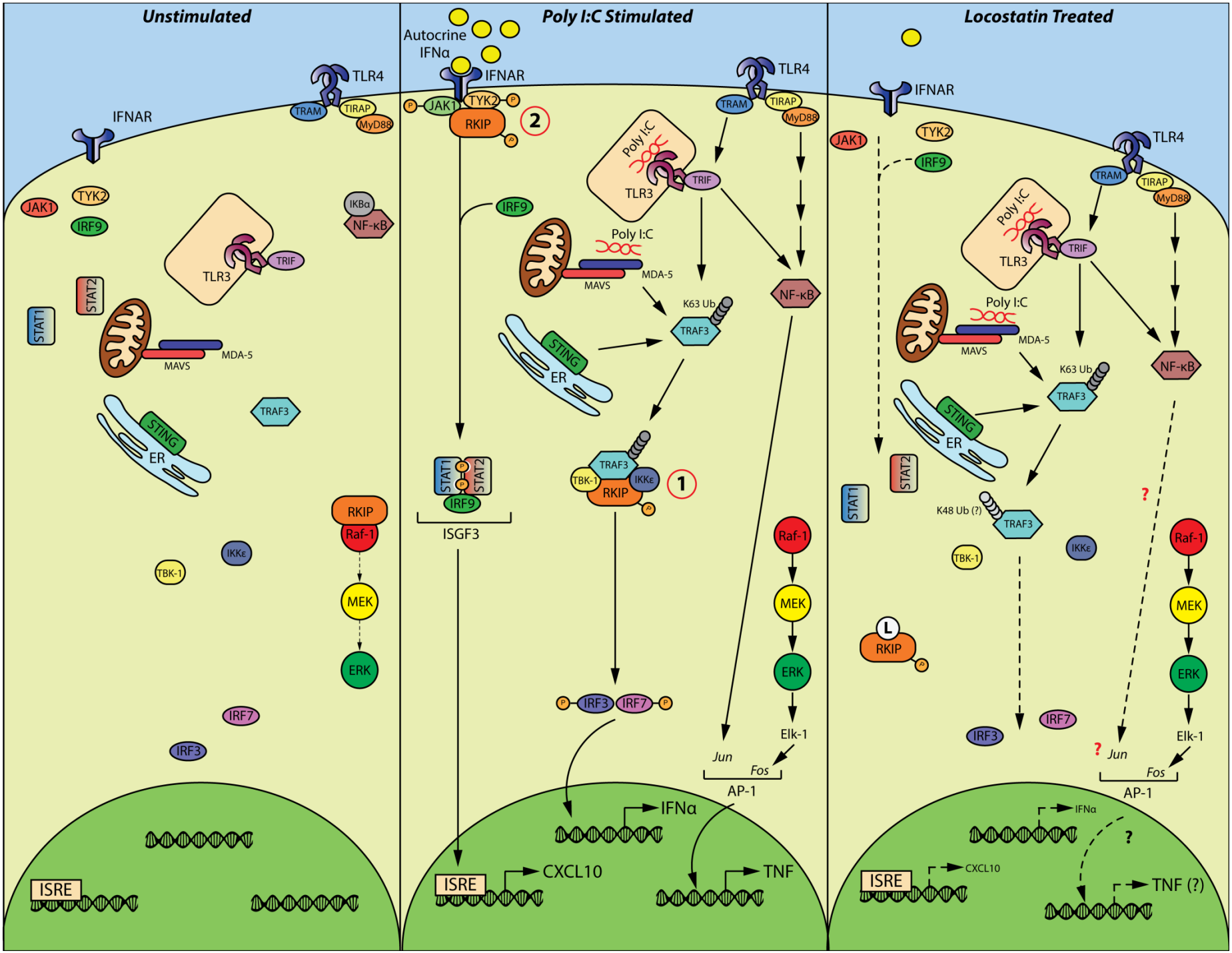
Unstimulated
Poly I:C Stimulated
Locostatin Treated
Autocrine IFNα
IFNAR
TLR4
TRAM
TIRAP
MyD88
JAK1
TYK2
IRF9
STAT1
STAT2
TLR3
TRIF
Poly I:C
MAVS
MDA-5
IKBα
NF-κB
TRAF3
K63 Ub
STING
ER
RKIP
Raf-1
MEK
ERK
Elk-1
Jun
Fos
AP-1
TBK-1
IKKε
IRF7
IRF3
ISGF3
IFNα
CXCL10
TNF
TNF (?)
K48 Ub (?)
ISRE
1
2
L
?

Figure 6-2: RKIP is necessary for maintenance of interferon-mediated effector functions in immune cells Through these studies, we have determined that RKIP imparts positive effects on both Type I and Type II IFNs. First, RKIP is necessary for the generation of $CD8^+$ Tc1 CTL effectors and proper production of their effector cytokine, IFNγ, during serial-TCR triggering. The exact molecular mechanism of this effect requires further study, however, it is clear that RKIP is most likely involved downstream of the TCR machinery. Additionally, RKIP is also necessary for the appropriate production of Type-I IFNs during sensing of nucleic acid PAMPs in APCs. This attenuated response in situations where RKIP function is inhibited can have wide-reaching effects, given the pleiotropic nature of Type-I IFN function including: an indirect effect on IFNγ production from Th1, CTLs, and NK cells through decreased STAT4 phosphorylation, decreased CXCR9/10-mediated chemotactic gradients, potentially attenuated anti-viral responses, and a worsening of some autoimmune diseases, such as multiple sclerosis, due to a decrease in $FoxA1^+$ Tregs expressing PD-L1. Nevertheless, the fact that RKIP can be inhibited using the small molecule inhibitor locostatin opens the door to future therapeutic interventions in inflammatory diseases that are mediated or potentiated by dysregulated IFN responses including: SIRS, SLE, RA, coeliac disease, and psoriasis.

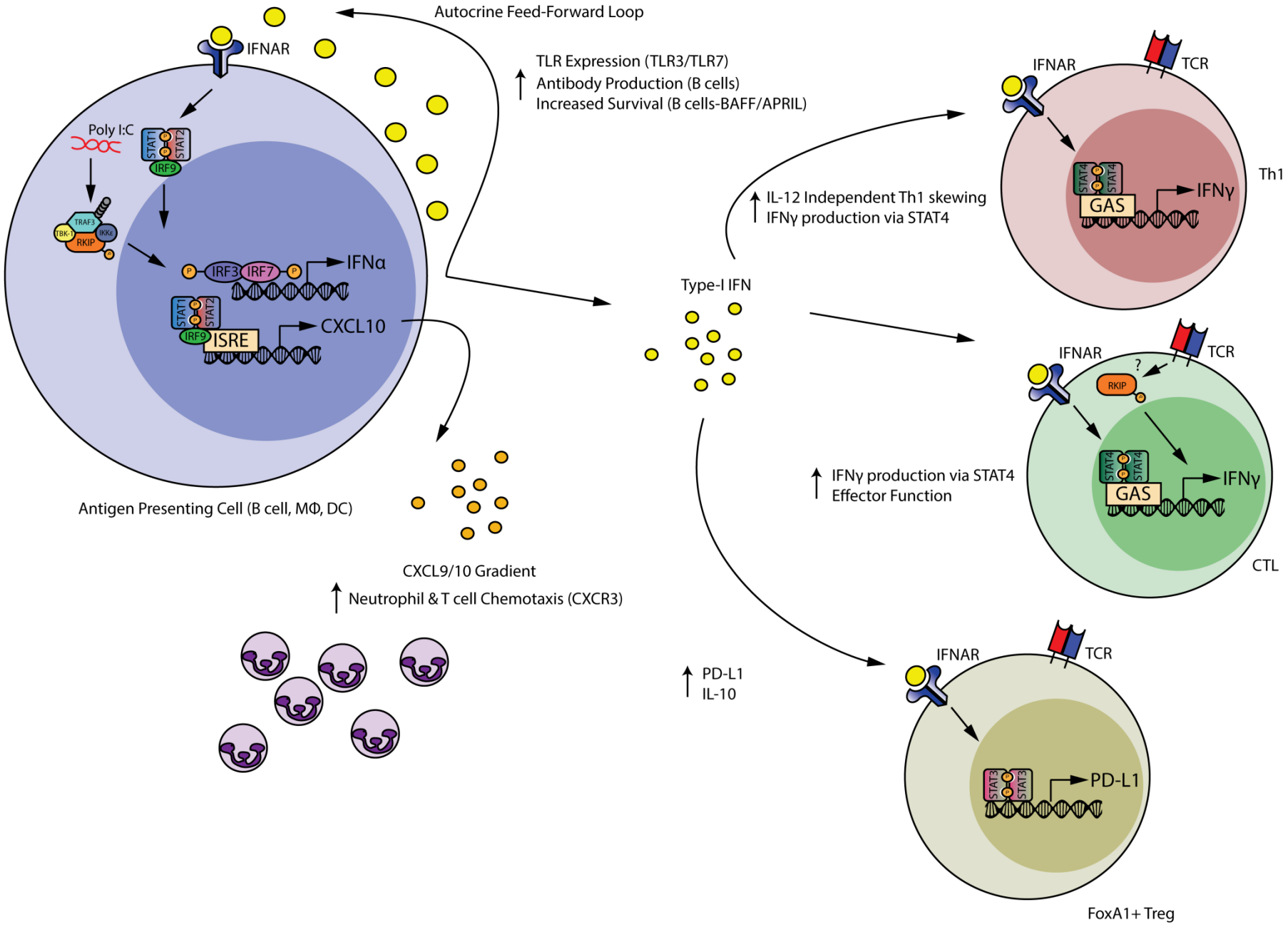
Autocrine Feed-Forward Loop
IFNAR
Poly I:C
STAT1
STAT2
IRF9
TRAF3
TBK-1
IKKε
RKIP
IRF3
IRF7
IFNα
ISRE
CXCL10
Antigen Presenting Cell (B cell, MΦ, DC)
TLR Expression (TLR3/TLR7)
Antibody Production (B cells)
Increased Survival (B cells-BAFF/APRIL)
Type-I IFN
IL-12 Independent Th1 skewing
IFNγ production via STAT4
IFNAR
TCR
STAT4
GAS
IFNγ
Th1
IFNγ production via STAT4
Effector Function
?
RKIP
CTL
CXCL9/10 Gradient
Neutrophil & T cell Chemotaxis (CXCR3)
PD-L1
IL-10
STAT3
PD-L1
FoxA1+ Treg

Figure 6-3: Utilizing ProteomeLab PF-2D to mine proteomic changes in RKIP$^{-/-}$ mice

Schematic of workflow and analysis of PF-2D proteomic mapping of naïve wild type and RKIP$^{-/-}$ naïve B cells; By using a full proteomic mining approach, we can gain new insight into the attenuated Type-I IFN transcriptome signature seen in RNAseq at the protein level. Additionally, we can determine whether transcript normalization after TLR ligation in B cells also normalizes the proteome. Finally, given that the PF-2D platform can also detect post-translational modifications of proteins by 1st dimensional pI shifts, a careful analysis of "fingerprints" may allow us to better understand exactly how RKIP imparts its effects in immune cells at the molecular level.

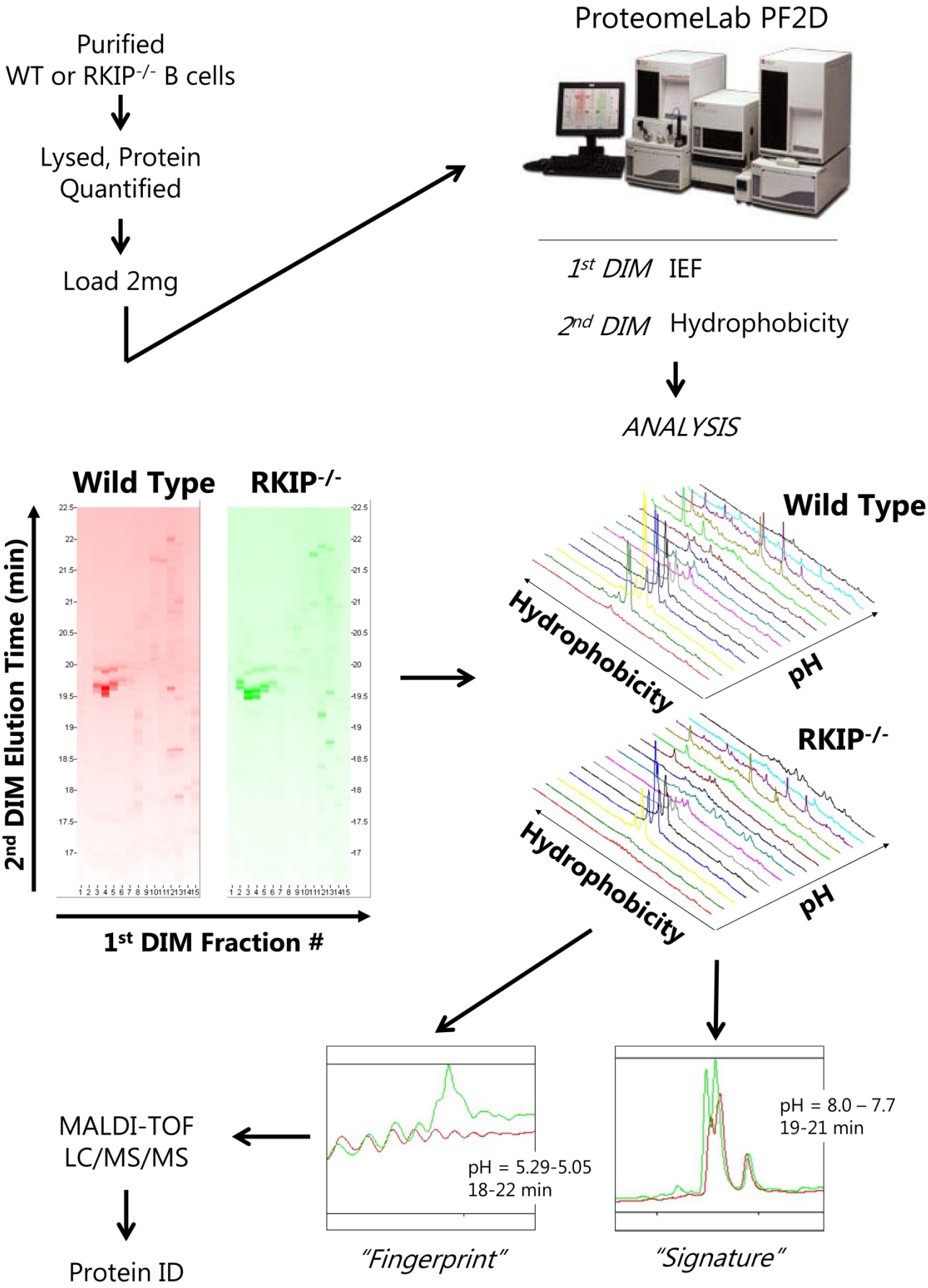
Purified
WT or RKIP-/- B cells
Lysed, Protein
Quantified
Load 2mg
ProteomeLab PF2D
1st DIM IEF
2nd DIM Hydrophobicity
ANALYSIS
Wild Type
RKIP-/-
2nd DIM Elution Time (min)
1st DIM Fraction #
Wild Type
Hydrophobicity
pH
RKIP-/-
Hydrophobicity
pH
MALDI-TOF
LC/MS/MS
Protein ID
pH = 5.29-5.05
18-22 min
"Fingerprint"
pH = 8.0 – 7.7
19-21 min
"Signature"

Figure 6-4: Avoiding the Tomato Effect: how much evidence is enough in the era of evidence based medicine? The "Tomato Effect" is a clinical rejection of potentially highly efficacious therapies due to a poor understanding of the mechanism by which they operate (352). To avoid this, especially in the era of evidence-based medicine, a significant amount of data must be obtained from different scientific approaches along a continuum in an effort to provide enough evidence for translation of a new therapeutic approach to the clinical setting. (Left Panel) Schematic of the "ideal" points of evidence that should be established in order to provide adequate scientific rationale for future human studies, ranging from low relevancy, high reproducibility systems approaches to highly relevant, but low reproducibility human studies; (Right Panel) The scientific approach utilized and evidence gathered during the current studies involving the interrogation of RKIP as a potential target for modulating inflammatory responses;

Ideal

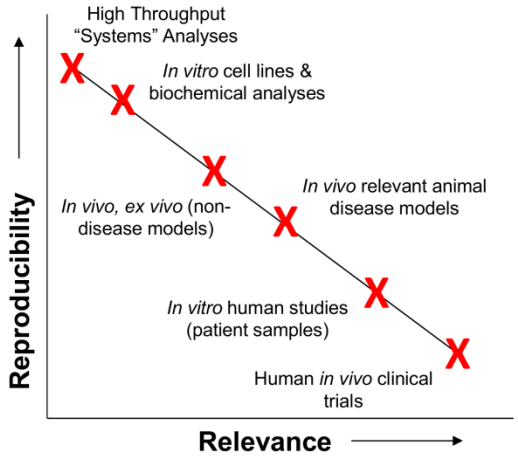

RKIP: A Case Study

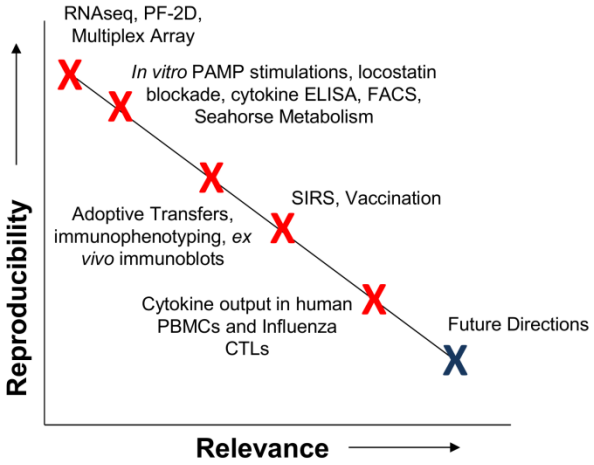

REFERENCES

1. Janeway, C. A., Jr., and R. Medzhitov. 2002. Innate immune recognition. *Annu Rev Immunol* 20: 197-216.

2. Cho, J. H., and P. K. Gregersen. 2011. Genomics and the multifactorial nature of human autoimmune disease. *N Engl J Med* 365: 1612-1623.

3. Westendorp, R. G. 2006. What is healthy aging in the 21st century? *Am J Clin Nutr* 83: 404S-409S.

4. Bailey, M., Z. Christoforidou, and M. Lewis. 2013. Evolution of immune systems: specificity and autoreactivity. *Autoimmun Rev* 12: 643-647.

5. Elliott, M. J., R. N. Maini, M. Feldmann, J. R. Kalden, C. Antoni, J. S. Smolen, B. Leeb, F. C. Breedveld, J. D. Macfarlane, H. Bijl, and et al. 1994. Randomised double-blind comparison of chimeric monoclonal antibody to tumour necrosis factor alpha (cA2) versus placebo in rheumatoid arthritis. *Lancet* 344: 1105-1110.

6. Beutler, B., I. W. Milsark, and A. C. Cerami. 1985. Passive immunization against cachectin/tumor necrosis factor protects mice from lethal effect of endotoxin. *Science* 229: 869-871.

7. Immunologists, A. A. o. 2008. An AAI recommendation for the NIH "Roadmap for Medical Research" FY 2011. In *The American Association of Immunologists newsletter*.

8. Song, X. Y., T. J. Torphy, D. E. Griswold, and D. Shealy. 2002. Coming of age: anti-cytokine therapies. *Mol Interv* 2: 36-46.

9. Schett, G., D. Elewaut, I. B. McInnes, J. M. Dayer, and M. F. Neurath. 2013. How cytokine networks fuel inflammation: Toward a cytokine-based disease taxonomy. *Nat Med* 19: 822-824.

10. Beutler, B., and A. Cerami. 1989. The biology of cachectin/TNF--a primary mediator of the host response. *Annu Rev Immunol* 7: 625-655.

11. Rubartelli, A., and M. T. Lotze. 2007. Inside, outside, upside down: damage-associated molecular-pattern molecules (DAMPs) and redox. *Trends Immunol* 28: 429-436.

12. Matzinger, P. 1994. Tolerance, danger, and the extended family. *Annu Rev Immunol* 12: 991-1045.

13. Casanova, J. L., L. Abel, and L. Quintana-Murci. 2011. Human TLRs and IL-1Rs in host defense: natural insights from evolutionary, epidemiological, and clinical genetics. *Annu Rev Immunol* 29: 447-491.

14. Takeda, K., T. Kaisho, and S. Akira. 2003. Toll-like receptors. *Annu Rev Immunol* 21: 335-376.

15. Klune, J. R., R. Dhupar, J. Cardinal, T. R. Billiar, and A. Tsung. 2008. HMGB1: endogenous danger signaling. *Mol Med* 14: 476-484.

16. Yang, H., H. S. Hreggvidsdottir, K. Palmblad, H. Wang, M. Ochani, J. Li, B. Lu, S. Chavan, M. Rosas-Ballina, Y. Al-Abed, S. Akira, A. Bierhaus, H. Erlandsson-Harris, U. Andersson, and K. J. Tracey. 2010. A critical cysteine is required for HMGB1 binding to Toll-like receptor 4 and activation of macrophage cytokine release. *Proc Natl Acad Sci U S A* 107: 11942-11947.

17. Karin, M., and Y. Ben-Neriah. 2000. Phosphorylation meets ubiquitination: the control of NF-[kappa]B activity. *Annu Rev Immunol* 18: 621-663.

18. Karin, M., and F. R. Greten. 2005. NF-kappaB: linking inflammation and immunity to cancer development and progression. *Nat Rev Immunol* 5: 749-759.

19. Wagner, E. F., and R. Eferl. 2005. Fos/AP-1 proteins in bone and the immune system. *Immunol Rev* 208: 126-140.

20. Watts, T. H. 2005. TNF/TNFR family members in costimulation of T cell responses. *Annu Rev Immunol* 23: 23-68.

21. Park, J. M., F. R. Greten, A. Wong, R. J. Westrick, J. S. Arthur, K. Otsu, A. Hoffmann, M. Montminy, and M. Karin. 2005. Signaling pathways and genes that inhibit pathogen-induced macrophage apoptosis--CREB and NF-kappaB as key regulators. *Immunity* 23: 319-329.

22. Yang, P., L. Guo, Z. J. Duan, C. G. Tepper, L. Xue, X. Chen, H. J. Kung, A. C. Gao, J. X. Zou, and H. W. Chen. 2012. Histone methyltransferase NSD2/MMSET mediates constitutive NF-kappaB signaling for cancer cell proliferation, survival, and tumor growth via a feed-forward loop. *Mol Cell Biol* 32: 3121-3131.

23. Yarilina, A., K. H. Park-Min, T. Antoniv, X. Hu, and L. B. Ivashkiv. 2008. TNF activates an IRF1-dependent autocrine loop leading to sustained expression of chemokines and STAT1-dependent type I interferon-response genes. *Nat Immunol* 9: 378-387.

24. Feldmann, M. 2002. Development of anti-TNF therapy for rheumatoid arthritis. *Nat Rev Immunol* 2: 364-371.

25. Saleh, M., and G. Trinchieri. 2011. Innate immune mechanisms of colitis and colitis-associated colorectal cancer. *Nat Rev Immunol* 11: 9-20.

26. Bone, R. C. 1992. Toward an epidemiology and natural history of SIRS (systemic inflammatory response syndrome). *Jama* 268: 3452-3455.

27. Rangel-Frausto, M. S., D. Pittet, M. Costigan, T. Hwang, C. S. Davis, and R. P. Wenzel. 1995. The natural history of the systemic inflammatory response syndrome (SIRS). A prospective study. *Jama* 273: 117-123.

28. Fry, D. E. 2012. Sepsis, systemic inflammatory response, and multiple organ dysfunction: the mystery continues. *The American surgeon* 78: 1-8.

29. Lethaby, A., M. A. Lopez-Olivo, L. Maxwell, A. Burls, P. Tugwell, and G. A. Wells. 2013. Etanercept for the treatment of rheumatoid arthritis. *Cochrane Database Syst Rev* 5: CD004525.

30. Panaccione, R., S. Ghosh, S. Middleton, J. R. Marquez, B. B. Scott, L. Flint, H. J. van Hoogstraten, A. C. Chen, H. Zheng, S. Danese, and P. Rutgeerts. 2014. Combination therapy with infliximab and azathioprine is superior to monotherapy with either agent in ulcerative colitis. *Gastroenterology* 146: 392-400 e393.

31. Kaltsonoudis, E., P. V. Voulgari, S. Konitsiotis, and A. A. Drosos. 2014. Demyelination and other neurological adverse events after anti-TNF therapy. *Autoimmun Rev* 13: 54-58.

32. Ulevitch, R. J. 2004. Therapeutics targeting the innate immune system. *Nat Rev Immunol* 4: 512-520.

33. Yamamoto, Y., and R. B. Gaynor. 2001. Therapeutic potential of inhibition of the NF-kappaB pathway in the treatment of inflammation and cancer. *J Clin Invest* 107: 135-142.

34. Calzado, M. A., S. Bacher, and M. L. Schmitz. 2007. NF-kappaB inhibitors for the treatment of inflammatory diseases and cancer. *Curr Med Chem* 14: 367-376.

35. Fraser, C. C. 2006. Exploring the positive and negative consequences of NF-kappaB inhibition for the treatment of human disease. *Cell Cycle* 5: 1160-1163.

36. Hennessy, E. J., A. E. Parker, and L. A. O'Neill. 2010. Targeting Toll-like receptors: emerging therapeutics? *Nat Rev Drug Discov* 9: 293-307.

37. Bennett-Guerrero, E., H. P. Grocott, J. H. Levy, K. A. Stierer, C. W. Hogue, A. T. Cheung, M. F. Newman, A. A. Carter, D. P. Rossignol, and C. D. Collard. 2007. A phase II, double-blind, placebo-controlled, ascending-dose study of Eritoran (E5564), a lipid A antagonist, in patients undergoing cardiac surgery with cardiopulmonary bypass. *Anesth Analg* 104: 378-383.

38. Theofilopoulos, A. N., R. Baccala, B. Beutler, and D. H. Kono. 2005. Type I interferons (alpha/beta) in immunity and autoimmunity. *Annu Rev Immunol* 23: 307-336.

39. Aguirre, S., A. M. Maestre, S. Pagni, J. R. Patel, T. Savage, D. Gutman, K. Maringer, D. Bernal-Rubio, R. S. Shabman, V. Simon, J. R. Rodriguez-Madoz, L. C. Mulder, G. N. Barber, and A. Fernandez-Sesma. 2012. DENV inhibits type I IFN production in infected cells by cleaving human STING. *PLoS Pathog* 8: e1002934.

40. Taniguchi, T., and A. Takaoka. 2001. A weak signal for strong responses: interferon-alpha/beta revisited. *Nat Rev Mol Cell Biol* 2: 378-386.

41. Liu, Y. J. 2005. IPC: professional type 1 interferon-producing cells and plasmacytoid dendritic cell precursors. *Annu Rev Immunol* 23: 275-306.

42. Blasius, A. L., and B. Beutler. 2010. Intracellular toll-like receptors. *Immunity* 32: 305-315.

43. Gonzalez-Navajas, J. M., J. Lee, M. David, and E. Raz. 2012. Immunomodulatory functions of type I interferons. *Nat Rev Immunol* 12: 125-135.

44. Honda, K., A. Takaoka, and T. Taniguchi. 2006. Type I interferon [corrected] gene induction by the interferon regulatory factor family of transcription factors. *Immunity* 25: 349-360.

45. Liu, B. S., H. L. Janssen, and A. Boonstra. 2012. Type I and III interferons enhance IL-10R expression on human monocytes and macrophages, resulting in IL-10-mediated suppression of TLR-induced IL-12. *Eur J Immunol* 42: 2431-2440.

46. Ziegler-Heitbrock, L., M. Lotzerich, A. Schaefer, T. Werner, M. Frankenberger, and E. Benkhart. 2003. IFN-alpha induces the human IL-10 gene by recruiting both IFN regulatory factor 1 and Stat3. *J Immunol* 171: 285-290.

47. Baccala, R., D. H. Kono, and A. N. Theofilopoulos. 2005. Interferons as pathogenic effectors in autoimmunity. *Immunol Rev* 204: 9-26.

48. Yao, Y., L. Richman, C. Morehouse, M. de los Reyes, B. W. Higgs, A. Boutrin, B. White, A. Coyle, J. Krueger, P. A. Kiener, and B. Jallal. 2008. Type I interferon: potential therapeutic target for psoriasis? *PLoS One* 3: e2737.

49. Hafler, D. A. 2004. Multiple sclerosis. *J Clin Invest* 113: 788-794.

50. Stewart, T. A. 2003. Neutralizing interferon alpha as a therapeutic approach to autoimmune diseases. *Cytokine Growth Factor Rev* 14: 139-154.

51. Devendra, D., and G. S. Eisenbarth. 2004. Interferon alpha--a potential link in the pathogenesis of viral-induced type 1 diabetes and autoimmunity. *Clin Immunol* 111: 225-233.

52. van Holten, J., K. Reedquist, P. Sattonet-Roche, T. J. Smeets, C. Plater-Zyberk, M. J. Vervoordeldonk, and P. P. Tak. 2004. Treatment with recombinant interferon-beta reduces inflammation and slows cartilage destruction in the collagen-induced arthritis model of rheumatoid arthritis. *Arthritis Res Ther* 6: R239-249.

53. van Holten, J., C. Plater-Zyberk, and P. P. Tak. 2002. Interferon-beta for treatment of rheumatoid arthritis? *Arthritis Res* 4: 346-352.

54. Borgia, G., L. Reynaud, I. Gentile, R. Cerini, R. Ciampi, M. Dello Russo, and M. Piazza. 2001. Myasthenia gravis during low-dose IFN-alpha therapy for chronic hepatitis C. *J Interferon Cytokine Res* 21: 469-470.

55. Gerner, M. Y., L. M. Heltemes-Harris, B. T. Fife, and M. F. Mescher. 2013. Cutting edge: IL-12 and type I IFN differentially program CD8 T cells for programmed death 1 re-expression levels and tumor control. *J Immunol* 191: 1011-1015.

56. Kirou, K. A., and E. Gkrouzman. 2013. Anti-interferon alpha treatment in SLE. *Clin Immunol* 148: 303-312.

57. Higgs, B. W., W. Zhu, C. Morehouse, W. I. White, P. Brohawn, X. Guo, M. Rebelatto, C. Le, A. Amato, D. Fiorentino, S. A. Greenberg, J. Drappa, L. Richman, W. Greth, B. Jallal, and Y. Yao. 2014. A phase 1b clinical trial evaluating sifalimumab, an anti-IFN-alpha monoclonal antibody, shows target neutralisation of a type I IFN signature in blood of dermatomyositis and polymyositis patients. *Ann Rheum Dis* 73: 256-262.

58. 1993. Interferon beta-1b is effective in relapsing-remitting multiple sclerosis. I. Clinical results of a multicenter, randomized, double-blind, placebo-controlled trial. The IFNB Multiple Sclerosis Study Group. *Neurology* 43: 655-661.

59. Latz, E., T. S. Xiao, and A. Stutz. 2013. Activation and regulation of the inflammasomes. *Nat Rev Immunol* 13: 397-411.

60. Vajjhala, P. R., R. E. Mirams, and J. M. Hill. 2012. Multiple binding sites on the pyrin domain of ASC protein allow self-association and interaction with NLRP3 protein. *J Biol Chem* 287: 41732-41743.

61. Davis, B. K., H. Wen, and J. P. Ting. 2011. The inflammasome NLRs in immunity, inflammation, and associated diseases. *Annu Rev Immunol* 29: 707-735.

62. Schroder, K., and J. Tschopp. 2010. The inflammasomes. *Cell* 140: 821-832.

63. Hornung, V., A. Ablasser, M. Charrel-Dennis, F. Bauernfeind, G. Horvath, D. R. Caffrey, E. Latz, and K. A. Fitzgerald. 2009. AIM2 recognizes cytosolic dsDNA and forms a caspase-1-activating inflammasome with ASC. *Nature* 458: 514-518.

64. Thomas, P. G., P. Dash, J. R. Aldridge, Jr., A. H. Ellebedy, C. Reynolds, A. J. Funk, W. J. Martin, M. Lamkanfi, R. J. Webby, K. L. Boyd, P. C. Doherty, and T. D. Kanneganti. 2009. The intracellular sensor NLRP3 mediates key innate and healing responses to influenza A virus via the regulation of caspase-1. *Immunity* 30: 566-575.

65. Munoz-Planillo, R., P. Kuffa, G. Martinez-Colon, B. L. Smith, T. M. Rajendiran, and G. Nunez. 2013. K(+) efflux is the common trigger of NLRP3 inflammasome activation by bacterial toxins and particulate matter. *Immunity* 38: 1142-1153.

66. Gombault, A., L. Baron, and I. Couillin. 2012. ATP release and purinergic signaling in NLRP3 inflammasome activation. *Front Immunol* 3: 414.

67. Bruchard, M., G. Mignot, V. Derangere, F. Chalmin, A. Chevriaux, F. Vegran, W. Boireau, B. Simon, B. Ryffel, J. L. Connat, J. Kanellopoulos, F. Martin, C. Rebe, L. Apetoh, and F. Ghiringhelli. 2013. Chemotherapy-triggered cathepsin B release in myeloid-derived suppressor cells activates the Nlrp3 inflammasome and promotes tumor growth. *Nat Med* 19: 57-64.

68. Niemi, K., L. Teirila, J. Lappalainen, K. Rajamaki, M. H. Baumann, K. Oorni, H. Wolff, P. T. Kovanen, S. Matikainen, and K. K. Eklund. 2011. Serum amyloid A activates the NLRP3 inflammasome via P2X7 receptor and a cathepsin B-sensitive pathway. *J Immunol* 186: 6119-6128.

69. Heid, M. E., P. A. Keyel, C. Kamga, S. Shiva, S. C. Watkins, and R. D. Salter. 2013. Mitochondrial reactive oxygen species induces NLRP3-dependent lysosomal damage and inflammasome activation. *J Immunol* 191: 5230-5238.

70. Mishra, B. B., V. A. Rathinam, G. W. Martens, A. J. Martinot, H. Kornfeld, K. A. Fitzgerald, and C. M. Sassetti. 2013. Nitric oxide controls the immunopathology of tuberculosis by inhibiting NLRP3 inflammasome-dependent processing of IL-1beta. *Nat Immunol* 14: 52-60.

71. Chen, G. Y., and G. Nunez. 2010. Sterile inflammation: sensing and reacting to damage. *Nat Rev Immunol* 10: 826-837.

72. Sheedy, F. J., A. Grebe, K. J. Rayner, P. Kalantari, B. Ramkhelawon, S. B. Carpenter, C. E. Becker, H. N. Ediriweera, A. E. Mullick, D. T. Golenbock, L. M. Stuart, E. Latz, K. A. Fitzgerald, and K. J. Moore. 2013. CD36 coordinates NLRP3 inflammasome activation by facilitating intracellular nucleation of soluble ligands into particulate ligands in sterile inflammation. *Nat Immunol* 14: 812-820.

73. Chawla, A., K. D. Nguyen, and Y. P. Goh. 2011. Macrophage-mediated inflammation in metabolic disease. *Nat Rev Immunol* 11: 738-749.

74. Wu, D., A. B. Molofsky, H. E. Liang, R. R. Ricardo-Gonzalez, H. A. Jouihan, J. K. Bando, A. Chawla, and R. M. Locksley. 2011. Eosinophils sustain adipose alternatively activated macrophages associated with glucose homeostasis. *Science* 332: 243-247.

75. Oury, C. 2014. CD36: linking lipids to the NLRP3 inflammasome, atherogenesis and atherothrombosis. *Cell Mol Immunol* 11: 8-10.

76. Mertens, M., and J. A. Singh. 2009. Anakinra for rheumatoid arthritis: a systematic review. *J Rheumatol* 36: 1118-1125.

77. Schlesinger, N. 2012. Canakinumab in gout. *Expert Opin Biol Ther* 12: 1265-1275.
78. Dinarello, C. A., A. Simon, and J. W. van der Meer. 2012. Treating inflammation by blocking interleukin-1 in a broad spectrum of diseases. *Nat Rev Drug Discov* 11: 633-652.

79. So, A., T. De Smedt, S. Revaz, and J. Tschopp. 2007. A pilot study of IL-1 inhibition by anakinra in acute gout. *Arthritis Res Ther* 9: R28.

80. Neogi, T. 2011. Clinical practice. Gout. *N Engl J Med* 364: 443-452.

81. Buch, M. H., S. J. Bingham, Y. Seto, D. McGonagle, V. Bejarano, J. White, and P. Emery. 2004. Lack of response to anakinra in rheumatoid arthritis following failure of tumor necrosis factor alpha blockade. *Arthritis Rheum* 50: 725-728.

82. Zhu, J., H. Yamane, and W. E. Paul. 2010. Differentiation of effector CD4 T cell populations (*). *Annu Rev Immunol* 28: 445-489.

83. Blum, J. S., P. A. Wearsch, and P. Cresswell. 2013. Pathways of antigen processing. *Annu Rev Immunol* 31: 443-473.

84. Malek, T. R. 2008. The biology of interleukin-2. *Annu Rev Immunol* 26: 453-479.

85. Yamane, H., and W. E. Paul. 2013. Early signaling events that underlie fate decisions of naive CD4(+) T cells toward distinct T-helper cell subsets. *Immunol Rev* 252: 12-23.

86. O'Shea, J. J., and W. E. Paul. 2010. Mechanisms underlying lineage commitment and plasticity of helper CD4+ T cells. *Science* 327: 1098-1102.

87. Kanno, Y., G. Vahedi, K. Hirahara, K. Singleton, and J. J. O'Shea. 2012. Transcriptional and epigenetic control of T helper cell specification: molecular mechanisms underlying commitment and plasticity. *Annu Rev Immunol* 30: 707-731.

88. Oestreich, K. J., and A. S. Weinmann. 2012. Transcriptional mechanisms that regulate T helper 1 cell differentiation. *Curr Opin Immunol* 24: 191-195.

89. Milstein, O., D. Hagin, A. Lask, S. Reich-Zeliger, E. Shezen, E. Ophir, Y. Eidelstein, R. Afik, Y. E. Antebi, M. L. Dustin, and Y. Reisner. 2011. CTLs respond with activation and granule secretion when serving as targets for T-cell recognition. *Blood* 117: 1042-1052.

90. Ando, K., K. Hiroishi, T. Kaneko, T. Moriyama, Y. Muto, N. Kayagaki, H. Yagita, K. Okumura, and M. Imawari. 1997. Perforin, Fas/Fas ligand, and TNF-alpha pathways as specific and bystander killing mechanisms of hepatitis C virus-specific human CTL. *J Immunol* 158: 5283-5291.

91. Mills, K. H. 2011. TLR-dependent T cell activation in autoimmunity. *Nat Rev Immunol* 11: 807-822.

92. Korn, T., E. Bettelli, M. Oukka, and V. K. Kuchroo. 2009. IL-17 and Th17 Cells. *Annu Rev Immunol* 27: 485-517.

93. Waite, J. C., and D. Skokos. 2012. Th17 response and inflammatory autoimmune diseases. *Int J Inflam* 2012: 819467.

94. Guo, L., G. Wei, J. Zhu, W. Liao, W. J. Leonard, K. Zhao, and W. Paul. 2009. IL-1 family members and STAT activators induce cytokine production by Th2, Th17, and Th1 cells. *Proc Natl Acad Sci U S A* 106: 13463-13468.

95. Yang, L., D. E. Anderson, C. Baecher-Allan, W. D. Hastings, E. Bettelli, M. Oukka, V. K. Kuchroo, and D. A. Hafler. 2008. IL-21 and TGF-beta are required for differentiation of human T(H)17 cells. *Nature* 454: 350-352.

96. Ivanov, II, B. S. McKenzie, L. Zhou, C. E. Tadokoro, A. Lepelley, J. J. Lafaille, D. J. Cua, and D. R. Littman. 2006. The orphan nuclear receptor RORgammat directs the differentiation program of proinflammatory IL-17+ T helper cells. *Cell* 126: 1121-1133.

97. Kolls, J. K., and A. Linden. 2004. Interleukin-17 family members and inflammation. *Immunity* 21: 467-476.

98. Ciric, B., M. El-behi, R. Cabrera, G. X. Zhang, and A. Rostami. 2009. IL-23 drives pathogenic IL-17-producing CD8+ T cells. *J Immunol* 182: 5296-5305.

99. Chabaud, M., F. Fossiez, J. L. Taupin, and P. Miossec. 1998. Enhancing effect of IL-17 on IL-1-induced IL-6 and leukemia inhibitory factor production by rheumatoid arthritis synoviocytes and its regulation by Th2 cytokines. *J Immunol* 161: 409-414.

100. Wong, C. K., L. C. Lit, L. S. Tam, E. K. Li, P. T. Wong, and C. W. Lam. 2008. Hyperproduction of IL-23 and IL-17 in patients with systemic lupus erythematosus: implications for Th17-mediated inflammation in auto-immunity. *Clin Immunol* 127: 385-393.

101. Wilson, N. J., K. Boniface, J. R. Chan, B. S. McKenzie, W. M. Blumenschein, J. D. Mattson, B. Basham, K. Smith, T. Chen, F. Morel, J. C. Lecron, R. A. Kastelein, D. J. Cua, T. K. McClanahan, E. P. Bowman, and R. de Waal Malefyt. 2007. Development, cytokine profile and function of human interleukin 17-producing helper T cells. *Nat Immunol* 8: 950-957.

102. Duerr, R. H., K. D. Taylor, S. R. Brant, J. D. Rioux, M. S. Silverberg, M. J. Daly, A. H. Steinhart, C. Abraham, M. Regueiro, A. Griffiths, T. Dassopoulos, A. Bitton, H. Yang, S. Targan, L. W. Datta, E. O. Kistner, L. P. Schumm, A. T. Lee, P. K. Gregersen, M. M. Barmada, J. I. Rotter, D. L. Nicolae, and J. H. Cho. 2006. A genome-wide association study identifies IL23R as an inflammatory bowel disease gene. *Science* 314: 1461-1463.

103. Oukka, M. 2008. Th17 cells in immunity and autoimmunity. *Ann Rheum Dis* 67 Suppl 3: iii26-29.

104. Gottlieb, A., A. Menter, A. Mendelsohn, Y. K. Shen, S. Li, C. Guzzo, S. Fretzin, R. Kunynetz, and A. Kavanaugh. 2009. Ustekinumab, a human interleukin 12/23 monoclonal antibody, for psoriatic arthritis: randomised, double-blind, placebo-controlled, crossover trial. *Lancet* 373: 633-640.

105. Sandborn, W. J., B. G. Feagan, R. N. Fedorak, E. Scherl, M. R. Fleisher, S. Katz, J. Johanns, M. Blank, and P. Rutgeerts. 2008. A randomized trial of Ustekinumab, a human interleukin-12/23 monoclonal antibody, in patients with moderate-to-severe Crohn's disease. *Gastroenterology* 135: 1130-1141.

106. Segal, B. M., C. S. Constantinescu, A. Raychaudhuri, L. Kim, R. Fidelus-Gort, and L. H. Kasper. 2008. Repeated subcutaneous injections of IL12/23 p40 neutralising antibody, ustekinumab, in patients with relapsing-remitting multiple sclerosis: a phase II, double-blind, placebo-controlled, randomised, dose-ranging study. *Lancet Neurol* 7: 796-804.

107. Ansel, K. M., I. Djuretic, B. Tanasa, and A. Rao. 2006. Regulation of Th2 differentiation and Il4 locus accessibility. *Annu Rev Immunol* 24: 607-656.

108. Schmitz, J., A. Owyang, E. Oldham, Y. Song, E. Murphy, T. K. McClanahan, G. Zurawski, M. Moshrefi, J. Qin, X. Li, D. M. Gorman, J. F. Bazan, and R. A. Kastelein. 2005. IL-33, an interleukin-1-like cytokine that signals via the IL-1 receptor-related protein ST2 and induces T helper type 2-associated cytokines. *Immunity* 23: 479-490.

109. Zhang, D. H., L. Yang, L. Cohn, L. Parkyn, R. Homer, P. Ray, and A. Ray. 1999. Inhibition of allergic inflammation in a murine model of asthma by expression of a dominant-negative mutant of GATA-3. *Immunity* 11: 473-482.

110. Van Dyken, S. J., and R. M. Locksley. 2013. Interleukin-4- and interleukin-13-mediated alternatively activated macrophages: roles in homeostasis and disease. *Annu Rev Immunol* 31: 317-343.

111. Gould, H. J., B. J. Sutton, A. J. Beavil, R. L. Beavil, N. McCloskey, H. A. Coker, D. Fear, and L. Smurthwaite. 2003. The biology of IGE and the basis of allergic disease. *Annu Rev Immunol* 21: 579-628.

112. Barnes, P. J. 2008. Immunology of asthma and chronic obstructive pulmonary disease. *Nat Rev Immunol* 8: 183-192.

113. Homer, C. J. 1997. Asthma disease management. *N Engl J Med* 337: 1461-1463.

114. Halloran, P. F. 2004. Immunosuppressive drugs for kidney transplantation. *N Engl J Med* 351: 2715-2729.

115. Halloran, P. F. 1996. The effect of immunosuppressive drugs on T cell signalling pathways: non-redundant steps in the T cell response. *Kidney Blood Press Res* 19: 174-176.

116. Dumont, F. J. 2000. FK506, an immunosuppressant targeting calcineurin function. *Curr Med Chem* 7: 731-748.

117. Cronstein, B. N. 2005. Low-dose methotrexate: a mainstay in the treatment of rheumatoid arthritis. *Pharmacol Rev* 57: 163-172.

118. Harwood, N. E., and F. D. Batista. 2010. Early events in B cell activation. *Annu Rev Immunol* 28: 185-210.

119. Yan, C. T., C. Boboila, E. K. Souza, S. Franco, T. R. Hickernell, M. Murphy, S. Gumaste, M. Geyer, A. A. Zarrin, J. P. Manis, K. Rajewsky, and F. W. Alt. 2007. IgH class switching and translocations use a robust non-classical end-joining pathway. *Nature* 449: 478-482.

120. Market, E., and F. N. Papavasiliou. 2003. V(D)J recombination and the evolution of the adaptive immune system. *PLoS Biol* 1: E16.

121. Lund, F. E. 2008. Cytokine-producing B lymphocytes-key regulators of immunity. *Curr Opin Immunol* 20: 332-338.

122. Mizoguchi, A., and A. K. Bhan. 2006. A case for regulatory B cells. *J Immunol* 176: 705-710.

123. Harris, D. P., L. Haynes, P. C. Sayles, D. K. Duso, S. M. Eaton, N. M. Lepak, L. L. Johnson, S. L. Swain, and F. E. Lund. 2000. Reciprocal regulation of polarized cytokine production by effector B and T cells. *Nat Immunol* 1: 475-482.

124. Sanz, I., and F. E. Lee. 2010. B cells as therapeutic targets in SLE. *Nat Rev Rheumatol* 6: 326-337.

125. Li, H., A. Llera, E. L. Malchiodi, and R. A. Mariuzza. 1999. The structural basis of T cell activation by superantigens. *Annu Rev Immunol* 17: 435-466.

126. Herman, A., J. W. Kappler, P. Marrack, and A. M. Pullen. 1991. Superantigens: mechanism of T-cell stimulation and role in immune responses. *Annu Rev Immunol* 9: 745-772.

127. Kotzin, B. L., D. Y. Leung, J. Kappler, and P. Marrack. 1993. Superantigens and their potential role in human disease. *Adv Immunol* 54: 99-166.

128. Kumar, S., S. L. Colpitts, A. Menoret, A. L. Budelsky, L. Lefrancois, and A. T. Vella. 2013. Rapid alphabeta T-cell responses orchestrate innate immunity in response to Staphylococcal enterotoxin A. *Mucosal Immunol* 6: 1006-1015.

129. Serre, L., B. Vallee, N. Bureaud, F. Schoentgen, and C. Zelwer. 1998. Crystal structure of the phosphatidylethanolamine-binding protein from bovine brain: a novel structural class of phospholipid-binding proteins. *Structure* 6: 1255-1265.

130. Serre, L., K. Pereira de Jesus, C. Zelwer, N. Bureaud, F. Schoentgen, and H. Benedetti. 2001. Crystal structures of YBHB and YBCL from Escherichia coli, two bacterial homologues to a Raf kinase inhibitor protein. *J Mol Biol* 310: 617-634.

131. Seddiqi, N., D. Segretain, S. Bucquoy, C. Pineau, B. Jegou, P. Jolles, and F. Schoentgen. 1996. Characterization and localization of the rat, mouse and human testicular phosphatidylethanolamine binding protein. *Experientia* 52: 101-110.

132. Yeung, K., T. Seitz, S. Li, P. Janosch, B. McFerran, C. Kaiser, F. Fee, K. D. Katsanakis, D. W. Rose, H. Mischak, J. M. Sedivy, and W. Kolch. 1999. Suppression of Raf-1 kinase activity and MAP kinase signalling by RKIP. *Nature* 401: 173-177.

133. Yeung, K. C., D. W. Rose, A. S. Dhillon, D. Yaros, M. Gustafsson, D. Chatterjee, B. McFerran, J. Wyche, W. Kolch, and J. M. Sedivy. 2001. Raf kinase inhibitor protein interacts with NF-kappaB-inducing kinase and TAK1 and inhibits NF-kappaB activation. *Mol Cell Biol* 21: 7207-7217.

134. Al-Mulla, F., M. S. Bitar, M. Al-Maghrebi, A. I. Behbehani, W. Al-Ali, O. Rath, B. Doyle, K. Y. Tan, A. Pitt, and W. Kolch. 2011. Raf kinase inhibitor protein RKIP enhances signaling by glycogen synthase kinase-3beta. *Cancer Res* 71: 1334-1343.

135. Dangi-Garimella, S., J. Yun, E. M. Eves, M. Newman, S. J. Erkeland, S. M. Hammond, A. J. Minn, and M. R. Rosner. 2009. Raf kinase inhibitory protein suppresses a metastasis signalling cascade involving LIN28 and let-7. *Embo J* 28: 347-358.

136. al-Mulla, F., M. S. Bitar, Z. Taqi, O. Rath, and W. Kolch. 2011. RAF kinase inhibitory protein (RKIP) modulates cell cycle kinetics and motility. *Mol Biosyst* 7: 928-941.

137. Thornton, T. M., G. Pedraza-Alva, B. Deng, C. D. Wood, A. Aronshtam, J. L. Clements, G. Sabio, R. J. Davis, D. E. Matthews, B. Doble, and M. Rincon. 2008. Phosphorylation by p38 MAPK as an alternative pathway for GSK3beta inactivation. *Science* 320: 667-670.

138. Schuierer, M. M., U. Heilmeier, A. Boettcher, P. Ugocsai, A. K. Bosserhoff, G. Schmitz, and T. Langmann. 2006. Induction of Raf kinase inhibitor protein contributes to macrophage differentiation. *Biochem Biophys Res Commun* 342: 1083-1087.

139. Reumer, A., A. Bogaerts, T. Van Loy, S. J. Husson, L. Temmerman, C. Choi, E. Clynen, B. Hassan, and L. Schoofs. 2009. Unraveling the protective effect of a Drosophila phosphatidylethanolamine-binding protein upon bacterial infection by means of proteomics. *Dev Comp Immunol* 33: 1186-1195.

140. Menoret, A., J. P. McAleer, S. M. Ngoi, S. Ray, N. A. Eddy, G. Fenteany, S. J. Lee, R. J. Rossi, B. Mukherji, D. L. Allen, N. G. Chakraborty, and A. T. Vella. 2009. The oxazolidinone derivative locostatin induces cytokine appeasement. *J Immunol* 183: 7489-7496.

141. 1999. TNF neutralization in MS: results of a randomized, placebo-controlled multicenter study. The Lenercept Multiple Sclerosis Study Group and The University of British Columbia MS/MRI Analysis Group. *Neurology* 53: 457-465.

142. Opal, S. M., C. J. Fisher, Jr., J. F. Dhainaut, J. L. Vincent, R. Brase, S. F. Lowry, J. C. Sadoff, G. J. Slotman, H. Levy, R. A. Balk, M. P. Shelly, J. P. Pribble, J. F. LaBrecque, J. Lookabaugh, H. Donovan, H. Dubin, R. Baughman, J. Norman, E. DeMaria, K. Matzel, E. Abraham, and M. Seneff. 1997. Confirmatory interleukin-1 receptor antagonist trial in severe sepsis: a phase III, randomized, double-blind, placebo-controlled, multicenter trial. The Interleukin-1 Receptor Antagonist Sepsis Investigator Group. *Crit Care Med* 25: 1115-1124.

143. Hueber, W., B. E. Sands, S. Lewitzky, M. Vandemeulebroecke, W. Reinisch, P. D. Higgins, J. Wehkamp, B. G. Feagan, M. D. Yao, M. Karczewski, J. Karczewski, N. Pezous, S. Bek, G. Bruin, B. Mellgard, C. Berger, M. Londei, A. P. Bertolino, G. Tougas, and S. P. Travis. 2012. Secukinumab, a human anti-IL-17A monoclonal antibody, for moderate to severe Crohn's disease: unexpected results of a randomised, double-blind placebo-controlled trial. *Gut* 61: 1693-1700.

144. Theroux, S., M. Pereira, K. S. Casten, R. D. Burwell, K. C. Yeung, J. M. Sedivy, and J. Klysik. 2007. Raf kinase inhibitory protein knockout mice: expression in the brain and olfaction deficit. *Brain research bulletin* 71: 559-567.

145. Nagy, A., M. Gertsenstein, K. Vintersten, and R. Behringer. 2003. *Manipulating the Mouse Embryo: A Laboratory Manual*, New York.

146. McAleer, J. P., B. Liu, Z. Li, S. M. Ngoi, J. Dai, M. Oft, and A. T. Vella. 2010. Potent intestinal Th17 priming through peripheral lipopolysaccharide-based immunization. *Journal of leukocyte biology* 88: 21-31.

147. McAleer, J. P., D. J. Zammit, L. Lefrancois, R. J. Rossi, and A. T. Vella. 2007. The lipopolysaccharide adjuvant effect on T cells relies on nonoverlapping contributions from the MyD88 pathway and CD11c+ cells. *J Immunol* 179: 6524-6535.

148. Unkeless, J. C. 1979. Characterization of a monoclonal antibody directed against mouse macrophage and lymphocyte Fc receptors. *J Exp Med* 150: 580-596.

149. Spandidos, A., X. Wang, H. Wang, and B. Seed. 2010. PrimerBank: a resource of human and mouse PCR primer pairs for gene expression detection and quantification. *Nucleic Acids Res* 38: D792-799.

150. Huang da, W., B. T. Sherman, and R. A. Lempicki. 2009. Systematic and integrative analysis of large gene lists using DAVID bioinformatics resources. *Nat Protoc* 4: 44-57.

151. Bone, R. C., R. A. Balk, F. B. Cerra, R. P. Dellinger, A. M. Fein, W. A. Knaus, R. M. Schein, and W. J. Sibbald. 1992. American College of Chest Physicians/Society of Critical Care Medicine Consensus Conference: definitions for sepsis and organ failure and guidelines for the use of innovative therapies in sepsis. *Crit Care Med* 20: 864-874.

152. Hotchkiss, R. S., and I. E. Karl. 2003. The pathophysiology and treatment of sepsis. *N Engl J Med* 348: 138-150.

153. Neviere, R. 2012. Sepsis and the systemic inflammatory response syndrome: Definitions, epidemiology, and prognosis. In *UpToDate*. P. Parsons, ed. Wolters Kluwer Health.

154. Angus, D. C., W. T. Linde-Zwirble, J. Lidicker, G. Clermont, J. Carcillo, and M. R. Pinsky. 2001. Epidemiology of severe sepsis in the United States: analysis of incidence, outcome, and associated costs of care. *Crit Care Med* 29: 1303-1310.

155. Abraham, E., A. Anzueto, G. Gutierrez, S. Tessler, G. San Pedro, R. Wunderink, A. Dal Nogare, S. Nasraway, S. Berman, R. Cooney, H. Levy, R. Baughman, M. Rumbak, R. B. Light, L. Poole, R. Allred, J. Constant, J. Pennington, and S. Porter. 1998. Double-blind randomised controlled trial of monoclonal antibody to human tumour necrosis factor in treatment of septic shock. NORASEPT II Study Group. *Lancet* 351: 929-933.

156. Fisher, C. J., Jr., J. M. Agosti, S. M. Opal, S. F. Lowry, R. A. Balk, J. C. Sadoff, E. Abraham, R. M. Schein, and E. Benjamin. 1996. Treatment of septic shock with the tumor necrosis factor receptor:Fc fusion protein. The Soluble TNF Receptor Sepsis Study Group. *N Engl J Med* 334: 1697-1702.

157. Russell, J. A. 2006. Management of sepsis. *N Engl J Med* 355: 1699-1713.

158. Annane, D., E. Bellissant, P. E. Bollaert, J. Briegel, M. Confalonieri, R. De Gaudio, D. Keh, Y. Kupfer, M. Oppert, and G. U. Meduri. 2009. Corticosteroids in the treatment of severe sepsis and septic shock in adults: a systematic review. *Jama* 301: 2362-2375.

159. Todd, J., M. Fishaut, F. Kapral, and T. Welch. 1978. Toxic-shock syndrome associated with phage-group-I Staphylococci. *Lancet* 2: 1116-1118.

160. Kappler, J. W., A. Herman, J. Clements, and P. Marrack. 1992. Mutations defining functional regions of the superantigen staphylococcal enterotoxin B. *J Exp Med* 175: 387-396.

161. Pontzer, C. H., M. J. Irwin, N. R. Gascoigne, and H. M. Johnson. 1992. T-cell antigen receptor binding sites for the microbial superantigen staphylococcal enterotoxin A. *Proc Natl Acad Sci U S A* 89: 7727-7731.

162. Rajagopalan, G., M. M. Sen, M. Singh, N. S. Murali, K. A. Nath, K. Iijima, H. Kita, A. A. Leontovich, U. Gopinathan, R. Patel, and C. S. David. 2006. Intranasal exposure to staphylococcal enterotoxin B elicits an acute systemic inflammatory response. *Shock* 25: 647-656.

163. Muralimohan, G., R. J. Rossi, L. A. Guernsey, R. S. Thrall, and A. T. Vella. 2008. Inhalation of Staphylococcus aureus enterotoxin A induces IFN-gamma and CD8 T cell-dependent airway and interstitial lung pathology in mice. *J Immunol* 181: 3698-3705.

164. Ward, N. S., B. Casserly, and A. Ayala. 2008. The compensatory anti-inflammatory response syndrome (CARS) in critically ill patients. *Clinics in chest medicine* 29: 617-625, viii.

165. Cauley, L. S., K. A. Cauley, F. Shub, G. Huston, and S. L. Swain. 1997. Transferable anergy: superantigen treatment induces CD4+ T cell tolerance that is reversible and requires CD4-CD8- cells and interferon gamma. *J Exp Med* 186: 71-81.

166. Vallabhapurapu, S., and M. Karin. 2009. Regulation and function of NF-kappaB transcription factors in the immune system. *Annu Rev Immunol* 27: 693-733.

167. Chang, L., and M. Karin. 2001. Mammalian MAP kinase signalling cascades. *Nature* 410: 37-40.

168. Yeung, K., P. Janosch, B. McFerran, D. W. Rose, H. Mischak, J. M. Sedivy, and W. Kolch. 2000. Mechanism of suppression of the Raf/MEK/extracellular signal-regulated kinase pathway by the raf kinase inhibitor protein. *Mol Cell Biol* 20: 3079-3085.

169. Tang, H., S. Park, S. C. Sun, R. Trumbly, G. Ren, E. Tsung, and K. C. Yeung. 2010. RKIP inhibits NF-kappaB in cancer cells by regulating upstream signaling components of the IkappaB kinase complex. *FEBS Lett* 584: 662-668.

170. Fu, Z., P. C. Smith, L. Zhang, M. A. Rubin, R. L. Dunn, Z. Yao, and E. T. Keller. 2003. Effects of raf kinase inhibitor protein expression on suppression of prostate cancer metastasis. *Journal of the National Cancer Institute* 95: 878-889.

171. Hagan, S., F. Al-Mulla, E. Mallon, K. Oien, R. Ferrier, B. Gusterson, J. J. Garcia, and W. Kolch. 2005. Reduction of Raf-1 kinase inhibitor protein expression correlates with breast cancer metastasis. *Clinical cancer research : an official journal of the American Association for Cancer Research* 11: 7392-7397.

172. Beshir, A. B., C. E. Argueta, L. C. Menikarachchi, J. A. Gascon, and G. Fenteany. 2011. Locostatin Disrupts Association of Raf Kinase Inhibitor Protein With Binding Proteins by Modifying a Conserved Histidine Residue in the Ligand-Binding Pocket. *Forum on immunopathological diseases and therapeutics* 2: 47-58.

173. McCormack, J. E., J. E. Callahan, J. Kappler, and P. C. Marrack. 1993. Profound deletion of mature T cells in vivo by chronic exposure to exogenous superantigen. *J Immunol* 150: 3785-3792.

174. Selberg, O., H. Hecker, M. Martin, A. Klos, W. Bautsch, and J. Kohl. 2000. Discrimination of sepsis and systemic inflammatory response syndrome by determination of circulating plasma concentrations of procalcitonin, protein complement 3a, and interleukin-6. *Crit Care Med* 28: 2793-2798.

175. Rodriguez-Gaspar, M., F. Santolaria, A. Jarque-Lopez, E. Gonzalez-Reimers, A. Milena, M. J. de la Vega, E. Rodriguez-Rodriguez, and J. L. Gomez-Sirvent. 2001. Prognostic value of cytokines in SIRS general medical patients. *Cytokine* 15: 232-236.

176. Zhang, N., M. H. Ahsan, A. F. Purchio, and D. B. West. 2005. Serum amyloid A-luciferase transgenic mice: response to sepsis, acute arthritis, and contact hypersensitivity and the effects of proteasome inhibition. *J Immunol* 174: 8125-8134.

177. Zein, J., G. Lee, M. Tawk, M. Dabaja, and G. Kinasewitz. 2004. Prognostic Significance of Elevated Serum Lactate Dehydrogenase (LDH) in Patients with Severe Sepsis. *Chest* 126: S873.

178. Moore, K. W., R. de Waal Malefyt, R. L. Coffman, and A. O'Garra. 2001. Interleukin-10 and the interleukin-10 receptor. *Annu Rev Immunol* 19: 683-765.

179. Florquin, S., Z. Amraoui, D. Abramowicz, and M. Goldman. 1994. Systemic release and protective role of IL-10 in staphylococcal enterotoxin B-induced shock in mice. *J Immunol* 153: 2618-2623.

180. O'Garra, A., P. L. Vieira, P. Vieira, and A. E. Goldfeld. 2004. IL-10-producing and naturally occurring CD4+ Tregs: limiting collateral damage. *J Clin Invest* 114: 1372-1378.

181. Seok, J., H. S. Warren, A. G. Cuenca, M. N. Mindrinos, H. V. Baker, W. Xu, D. R. Richards, G. P. McDonald-Smith, H. Gao, L. Hennessy, C. C. Finnerty, C. M. Lopez, S. Honari, E. E. Moore, J. P. Minei, J. Cuschieri, P. E. Bankey, J. L. Johnson, J. Sperry, A. B. Nathens, T. R. Billiar, M. A. West, M. G. Jeschke, M. B. Klein, R. L. Gamelli, N. S. Gibran, B. H. Brownstein, C. Miller-Graziano, S. E. Calvano, P. H. Mason, J. P. Cobb, L. G. Rahme, S. F. Lowry, R. V. Maier, L. L. Moldawer, D. N. Herndon, R. W. Davis, W. Xiao, and R. G. Tompkins. 2013. Genomic responses in mouse models poorly mimic human inflammatory diseases. *Proc Natl Acad Sci U S A* 110: 3507-3512.

182. Mueller, D. L., M. K. Jenkins, and R. H. Schwartz. 1989. Clonal expansion versus functional clonal inactivation: a costimulatory signalling pathway determines the outcome of T cell antigen receptor occupancy. *Annu Rev Immunol* 7: 445-480.

183. Annane, D., V. Sebille, C. Charpentier, P. E. Bollaert, B. Francois, J. M. Korach, G. Capellier, Y. Cohen, E. Azoulay, G. Troche, P. Chaumet-Riffaud, and E. Bellissant. 2002. Effect of treatment with low doses of hydrocortisone and fludrocortisone on mortality in patients with septic shock. *Jama* 288: 862-871.

184. Zhu, S., K. T. Mc Henry, W. S. Lane, and G. Fenteany. 2005. A chemical inhibitor reveals the role of Raf kinase inhibitor protein in cell migration. *Chemistry & biology* 12: 981-991.

185. Shemon, A. N., E. M. Eves, M. C. Clark, G. Heil, A. Granovsky, L. Zeng, A. Imamoto, S. Koide, and M. R. Rosner. 2009. Raf Kinase Inhibitory Protein protects cells against locostatin-mediated inhibition of migration. *PLoS One* 4: e6028.

186. McAleer, J. P., and A. T. Vella. 2010. Educating CD4 T cells with vaccine adjuvants: lessons from lipopolysaccharide. *Trends Immunol* 31: 429-435.

187. Fenteany, G., R. F. Standaert, G. A. Reichard, E. J. Corey, and S. L. Schreiber. 1994. A beta-lactone related to lactacystin induces neurite outgrowth in a neuroblastoma cell line and inhibits cell cycle progression in an osteosarcoma cell line. *Proc Natl Acad Sci U S A* 91: 3358-3362.

188. Liu, X., and F. Fagotto. 2011. A method to separate nuclear, cytosolic, and membrane-associated signaling molecules in cultured cells. *Sci Signal* 4: pl2.

189. Janeway, C. A., Jr. 2013. Pillars article: approaching the asymptote? Evolution and revolution in immunology. Cold spring harb symp quant biol. 1989. 54: 1-13. *J Immunol* 191: 4475-4487.

190. Song, W. Y., G. L. Wang, L. L. Chen, H. S. Kim, L. Y. Pi, T. Holsten, J. Gardner, B. Wang, W. X. Zhai, L. H. Zhu, C. Fauquet, and P. Ronald. 1995. A receptor kinase-like protein encoded by the rice disease resistance gene, Xa21. *Science* 270: 1804-1806.

191. Lemaitre, B., E. Nicolas, L. Michaut, J. M. Reichhart, and J. A. Hoffmann. 1996. The dorsoventral regulatory gene cassette spatzle/Toll/cactus controls the potent antifungal response in Drosophila adults. *Cell* 86: 973-983.

192. Poltorak, A., X. He, I. Smirnova, M. Y. Liu, C. Van Huffel, X. Du, D. Birdwell, E. Alejos, M. Silva, C. Galanos, M. Freudenberg, P. Ricciardi-Castagnoli, B. Layton, and B. Beutler. 1998. Defective LPS signaling in C3H/HeJ and C57BL/10ScCr mice: mutations in Tlr4 gene. *Science* 282: 2085-2088.

193. Medzhitov, R., P. Preston-Hurlburt, and C. A. Janeway, Jr. 1997. A human homologue of the Drosophila Toll protein signals activation of adaptive immunity. *Nature* 388: 394-397.

194. Anderson, K. V., L. Bokla, and C. Nusslein-Volhard. 1985. Establishment of dorsal-ventral polarity in the Drosophila embryo: the induction of polarity by the Toll gene product. *Cell* 42: 791-798.

195. Trinchieri, G., and A. Sher. 2007. Cooperation of Toll-like receptor signals in innate immune defence. *Nat Rev Immunol* 7: 179-190.

196. Medzhitov, R., P. Preston-Hurlburt, E. Kopp, A. Stadlen, C. Chen, S. Ghosh, and C. A. Janeway, Jr. 1998. MyD88 is an adaptor protein in the hToll/IL-1 receptor family signaling pathways. *Mol Cell* 2: 253-258.

197. Muzio, M., G. Natoli, S. Saccani, M. Levrero, and A. Mantovani. 1998. The human toll signaling pathway: divergence of nuclear factor kappaB and JNK/SAPK activation upstream of tumor necrosis factor receptor-associated factor 6 (TRAF6). *J Exp Med* 187: 2097-2101.

198. Schnare, M., A. C. Holt, K. Takeda, S. Akira, and R. Medzhitov. 2000. Recognition of CpG DNA is mediated by signaling pathways dependent on the adaptor protein MyD88. *Curr Biol* 10: 1139-1142.

199. Oshiumi, H., M. Matsumoto, K. Funami, T. Akazawa, and T. Seya. 2003. TICAM-1, an adaptor molecule that participates in Toll-like receptor 3-mediated interferon-beta induction. *Nat Immunol* 4: 161-167.

200. Yamamoto, M., S. Sato, H. Hemmi, K. Hoshino, T. Kaisho, H. Sanjo, O. Takeuchi, M. Sugiyama, M. Okabe, K. Takeda, and S. Akira. 2003. Role of adaptor TRIF in the MyD88-independent toll-like receptor signaling pathway. *Science* 301: 640-643.

201. Hoebe, K., E. M. Janssen, S. O. Kim, L. Alexopoulou, R. A. Flavell, J. Han, and B. Beutler. 2003. Upregulation of costimulatory molecules induced by lipopolysaccharide and double-stranded RNA occurs by Trif-dependent and Trif-independent pathways. *Nat Immunol* 4: 1223-1229.

202. Tabeta, K., P. Georgel, E. Janssen, X. Du, K. Hoebe, K. Crozat, S. Mudd, L. Shamel, S. Sovath, J. Goode, L. Alexopoulou, R. A. Flavell, and B. Beutler. 2004. Toll-like receptors 9 and 3 as essential components of innate immune defense against mouse cytomegalovirus infection. *Proc Natl Acad Sci U S A* 101: 3516-3521.

203. Ishikawa, H., and G. N. Barber. 2008. STING is an endoplasmic reticulum adaptor that facilitates innate immune signalling. *Nature* 455: 674-678.

204. Wright, K. T., and A. T. Vella. 2013. RKIP contributes to IFN-gamma synthesis by CD8+ T cells after serial TCR triggering in systemic inflammatory response syndrome. *J Immunol* 191: 708-716.

205. Patil, A., Y. Kumagai, K. C. Liang, Y. Suzuki, and K. Nakai. 2013. Linking transcriptional changes over time in stimulated dendritic cells to identify gene networks activated during the innate immune response. *PLoS Comput Biol* 9: e1003323.

206. Therrien, M., H. C. Chang, N. M. Solomon, F. D. Karim, D. A. Wassarman, and G. M. Rubin. 1995. KSR, a novel protein kinase required for RAS signal transduction. *Cell* 83: 879-888.

207. Schaeffer, H. J., A. D. Catling, S. T. Eblen, L. S. Collier, A. Krauss, and M. J. Weber. 1998. MP1: a MEK binding partner that enhances enzymatic activation of the MAP kinase cascade. *Science* 281: 1668-1671.

208. Luttrell, L. M., F. L. Roudabush, E. W. Choy, W. E. Miller, M. E. Field, K. L. Pierce, and R. J. Lefkowitz. 2001. Activation and targeting of extracellular signal-regulated kinases by beta-arrestin scaffolds. *Proc Natl Acad Sci U S A* 98: 2449-2454.

209. Sobering, A. K., R. Watanabe, M. J. Romeo, B. C. Yan, C. A. Specht, P. Orlean, H. Riezman, and D. E. Levin. 2004. Yeast Ras regulates the complex that catalyzes the first step in GPI-anchor biosynthesis at the ER. *Cell* 117: 637-648.

210. Torii, S., M. Kusakabe, T. Yamamoto, M. Maekawa, and E. Nishida. 2004. Sef is a spatial regulator for Ras/MAP kinase signaling. *Dev Cell* 7: 33-44.

211. Chiu, R., W. J. Boyle, J. Meek, T. Smeal, T. Hunter, and M. Karin. 1988. The c-Fos protein interacts with c-Jun/AP-1 to stimulate transcription of AP-1 responsive genes. *Cell* 54: 541-552.

212. Lorenz, K., M. J. Lohse, and U. Quitterer. 2003. Protein kinase C switches the Raf kinase inhibitor from Raf-1 to GRK-2. *Nature* 426: 574-579.

213. Cook, D. N., D. S. Pisetsky, and D. A. Schwartz. 2004. Toll-like receptors in the pathogenesis of human disease. *Nat Immunol* 5: 975-979.

214. Kiechl, S., E. Lorenz, M. Reindl, C. J. Wiedermann, F. Oberhollenzer, E. Bonora, J. Willeit, and D. A. Schwartz. 2002. Toll-like receptor 4 polymorphisms and atherogenesis. *N Engl J Med* 347: 185-192.

215. Ishihara, S., M. A. Rumi, C. F. Ortega-Cava, H. Kazumori, Y. Kadowaki, N. Ishimura, and Y. Kinoshita. 2006. Therapeutic targeting of toll-like receptors in gastrointestinal inflammation. *Curr Pharm Des* 12: 4215-4228.

216. Sacre, S. M., E. Andreakos, S. Kiriakidis, P. Amjadi, A. Lundberg, G. Giddins, M. Feldmann, F. Brennan, and B. M. Foxwell. 2007. The Toll-like receptor adaptor proteins MyD88 and Mal/TIRAP contribute to the inflammatory and destructive processes in a human model of rheumatoid arthritis. *Am J Pathol* 170: 518-525.

217. Schroder, N. W., and M. Maurer. 2007. The role of innate immunity in asthma: leads and lessons from mouse models. *Allergy* 62: 579-590.

218. Zhai, Y., X. D. Shen, R. O'Connell, F. Gao, C. Lassman, R. W. Busuttil, G. Cheng, and J. W. Kupiec-Weglinski. 2004. Cutting edge: TLR4 activation mediates liver ischemia/reperfusion inflammatory response via IFN regulatory factor 3-dependent MyD88-independent pathway. *J Immunol* 173: 7115-7119.

219. Ondiveeran, H. K., and A. Fox-Robichaud. 2004. Drug evaluation: E-5564. *IDrugs* 7: 582-590.

220. Kaplan, B. I., and P. Tipirneni. 2007. Lessons for the future: a review of sepsis past and present. *IDrugs* 10: 264-269.

221. Vanags, D., B. Williams, B. Johnson, S. Hall, P. Nash, A. Taylor, J. Weiss, and D. Feeney. 2006. Therapeutic efficacy and safety of chaperonin 10 in patients with rheumatoid arthritis: a double-blind randomised trial. *Lancet* 368: 855-863.

222. Gearing, A. J. 2007. Targeting toll-like receptors for drug development: a summary of commercial approaches. *Immunol Cell Biol* 85: 490-494.

223. Martin, F., and A. C. Chan. 2006. B cell immunobiology in disease: evolving concepts from the clinic. *Annu Rev Immunol* 24: 467-496.

224. Zinkernagel, R. M. 2003. On natural and artificial vaccinations. *Annu Rev Immunol* 21: 515-546.

225. Riley, E. M., and V. A. Stewart. 2013. Immune mechanisms in malaria: new insights in vaccine development. *Nat Med* 19: 168-178.

226. Jensen-Jarolim, E., and J. Singer. 2011. Cancer vaccines inducing antibody production: more pros than cons. *Expert Rev Vaccines* 10: 1281-1289.

227. Fillatreau, S. 2013. Cytokine-producing B cells as regulators of pathogenic and protective immune responses. *Ann Rheum Dis* 72 Suppl 2: ii80-84.

228. Edwards, J. C., L. Szczepanski, J. Szechinski, A. Filipowicz-Sosnowska, P. Emery, D. R. Close, R. M. Stevens, and T. Shaw. 2004. Efficacy of B-cell-targeted therapy with rituximab in patients with rheumatoid arthritis. *N Engl J Med* 350: 2572-2581.

229. Carson, K. R., D. Focosi, E. O. Major, M. Petrini, E. A. Richey, D. P. West, and C. L. Bennett. 2009. Monoclonal antibody-associated progressive multifocal leucoencephalopathy in patients treated with rituximab, natalizumab, and efalizumab: a Review from the Research on Adverse Drug Events and Reports (RADAR) Project. *Lancet Oncol* 10: 816-824.

230. Gavin, A. L., K. Hoebe, B. Duong, T. Ota, C. Martin, B. Beutler, and D. Nemazee. 2006. Adjuvant-enhanced antibody responses in the absence of toll-like receptor signaling. *Science* 314: 1936-1938.

231. Giannini, S. L., E. Hanon, P. Moris, M. Van Mechelen, S. Morel, F. Dessy, M. A. Fourneau, B. Colau, J. Suzich, G. Losonksy, M. T. Martin, G. Dubin, and M. A. Wettendorff. 2006. Enhanced humoral and memory B cellular immunity using HPV16/18 L1 VLP vaccine formulated with the MPL/aluminium salt combination (AS04) compared to aluminium salt only. *Vaccine* 24: 5937-5949.

232. Garraud, O., G. Borhis, G. Badr, S. Degrelle, B. Pozzetto, F. Cognasse, and Y. Richard. 2012. Revisiting the B-cell compartment in mouse and humans: more than one B-cell subset exists in the marginal zone and beyond. *BMC Immunol* 13: 63.

233. Green, N. M., and A. Marshak-Rothstein. 2011. Toll-like receptor driven B cell activation in the induction of systemic autoimmunity. *Semin Immunol* 23: 106-112.

234. Moir, S., and A. S. Fauci. 2009. B cells in HIV infection and disease. *Nat Rev Immunol* 9: 235-245.

235. Bluml, S., K. McKeever, R. Ettinger, J. Smolen, and R. Herbst. 2013. B-cell targeted therapeutics in clinical development. *Arthritis Res Ther* 15 Suppl 1: S4.

236. Krieg, A. M., A. K. Yi, S. Matson, T. J. Waldschmidt, G. A. Bishop, R. Teasdale, G. A. Koretzky, and D. M. Klinman. 1995. CpG motifs in bacterial DNA trigger direct B-cell activation. *Nature* 374: 546-549.

237. Chang, C. H., J. D. Curtis, L. B. Maggi, Jr., B. Faubert, A. V. Villarino, D. O'Sullivan, S. C. Huang, G. J. van der Windt, J. Blagih, J. Qiu, J. D. Weber, E. J. Pearce, R. G. Jones, and E. L. Pearce. 2013. Posttranscriptional control of T cell effector function by aerobic glycolysis. *Cell* 153: 1239-1251.

238. Desmet, C. J., and K. J. Ishii. 2012. Nucleic acid sensing at the interface between innate and adaptive immunity in vaccination. *Nat Rev Immunol* 12: 479-491.

239. Reed, S. G., M. T. Orr, and C. B. Fox. 2013. Key roles of adjuvants in modern vaccines. *Nat Med* 19: 1597-1608.

240. Moir, S., A. Malaspina, and A. S. Fauci. 2011. Prospects for an HIV vaccine: leading B cells down the right path. *Nat Struct Mol Biol* 18: 1317-1321.

241. Sallusto, F., A. Lanzavecchia, K. Araki, and R. Ahmed. 2010. From vaccines to memory and back. *Immunity* 33: 451-463.

242. Browne, E. P. 2012. Regulation of B-cell responses by Toll-like receptors. *Immunology* 136: 370-379.

243. Rawlings, D. J., M. A. Schwartz, S. W. Jackson, and A. Meyer-Bahlburg. 2012. Integration of B cell responses through Toll-like receptors and antigen receptors. *Nat Rev Immunol* 12: 282-294.

244. Agrawal, S., and S. Gupta. 2011. TLR1/2, TLR7, and TLR9 signals directly activate human peripheral blood naive and memory B cell subsets to produce cytokines, chemokines, and hematopoietic growth factors. *J Clin Immunol* 31: 89-98.

245. Zouggari, Y., H. Ait-Oufella, P. Bonnin, T. Simon, A. P. Sage, C. Guerin, J. Vilar, G. Caligiuri, D. Tsiantoulas, L. Laurans, E. Dumeau, S. Kotti, P. Bruneval, I. F. Charo, C. J. Binder, N. Danchin, A. Tedgui, T. F. Tedder, J. S. Silvestre, and Z. Mallat. 2013. B lymphocytes trigger monocyte mobilization and impair heart function after acute myocardial infarction. *Nat Med* 19: 1273-1280.

246. Pulendran, B., and R. Ahmed. 2011. Immunological mechanisms of vaccination. *Nat Immunol* 12: 509-517.

247. Coffman, R. L., A. Sher, and R. A. Seder. 2010. Vaccine adjuvants: putting innate immunity to work. *Immunity* 33: 492-503.

248. Gaucher, D., R. Therrien, N. Kettaf, B. R. Angermann, G. Boucher, A. Filali-Mouhim, J. M. Moser, R. S. Mehta, D. R. Drake, 3rd, E. Castro, R. Akondy, A. Rinfret, B. Yassine-Diab, E. A. Said, Y. Chouikh, M. J. Cameron, R. Clum, D. Kelvin, R. Somogyi, L. D. Greller, R. S. Balderas, P. Wilkinson, G. Pantaleo, J. Tartaglia, E. K. Haddad, and R. P. Sekaly. 2008. Yellow fever vaccine induces integrated multilineage and polyfunctional immune responses. *J Exp Med* 205: 3119-3131.

249. Querec, T. D., and B. Pulendran. 2007. Understanding the role of innate immunity in the mechanism of action of the live attenuated Yellow Fever Vaccine 17D. *Adv Exp Med Biol* 590: 43-53.

250. Caskey, M., F. Lefebvre, A. Filali-Mouhim, M. J. Cameron, J. P. Goulet, E. K. Haddad, G. Breton, C. Trumpfheller, S. Pollak, I. Shimeliovich, A. Duque-Alarcon, L. Pan, A. Nelkenbaum, A. M. Salazar, S. J. Schlesinger, R. M. Steinman, and R. P. Sekaly. 2011. Synthetic double-stranded RNA induces innate immune responses similar to a live viral vaccine in humans. *J Exp Med* 208: 2357-2366.

251. Marshak-Rothstein, A., and I. R. Rifkin. 2007. Immunologically active autoantigens: the role of toll-like receptors in the development of chronic inflammatory disease. *Annu Rev Immunol* 25: 419-441.

252. Pasare, C., and R. Medzhitov. 2005. Control of B-cell responses by Toll-like receptors. *Nature* 438: 364-368.

253. Rajagopal, D., C. Paturel, Y. Morel, S. Uematsu, S. Akira, and S. S. Diebold. 2010. Plasmacytoid dendritic cell-derived type I interferon is crucial for the adjuvant activity of Toll-like receptor 7 agonists. *Blood* 115: 1949-1957.

254. Everts, B., E. Amiel, S. C. Huang, A. M. Smith, C. H. Chang, W. Y. Lam, V. Redmann, T. C. Freitas, J. Blagih, G. J. van der Windt, M. N. Artyomov, R. G. Jones, E. L. Pearce, and E. J. Pearce. 2014. TLR-driven early glycolytic reprogramming via the kinases TBK1-IKKvarepsilon supports the anabolic demands of dendritic cell activation. *Nat Immunol* 15: 323-332.

255. Bennett, L., A. K. Palucka, E. Arce, V. Cantrell, J. Borvak, J. Banchereau, and V. Pascual. 2003. Interferon and granulopoiesis signatures in systemic lupus erythematosus blood. *J Exp Med* 197: 711-723.

256. Curbishley, S. M., B. Eksteen, R. P. Gladue, P. Lalor, and D. H. Adams. 2005. CXCR 3 activation promotes lymphocyte transendothelial migration across human hepatic endothelium under fluid flow. *Am J Pathol* 167: 887-899.

257. Green, N. M., A. Laws, K. Kiefer, L. Busconi, Y. M. Kim, M. M. Brinkmann, E. H. Trail, K. Yasuda, S. R. Christensen, M. J. Shlomchik, S. Vogel, J. H. Connor, H. Ploegh, D. Eilat, I. R. Rifkin, J. M. van Seventer, and A. Marshak-Rothstein. 2009. Murine B cell response to TLR7 ligands depends on an IFN-beta feedback loop. *J Immunol* 183: 1569-1576.

258. Chang, W. L., E. S. Coro, F. C. Rau, Y. Xiao, D. J. Erle, and N. Baumgarth. 2007. Influenza virus infection causes global respiratory tract B cell response modulation via innate immune signals. *J Immunol* 178: 1457-1467.

259. Krumbholz, M., H. Faber, F. Steinmeyer, L. A. Hoffmann, T. Kumpfel, H. Pellkofer, T. Derfuss, C. Ionescu, M. Starck, C. Hafner, R. Hohlfeld, and E. Meinl. 2008. Interferon-beta increases BAFF levels in multiple sclerosis: implications for B cell autoimmunity. *Brain* 131: 1455-1463.

260. Kina, T., K. Ikuta, E. Takayama, K. Wada, A. S. Majumdar, I. L. Weissman, and Y. Katsura. 2000. The monoclonal antibody TER-119 recognizes a molecule associated with glycophorin A and specifically marks the late stages of murine erythroid lineage. *Br J Haematol* 109: 280-287.

261. Bagriacik, E. U., M. D. Armstrong, M. Okabe, and J. R. Klein. 1999. Differential expression of CD43 isoforms on murine T cells and their relationship to acute intestinal graft versus host disease: studies using enhanced-green fluorescent protein transgenic mice. *Int Immunol* 11: 1651-1662.

262. Tavel, L., L. Jaquillard, A. I. Karsisiotis, F. Saab, L. Jouvensal, A. Brans, A. F. Delmas, F. Schoentgen, M. Cadene, and C. Damblon. 2012. Ligand binding study of human PEBP1/RKIP: interaction with nucleotides and Raf-1 peptides evidenced by NMR and mass spectrometry. *PLoS One* 7: e36187.

263. Park, S., O. Rath, S. Beach, X. Xiang, S. M. Kelly, Z. Luo, W. Kolch, and K. C. Yeung. 2006. Regulation of RKIP binding to the N-region of the Raf-1 kinase. *FEBS Lett* 580: 6405-6412.

264. Kang, D. C., R. V. Gopalkrishnan, Q. Wu, E. Jankowsky, A. M. Pyle, and P. B. Fisher. 2002. mda-5: An interferon-inducible putative RNA helicase with double-stranded RNA-dependent ATPase activity and melanoma growth-suppressive properties. *Proc Natl Acad Sci U S A* 99: 637-642.

265. Alexopoulou, L., A. C. Holt, R. Medzhitov, and R. A. Flavell. 2001. Recognition of double-stranded RNA and activation of NF-kappaB by Toll-like receptor 3. *Nature* 413: 732-738.

266. Marshall-Clarke, S., J. E. Downes, I. R. Haga, A. G. Bowie, P. Borrow, J. L. Pennock, R. K. Grencis, and P. Rothwell. 2007. Polyinosinic acid is a ligand for toll-like receptor 3. *J Biol Chem* 282: 24759-24766.

267. Kumar, H., S. Koyama, K. J. Ishii, T. Kawai, and S. Akira. 2008. Cutting edge: cooperation of IPS-1- and TRIF-dependent pathways in poly IC-enhanced antibody production and cytotoxic T cell responses. *J Immunol* 180: 683-687.

268. Kayagaki, N., Q. Phung, S. Chan, R. Chaudhari, C. Quan, K. M. O'Rourke, M. Eby, E. Pietras, G. Cheng, J. F. Bazan, Z. Zhang, D. Arnott, and V. M. Dixit. 2007. DUBA: a deubiquitinase that regulates type I interferon production. *Science* 318: 1628-1632.

269. Tseng, P. H., A. Matsuzawa, W. Zhang, T. Mino, D. A. Vignali, and M. Karin. 2010. Different modes of ubiquitination of the adaptor TRAF3 selectively activate the expression of type I interferons and proinflammatory cytokines. *Nat Immunol* 11: 70-75.

270. Oganesyan, G., S. K. Saha, B. Guo, J. Q. He, A. Shahangian, B. Zarnegar, A. Perry, and G. Cheng. 2006. Critical role of TRAF3 in the Toll-like receptor-dependent and -independent antiviral response. *Nature* 439: 208-211.

271. Sharma, S., B. R. tenOever, N. Grandvaux, G. P. Zhou, R. Lin, and J. Hiscott. 2003. Triggering the interferon antiviral response through an IKK-related pathway. *Science* 300: 1148-1151.

272. Fitzgerald, K. A., S. M. McWhirter, K. L. Faia, D. C. Rowe, E. Latz, D. T. Golenbock, A. J. Coyle, S. M. Liao, and T. Maniatis. 2003. IKKepsilon and TBK1 are essential components of the IRF3 signaling pathway. *Nat Immunol* 4: 491-496.

273. Ivashkiv, L. B., and L. T. Donlin. 2014. Regulation of type I interferon responses. *Nat Rev Immunol* 14: 36-49.

274. Deiss, K., C. Kisker, M. J. Lohse, and K. Lorenz. 2012. Raf kinase inhibitor protein (RKIP) dimer formation controls its target switch from Raf1 to G protein-coupled receptor kinase (GRK) 2. *J Biol Chem* 287: 23407-23417.

275. Hu, X., S. D. Chakravarty, and L. B. Ivashkiv. 2008. Regulation of interferon and Toll-like receptor signaling during macrophage activation by opposing feedforward and feedback inhibition mechanisms. *Immunol Rev* 226: 41-56.

276. Baccala, R., K. Hoebe, D. H. Kono, B. Beutler, and A. N. Theofilopoulos. 2007. TLR-dependent and TLR-independent pathways of type I interferon induction in systemic autoimmunity. *Nat Med* 13: 543-551.

277. Banchereau, J., and V. Pascual. 2006. Type I interferon in systemic lupus erythematosus and other autoimmune diseases. *Immunity* 25: 383-392.

278. de Weerd, N. A., S. A. Samarajiwa, and P. J. Hertzog. 2007. Type I interferon receptors: biochemistry and biological functions. *J Biol Chem* 282: 20053-20057.

279. Gilliet, M., W. Cao, and Y. J. Liu. 2008. Plasmacytoid dendritic cells: sensing nucleic acids in viral infection and autoimmune diseases. *Nat Rev Immunol* 8: 594-606.

280. Longhi, M. P., C. Trumpfheller, J. Idoyaga, M. Caskey, I. Matos, C. Kluger, A. M. Salazar, M. Colonna, and R. M. Steinman. 2009. Dendritic cells require a systemic type I interferon response to mature and induce CD4+ Th1 immunity with poly IC as adjuvant. *J Exp Med* 206: 1589-1602.

281. Panchanathan, R., and D. Choubey. 2013. Murine BAFF expression is up-regulated by estrogen and interferons: implications for sex bias in the development of autoimmunity. *Mol Immunol* 53: 15-23.

282. Vincent, F. B., D. Saulep-Easton, W. A. Figgett, K. A. Fairfax, and F. Mackay. 2013. The BAFF/APRIL system: emerging functions beyond B cell biology and autoimmunity. *Cytokine Growth Factor Rev* 24: 203-215.

283. Swanson, C. L., T. J. Wilson, P. Strauch, M. Colonna, R. Pelanda, and R. M. Torres. 2010. Type I IFN enhances follicular B cell contribution to the T cell-independent antibody response. *J Exp Med* 207: 1485-1500.

284. Kelly-Scumpia, K. M., P. O. Scumpia, M. J. Delano, J. S. Weinstein, A. G. Cuenca, J. L. Wynn, and L. L. Moldawer. 2010. Type I interferon signaling in hematopoietic cells is required for survival in mouse polymicrobial sepsis by regulating CXCL10. *J Exp Med* 207: 319-326.

285. Dufour, J. H., M. Dziejman, M. T. Liu, J. H. Leung, T. E. Lane, and A. D. Luster. 2002. IFN-gamma-inducible protein 10 (IP-10; CXCL10)-deficient mice reveal a role for IP-10 in effector T cell generation and trafficking. *J Immunol* 168: 3195-3204.

286. Ghislain, J. J., T. Wong, M. Nguyen, and E. N. Fish. 2001. The interferon-inducible Stat2:Stat1 heterodimer preferentially binds in vitro to a consensus element found in the promoters of a subset of interferon-stimulated genes. *J Interferon Cytokine Res* 21: 379-388.

287. Ohmori, Y., and T. A. Hamilton. 1995. The interferon-stimulated response element and a kappa B site mediate synergistic induction of murine IP-10 gene transcription by IFN-gamma and TNF-alpha. *J Immunol* 154: 5235-5244.

288. Jia, T., I. Leiner, G. Dorothee, K. Brandl, and E. G. Pamer. 2009. MyD88 and Type I interferon receptor-mediated chemokine induction and monocyte recruitment during Listeria monocytogenes infection. *J Immunol* 183: 1271-1278.

289. Trinchieri, G. 2010. Type I interferon: friend or foe? *J Exp Med* 207: 2053-2063.

290. Prchal, M., A. Pilz, O. Simma, K. Lingnau, A. von Gabain, B. Strobl, M. Muller, and T. Decker. 2009. Type I interferons as mediators of immune adjuvants for T- and B cell-dependent acquired immunity. *Vaccine* 27 Suppl 6: G17-20.

291. Cousens, L. P., R. Peterson, S. Hsu, A. Dorner, J. D. Altman, R. Ahmed, and C. A. Biron. 1999. Two roads diverged: interferon alpha/beta- and interleukin 12-mediated pathways in promoting T cell interferon gamma responses during viral infection. *J Exp Med* 189: 1315-1328.

292. Nguyen, K. B., L. P. Cousens, L. A. Doughty, G. C. Pien, J. E. Durbin, and C. A. Biron. 2000. Interferon alpha/beta-mediated inhibition and promotion of interferon gamma: STAT1 resolves a paradox. *Nat Immunol* 1: 70-76.

293. Nguyen, K. B., W. T. Watford, R. Salomon, S. R. Hofmann, G. C. Pien, A. Morinobu, M. Gadina, J. J. O'Shea, and C. A. Biron. 2002. Critical role for STAT4 activation by type 1 interferons in the interferon-gamma response to viral infection. *Science* 297: 2063-2066.

294. Freudenberg, M. A., T. Merlin, C. Kalis, Y. Chvatchko, H. Stubig, and C. Galanos. 2002. Cutting edge: a murine, IL-12-independent pathway of IFN-gamma induction by gram-negative bacteria based on STAT4 activation by Type I IFN and IL-18 signaling. *J Immunol* 169: 1665-1668.

295. Cho, S. S., C. M. Bacon, C. Sudarshan, R. C. Rees, D. Finbloom, R. Pine, and J. J. O'Shea. 1996. Activation of STAT4 by IL-12 and IFN-alpha: evidence for the involvement of ligand-induced tyrosine and serine phosphorylation. *J Immunol* 157: 4781-4789.

296. Rogge, L., D. D'Ambrosio, M. Biffi, G. Penna, L. J. Minetti, D. H. Presky, L. Adorini, and F. Sinigaglia. 1998. The role of Stat4 in species-specific regulation of Th cell development by type I IFNs. *J Immunol* 161: 6567-6574.

297. Wang, Y., M. Cella, S. Gilfillan, and M. Colonna. 2010. Cutting edge: polyinosinic:polycytidylic acid boosts the generation of memory CD8 T cells through melanoma differentiation-associated protein 5 expressed in stromal cells. *J Immunol* 184: 2751-2755.

298. Curtsinger, J. M., J. O. Valenzuela, P. Agarwal, D. Lins, and M. F. Mescher. 2005. Type I IFNs provide a third signal to CD8 T cells to stimulate clonal expansion and differentiation. *J Immunol* 174: 4465-4469.

299. Kolumam, G. A., S. Thomas, L. J. Thompson, J. Sprent, and K. Murali-Krishna. 2005. Type I interferons act directly on CD8 T cells to allow clonal expansion and memory formation in response to viral infection. *J Exp Med* 202: 637-650.

300. Thompson, L. J., G. A. Kolumam, S. Thomas, and K. Murali-Krishna. 2006. Innate inflammatory signals induced by various pathogens differentially dictate the IFN-I dependence of CD8 T cells for clonal expansion and memory formation. *J Immunol* 177: 1746-1754.

301. Platanias, L. C. 2005. Mechanisms of type-I- and type-II-interferon-mediated signalling. *Nat Rev Immunol* 5: 375-386.

302. Tanabe, Y., T. Nishibori, L. Su, R. M. Arduini, D. P. Baker, and M. David. 2005. Cutting edge: role of STAT1, STAT3, and STAT5 in IFN-alpha beta responses in T lymphocytes. *J Immunol* 174: 609-613.

303. Chang, E. Y., B. Guo, S. E. Doyle, and G. Cheng. 2007. Cutting edge: involvement of the type I IFN production and signaling pathway in lipopolysaccharide-induced IL-10 production. *J Immunol* 178: 6705-6709.

304. Wang, X., M. Chen, K. P. Wandinger, G. Williams, and S. Dhib-Jalbut. 2000. IFN-beta-1b inhibits IL-12 production in peripheral blood mononuclear cells in an IL-10-dependent mechanism: relevance to IFN-beta-1b therapeutic effects in multiple sclerosis. *J Immunol* 165: 548-557.

305. Wang, H., J. Brown, C. A. Garcia, Y. Tang, M. R. Benakanakere, T. Greenway, P. Alard, D. F. Kinane, and M. Martin. 2011. The role of glycogen synthase kinase 3 in regulating IFN-beta-mediated IL-10 production. *J Immunol* 186: 675-684.

306. Delgoffe, G. M., and D. A. Vignali. 2014. A Fox of a different color: FoxA1 programs a new regulatory T cell subset. *Nat Med* 20: 236-237.

307. Liu, Y., R. Carlsson, M. Comabella, J. Wang, M. Kosicki, B. Carrion, M. Hasan, X. Wu, X. Montalban, M. H. Dziegiel, F. Sellebjerg, P. S. Sorensen, K. Helin, and S. Issazadeh-Navikas. 2014. FoxA1 directs the lineage and immunosuppressive properties of a novel regulatory T cell population in EAE and MS. *Nat Med* 20: 272-282.

308. Bowie, A. G., and L. Unterholzner. 2008. Viral evasion and subversion of pattern-recognition receptor signalling. *Nat Rev Immunol* 8: 911-922.

309. Nagano, Y., and Y. Kojima. 1954. [Immunizing property of vaccinia virus inactivated by ultraviolets rays]. *C R Seances Soc Biol Fil* 148: 1700-1702.

310. Watanabe, Y. 2004. Fifty years of interference. *Nat Immunol* 5: 1193.

311. Ozato, K., K. Uno, and Y. Iwakura. 2007. Another road to interferon: Yasuichi Nagano's journey. *J Interferon Cytokine Res* 27: 349-352.

312. Isaacs, A., and J. Lindenmann. 1957. Virus interference. I. The interferon. *Proc R Soc Lond B Biol Sci* 147: 258-267.

313. Sadler, A. J., and B. R. Williams. 2008. Interferon-inducible antiviral effectors. *Nat Rev Immunol* 8: 559-568.

314. Savan, R., S. Ravichandran, J. R. Collins, M. Sakai, and H. A. Young. 2009. Structural conservation of interferon gamma among vertebrates. *Cytokine Growth Factor Rev* 20: 115-124.

315. Manry, J., G. Laval, E. Patin, S. Fornarino, Y. Itan, M. Fumagalli, M. Sironi, M. Tichit, C. Bouchier, J. L. Casanova, L. B. Barreiro, and L. Quintana-Murci. 2011. Evolutionary genetic dissection of human interferons. *J Exp Med* 208: 2747-2759.

316. Chen, W., Z. Jia, T. Zhang, N. Zhang, C. Lin, F. Gao, L. Wang, X. Li, Y. Jiang, G. F. Gao, and C. Xia. 2010. MHC class I presentation and regulation by IFN in bony fish determined by molecular analysis of the class I locus in grass carp. *J Immunol* 185: 2209-2221.

317. Shisheva, A., S. J. Doxsey, J. M. Buxton, and M. P. Czech. 1995. Pericentriolar targeting of GDP-dissociation inhibitor isoform 2. *Eur J Cell Biol* 68: 143-158.

318. Cardenas, W. B., Y. M. Loo, M. Gale, Jr., A. L. Hartman, C. R. Kimberlin, L. Martinez-Sobrido, E. O. Saphire, and C. F. Basler. 2006. Ebola virus VP35 protein binds double-stranded RNA and inhibits alpha/beta interferon production induced by RIG-I signaling. *J Virol* 80: 5168-5178.

319. Chang, H. W., J. C. Watson, and B. L. Jacobs. 1992. The E3L gene of vaccinia virus encodes an inhibitor of the interferon-induced, double-stranded RNA-dependent protein kinase. *Proc Natl Acad Sci U S A* 89: 4825-4829.

320. Hatada, E., and R. Fukuda. 1992. Binding of influenza A virus NS1 protein to dsRNA in vitro. *J Gen Virol* 73 (Pt 12): 3325-3329.

321. Li, K., E. Foy, J. C. Ferreon, M. Nakamura, A. C. Ferreon, M. Ikeda, S. C. Ray, M. Gale, Jr., and S. M. Lemon. 2005. Immune evasion by hepatitis C virus NS3/4A protease-mediated cleavage of the Toll-like receptor 3 adaptor protein TRIF. *Proc Natl Acad Sci U S A* 102: 2992-2997.

322. Abe, T., Y. Kaname, I. Hamamoto, Y. Tsuda, X. Wen, S. Taguwa, K. Moriishi, O. Takeuchi, T. Kawai, T. Kanto, N. Hayashi, S. Akira, and Y. Matsuura. 2007. Hepatitis C virus nonstructural protein 5A modulates the toll-like receptor-MyD88-dependent signaling pathway in macrophage cell lines. *J Virol* 81: 8953-8966.

323. Gale, M. J., Jr., M. J. Korth, N. M. Tang, S. L. Tan, D. A. Hopkins, T. E. Dever, S. J. Polyak, D. R. Gretch, and M. G. Katze. 1997. Evidence that hepatitis C virus resistance to interferon is mediated through repression of the PKR protein kinase by the nonstructural 5A protein. *Virology* 230: 217-227.

324. Otsuka, M., N. Kato, M. Moriyama, H. Taniguchi, Y. Wang, N. Dharel, T. Kawabe, and M. Omata. 2005. Interaction between the HCV NS3 protein and the host TBK1 protein leads to inhibition of cellular antiviral responses. *Hepatology* 41: 1004-1012.

325. Romano, P. R., F. Zhang, S. L. Tan, M. T. Garcia-Barrio, M. G. Katze, T. E. Dever, and A. G. Hinnebusch. 1998. Inhibition of double-stranded RNA-dependent protein kinase PKR by vaccinia virus E3: role of complex formation and the E3 N-terminal domain. *Mol Cell Biol* 18: 7304-7316.

326. Keating, S. E., G. M. Maloney, E. M. Moran, and A. G. Bowie. 2007. IRAK-2 participates in multiple toll-like receptor signaling pathways to NFkappaB via activation of TRAF6 ubiquitination. *J Biol Chem* 282: 33435-33443.

327. Pichlmair, A., O. Schulz, C. P. Tan, T. I. Naslund, P. Liljestrom, F. Weber, and C. Reis e Sousa. 2006. RIG-I-mediated antiviral responses to single-stranded RNA bearing 5'-phosphates. *Science* 314: 997-1001.

328. Folly, B. B., A. M. Weffort-Santos, C. G. Fathman, and L. R. Soares. 2011. Dengue-2 structural proteins associate with human proteins to produce a coagulation and innate immune response biased interactome. *BMC Infect Dis* 11: 34.

329. Diekema, D. J., and R. N. Jones. 2001. Oxazolidinone antibiotics. *Lancet* 358: 1975-1982.

330. Present, D. H., P. Rutgeerts, S. Targan, S. B. Hanauer, L. Mayer, R. A. van Hogezand, D. K. Podolsky, B. E. Sands, T. Braakman, K. L. DeWoody, T. F. Schaible, and S. J. van Deventer. 1999. Infliximab for the treatment of fistulas in patients with Crohn's disease. *N Engl J Med* 340: 1398-1405.

331. Hua, J., K. Kirou, C. Lee, and M. K. Crow. 2006. Functional assay of type I interferon in systemic lupus erythematosus plasma and association with anti-RNA binding protein autoantibodies. *Arthritis Rheum* 54: 1906-1916.

332. Kirou, K. A., C. Lee, S. George, K. Louca, M. G. Peterson, and M. K. Crow. 2005. Activation of the interferon-alpha pathway identifies a subgroup of systemic lupus erythematosus patients with distinct serologic features and active disease. *Arthritis Rheum* 52: 1491-1503.

333. Baechler, E. C., F. M. Batliwalla, G. Karypis, P. M. Gaffney, W. A. Ortmann, K. J. Espe, K. B. Shark, W. J. Grande, K. M. Hughes, V. Kapur, P. K. Gregersen, and T. W. Behrens. 2003. Interferon-inducible gene expression signature in peripheral blood cells of patients with severe lupus. *Proc Natl Acad Sci U S A* 100: 2610-2615.

334. Yao, Y., L. Richman, B. W. Higgs, C. A. Morehouse, M. de los Reyes, P. Brohawn, J. Zhang, B. White, A. J. Coyle, P. A. Kiener, and B. Jallal. 2009. Neutralization of interferon-alpha/beta-inducible genes and downstream effect in a phase I trial of an anti-interferon-alpha monoclonal antibody in systemic lupus erythematosus. *Arthritis Rheum* 60: 1785-1796.

335. Wilson, L. E., D. Widman, S. H. Dikman, and P. D. Gorevic. 2002. Autoimmune disease complicating antiviral therapy for hepatitis C virus infection. *Semin Arthritis Rheum* 32: 163-173.

336. Nestle, F. O., C. Conrad, A. Tun-Kyi, B. Homey, M. Gombert, O. Boyman, G. Burg, Y. J. Liu, and M. Gilliet. 2005. Plasmacytoid predendritic cells initiate psoriasis through interferon-alpha production. *J Exp Med* 202: 135-143.

337. Dzionek, A., Y. Sohma, J. Nagafune, M. Cella, M. Colonna, F. Facchetti, G. Gunther, I. Johnston, A. Lanzavecchia, T. Nagasaka, T. Okada, W. Vermi, G. Winkels, T. Yamamoto, M. Zysk, Y. Yamaguchi, and J. Schmitz. 2001. BDCA-2, a novel plasmacytoid dendritic cell-specific type II C-type lectin, mediates antigen capture and is a potent inhibitor of interferon alpha/beta induction. *J Exp Med* 194: 1823-1834.

338. Freeman, H. J., A. Chopra, M. T. Clandinin, and A. B. Thomson. 2011. Recent advances in celiac disease. *World J Gastroenterol* 17: 2259-2272.

339. MacDonald, T. T., and J. Spencer. 1988. Evidence that activated mucosal T cells play a role in the pathogenesis of enteropathy in human small intestine. *J Exp Med* 167: 1341-1349.

340. Di Sabatino, A., K. M. Pickard, J. N. Gordon, V. Salvati, G. Mazzarella, R. M. Beattie, A. Vossenkaemper, L. Rovedatti, N. A. Leakey, N. M. Croft, R. Troncone, G. R. Corazza, A. J. Stagg, G. Monteleone, and T. T. MacDonald. 2007. Evidence for the role of interferon-alfa production by dendritic cells in the Th1 response in celiac disease. *Gastroenterology* 133: 1175-1187.

341. Ann Marrie, R., and R. A. Rudick. 2006. Drug Insight: interferon treatment in multiple sclerosis. *Nat Clin Pract Neurol* 2: 34-44.

342. Teige, I., A. Treschow, A. Teige, R. Mattsson, V. Navikas, T. Leanderson, R. Holmdahl, and S. Issazadeh-Navikas. 2003. IFN-beta gene deletion leads to augmented and chronic demyelinating experimental autoimmune encephalomyelitis. *J Immunol* 170: 4776-4784.

343. Brod, S. A., and D. K. Burns. 1994. Suppression of relapsing experimental autoimmune encephalomyelitis in the SJL/J mouse by oral administration of type I interferons. *Neurology* 44: 1144-1148.

344. Guo, B., E. Y. Chang, and G. Cheng. 2008. The type I IFN induction pathway constrains Th17-mediated autoimmune inflammation in mice. *J Clin Invest* 118: 1680-1690.

345. Astry, B., E. Harberts, and K. D. Moudgil. 2011. A cytokine-centric view of the pathogenesis and treatment of autoimmune arthritis. *J Interferon Cytokine Res* 31: 927-940.

346. Musch, E., T. Andus, M. Malek, A. Chrissafidou, and M. Schulz. 2007. Successful treatment of steroid refractory active ulcerative colitis with natural interferon-beta--an open long-term trial. *Z Gastroenterol* 45: 1235-1240.

347. Nikolaus, S., P. Rutgeerts, R. Fedorak, A. H. Steinhart, G. E. Wild, D. Theuer, J. Mohrle, and S. Schreiber. 2003. Interferon beta-1a in ulcerative colitis: a placebo controlled, randomised, dose escalating study. *Gut* 52: 1286-1290.

348. Madsen, S. M., P. Schlichting, B. Davidsen, O. H. Nielsen, B. Federspiel, P. Riis, and P. Munkholm. 2001. An open-labeled, randomized study comparing systemic interferon-alpha-2A and prednisolone enemas in the treatment of left-sided ulcerative colitis. *Am J Gastroenterol* 96: 1807-1815.

349. Pena Rossi, C., S. B. Hanauer, R. Tomasevic, J. O. Hunter, I. Shafran, and H. Graffner. 2009. Interferon beta-1a for the maintenance of remission in patients with Crohn's disease: results of a phase II dose-finding study. *BMC Gastroenterol* 9: 22.

350. Musch, E., T. Andus, W. Kruis, A. Raedler, M. Spehlmann, S. Schreiber, B. Krakamp, M. Malek, H. Malchow, F. Zavada, and G. Engelberg Feurle. 2005. Interferon-beta-1a for the treatment of steroid-refractory ulcerative colitis: a randomized, double-blind, placebo-controlled trial. *Clin Gastroenterol Hepatol* 3: 581-586.

351. Sigidin, Y. A., G. V. Loukina, B. Skurkovich, and S. Skurkovich. 2001. Randomized, double-blind trial of anti-interferon-gamma antibodies in rheumatoid arthritis. *Scand J Rheumatol* 30: 203-207.

352. Goodwin, J. S., and J. M. Goodwin. 1984. The tomato effect. Rejection of highly efficacious therapies. *Jama* 251: 2387-2390.